

**Distribution and Isotopic Composition of Living Planktonic Foraminifera
N. pachyderma (sinistral) and *T. quinqueloba* in the High Latitude North Atlantic**

Dissertation
zur Erlangung des Doktorgrades
der Mathematisch-Naturwissenschaftlichen Fakultät
der Christian-Albrechts-Universität zu Kiel

by
Elena Stangeew

Kiel 2001

Referent: Prof. Dr. M. Spindler

Koreferent: Prof. Dr. W.-Chr. Dullo

Tag der mündlichen Prüfung: 25.07.2001

Zum Druck genehmigt: Kiel, den 25.07.2001

Prof. Dr. Th. Bauer
Der Dekan

Kurzfassung

Anhand der Untersuchungen von Multinetzfängen (63 µm Maschenweite) wurde in der vorliegenden Arbeit die Verbreitung unterschiedlicher Arten der planktischen Foraminiferen in polaren Gebieten: der Labrador-, Grönlandsee und der Framstraße analysiert. Die Zusammensetzung der Artengemeinschaft wird in diesen Regionen in erster Linie durch die Temperatur in unterschiedlichen Wassermassen kontrolliert, wobei hauptsächlich sechs Arten auftreten: links- und rechtsdrehende *N. pachyderma*, *T. quinqueloba*, *G. bulloides*, *G. glutinata* und *G. uvula*. Die Anwendung der kleinmaschigen Multinetze führte zu einem niedrigeren Temperaturoptimum der dominanten Arten *Neogloboquadrina pachyderma* (sinistral) und *Turborotalita quinqueloba* als für die Größenklassen >200 µm beschrieben wurde. Die Änderungen der horizontalen und vertikalen Verbreitung von *N. pachyderma* (s.) und *T. quinqueloba* sowie der Verteilung der mittleren Gehäusegröße wird in der Untersuchungsregion neben den hydrographischen Parametern in erster Linie durch die synchrone Reproduktion in Abhängigkeit von dem Lunarzyklus beeinflusst. Die Untersuchung von Proben, die mit einer ausreichenden zeitlichen Auflösung in der Labrador See genommen wurden, ergab jeweils eine semilunare und lunare Periodizität für *N. pachyderma* (s.) und *T. quinqueloba*. Das Auftreten von Individuen mit einer Kümmerkammer und einer sekundären Kalzifizierung in den späteren Entwicklungsstadien folgte dem Reproduktionszyklus beider Arten.

Die zum ersten Mal durchgeführte detaillierte Untersuchung des Isotopensignals in Abhängigkeit von Größe und Gewicht bei *N. pachyderma* (s.) aus Planktonfängen ergab, daß das Gewicht und somit der Grad der Kalzifizierung nicht die primären Faktoren sind, die das Isotopensignal der verkrusteten *N. pachyderma* (s.) kontrollieren.

Der ¹⁸O-Vitaleffekt wird in erster Linie durch der thermische Schichtung der Wassersäule verursacht, während der ¹³C-Vitaleffekt stark durch den Verlauf der ontogenischen Entwicklung bestimmt wird. Der größenabhängige Verlauf der ¹³C-Werte von *N. pachyderma* (s.) folgt der für planktische Foraminiferen typischen logarithmischen Wachstumskurve. In der Framstraße (80°N) durchgeführte Isotopenuntersuchung an der symbiontentragenden Art *T. quinqueloba* zeigten einen zusätzlichen Einfluß der Symbiontenaktivität auf das ¹³C-Signal dieser Art.

Die bei der Untersuchung des ¹⁸O: ¹³C-Zusammenhangs von *N. pachyderma* (s.) festgestellte Steigung von 0.32 wurde in der vorliegenden Arbeit benutzt um die Vitaleffekte für beide Arten zu berechnen. Dabei wurde ein relativ geringer ¹⁸O-Vitaleffekt gegenüber den zu erwartenden Gleichgewichtswerten vom anorganischen Kalzit von -0.5 bis -0.7 ‰ für *N. pachyderma* (s.) und -0.8 ‰ für *T. quinqueloba* berechnet. Der ¹³C-Vitaleffekt gegenüber ¹³C_{Eq} lag bei -1.7 bis -2.1 ‰ für *N. pachyderma* (s.) und bei -2.5 ‰ für *T. quinqueloba*. In Übereinstimmung mit früheren Arbeiten wurde festgestellt, daß die beiden Arten innerhalb eines engen Temperaturbereiches kalzifizieren. Der Aufbau der Kalzitkruste erfolgt vor dem Absinken in tiefere Wasserschichten (in der Regel in 100-200 m Tiefe) und kann in Abhängigkeit von den Reproduktionszyklus der jeweiligen Art zwischen den oberen 0-50 m und 50-75 m variieren.

Für die im atlantischen Wasser des Westspitzbergenstroms (80°N) gemessenen Isotopenwerte von *N. pachyderma* (s.) und *T. quinqueloba*, die sich außerhalb des Gleichgewichts mit dem umgebenden Wasser befanden, wurde eine Kalzifizierung bei ca. 2.5°C höheren Wassertempere-

II

ren festgestellt, was für die Advektion beider Arten aus niedrigeren Breiten spricht.

Bei dem entlang des 80°N-Transekts in der Framstraße durchgeführten Vergleich zwischen dem Isotopensignal von *N. pachyderma* (s.) in der Wassersäule und in den Oberflächensedimenten wurden jeweils 0.2 ‰ und 0.3 ‰ höhere ¹⁸O- und ¹³C-Werte in den Sedimenten festgestellt.

Abstract

With the examination of multinet catches (63 μm mesh size), the present study analyzes the distribution of planktonic foraminifera in Polar regions: the Labrador Sea, Greenland Sea at 75°N and Fram Strait at 80°N. The community of the planktonic foraminifera, which in the study area mainly consists of six species: left and right-coiling *N. pachyderma*, *T. quinqueloba*, *G. bulloides*, *G. glutinata* and *G. uvula*, is primarily controlled by the temperature in the different water masses. The use of small mesh multinetts led to a slightly lower temperature optimum of the dominant species: *Neogloboquadrina pachyderma* (sinistral) and *Turborotalita quinqueloba* than what had been described for the size classes $>200 \mu\text{m}$.

Besides hydrographic parameters, the changes in the horizontal and vertical distribution of *N. pachyderma* (s.) and *T. quinqueloba* as well as their shell size distribution in the study area are primarily influenced by the synchronic reproduction, which is coupled to the lunar cycle. The examination of samples taken with sufficient temporal resolution in the Labrador Sea indicated *N. pachyderma* (s.) and *T. quinqueloba* to respectively show a semi-lunar and lunar periodicity. The occurrence of kummerform phenotypes and secondary calcification in the later development stages followed the reproductive cycles of both species.

Detailed examinations of the isotope signal in dependency of the shell size and weight for *N. pachyderma* (s.) from plankton tows, indicated the weight or degree of calcification to not be the primary factor controlling the isotope signal of encrusted specimens.

The ^{18}O vital effect is primarily caused by the thermal stratification of the water column, whereas the ^{13}C vital effect mainly results from the ontogenetic development. The size dependent course of ^{13}C values of *N. pachyderma* (s.) follows the typical logarithmic growth curve of planktonic foraminifera. Examinations of the symbiont-bearing species *T. quinqueloba* conducted in the Fram Strait (80°N) indicated an additional influence of symbiontactivity on the ^{13}C signal of this species.

Upon examination of the ^{18}O : ^{13}C disequilibrium, the established slope of 0.32 was used in the present study to calculate the vital effects for both species. A relatively low ^{18}O vital effect compared to ^{18}O values of inorganic calcite precipitated in equilibrium with ambient sea water was thus calculated: at -0.5 to -0.7 ‰ for *N. pachyderma* (s.) and -0.8 ‰ for *T. quinqueloba*. The ^{13}C vital effect relative to $^{13}\text{C}_{\text{Eq}}$ was at -1.7 to -2.1 ‰ for *N. pachyderma* (s.) and at -2.5 ‰ for *T. quinqueloba*. In agreement with previous studies, it has been established that both species calcify within a narrow temperature range. The secondary calcification occurs before the sinking into the deeper water layers (as a rule into 100-200 m depth) and may vary between the upper 0-50 m and 50-75 m in response to the reproductive cycles.

In the West Spitzbergen Current (80°N) measured isotope values of *N. pachyderma* (s.) and *T. quinqueloba* were out of equilibrium with the surrounding water. A calcification at 2.5 °C higher temperatures was assumed, indicating the advection of planktonic foraminifera from lower latitudes.

The isotope signal of *N. pachyderma* (s.) in plankton tows from the Fram Strait (80°N), showed a good match with surface sediments, where the ^{18}O and ^{13}C values were higher by 0.2 ‰ and 0.3 ‰, respectively.

Contents

1. Introduction	1
1.1 Oceanography of the Study Area.....	2
2. Material and Methods	
2.1 Multinet Samples and Hydrographic Measurements.....	4
2.1.2 Foraminiferal Shell Mass and Stable Isotope Analysis	6
2.1.3 Water Column $^{18}\text{O}_{\text{Eq}}$ and $^{13}\text{C}_{\text{Eq}}$	6
3. Results	
3.1 Labrador Sea: Hydrographic Setting and Total Planktonic Foraminifera Distribution ..	8
3.1.1 Abundance and Shell Size Distribution of <i>N. pachyderma</i> (s.) and <i>T. quinqueloba</i> ..	11
3.1.2 Shell Size, Mass and Stable Isotope Composition of <i>N. pachyderma</i> (s.).....	13
3.2 Greenland Sea: Hydrographic Setting and Total Foraminiferal Distribution along the 75°N-Transect.....	18
3.2.1 Abundance and Shell Size Distribution of <i>N. pachyderma</i> (s.) and <i>T. quinqueloba</i> ..	22
3.3 Fram Strait: Hydrographic Setting and Total Foraminiferal Distribution along the 80°N-Transect.....	24
3.3.1 Abundance and Shell Size Distribution of <i>N. pachyderma</i> (s.) and <i>T. quinqueloba</i> ..	28
3.3.2 Stable Isotope Composition of <i>N. pachyderma</i> (s.) and <i>T. quinqueloba</i>	29
4. Discussion	
4.1 Distribution of Planktonic Foraminifera in the Study Area	34
4.1.1 Species Distribution Pattern.....	34
4.1.2 Absolute Abundance and Depth Distribution of <i>N. pachyderma</i> (s.) and <i>T. quinqueloba</i>	38
4.1.3 Reproductive Cycles.....	43
4.2 Isotopic Composition of <i>N. pachyderma</i> (s.) and <i>T. quinqueloba</i>	51

4.2.1	Effect of Size, Weight and Encrustation on the Stable Isotope Composition of <i>N. pachyderma</i> (s.) and <i>T. quinqueloba</i>	51
4.2.2	The Estimation of Disequilibrium in ^{18}O and ^{13}C	55
4.2.3	Comparison between the Isotope Signal of <i>N. pachyderma</i> (s.) from Plankton Tows and from Surface Sediments in the Fram Strait.....	59
5.	Conclusions	61
6.	References	63
7.	Appendix	70
	Acknowledgments	90

1. Introduction

Planktonic foraminifera are drifting passively in oceanic currents as part of the marine protozoan plankton. The hydrologic conditions in the water masses control the distribution of different species among the currents as well as the stable isotope composition (^{18}O and ^{13}C) of their calcite shells. Based on this, many paleoceanographic studies use the species composition and isotope signal of fossils to determine the temperature, salinity and productivity of the past oceanic surface layer.

In order to interpret foraminiferal data in sediment records, the first calibrations between the surface currents and foraminiferal assemblage in the North Atlantic and Arctic regions were limited to size classes $> 200\ \mu\text{m}$ (Be & Tolderlund, 1971; Stehmann, 1972; Vilks, 1975), resulting in the presentation of a temperature dependent spread pattern of planktonic foraminifera (Be & Tolderlund, 1971). Recent research, which examined smaller size classes, however shows that different development stages and size classes may have a different depth distribution, indicating a lack of correlation between surface temperatures and foraminiferal assemblage (Carstens & Wefer, 1992; Jensen, 1998). Additionally, local influences like ice coverage and surface hydrography may lead to a change of the abundance and depth at which planktonic foraminifera live (Carstens et al., 1997; Volkman, 2000a). Many questions remain concerning the reproduction of planktonic foraminifera at high latitudes, but several findings indicate it to be similar to that of tropical species (Carstens, unpublished data; Volkman, 2000a), being tied to the lunar cycle (Be & Anderson, 1976; Spindler et al., 1979; Almogilabin, 1984; Bijma et al., 1990a). The survey of temporal and spatial variations in the distribution of the dominant species *Neogloboquadrina pachyderma* (sinistral) and *Turborotalita quinqueloba* is the focus of this work. Special emphasis is put on how the vertical, horizontal and size distribution of these species reflect the environmental conditions of their life habitat. The knowledge of these species-specific living and calcification depths hereby gained will primarily be used in the interpretation of the isotope signal from their calcite shells (Emiliani, 1954; Duplessy et al., 1981b; Berger, 1981).

The oxygen isotope composition in the foraminiferal shells is dependent upon calcification temperature and ^{18}O composition of the sea water (Urey, 1947; Epstein et al., 1951). The ^{18}O composition of sea water is determined by salinity (Craig & Gordon, 1965). Therefore the ^{18}O values of foraminiferal shells allow conclusions on temperature, ^{18}O and salinity in the habitat depth of each species. The carbon isotope values of planktonic foraminifera are controlled by the $^{13}\text{C}_{\text{DIC}}$ (Dissolved Inorganic Carbon) in seawater (Berger et al., 1978; Bouvier-Soumagnac & Duplessy, 1985; Spero, 1992). The $^{13}\text{C}_{\text{DIC}}$ is mainly influenced by biological processes and air-sea CO_2 exchange (Broecker & Peng, 1982; Lynch-Stieglitz et al., 1994).

Due to nutrient depletion and preferential C^{12} -uptake (relative to C^{13}) during photosynthesis, the $^{13}C_{DIC}$ values correlate inversely with nutrient concentrations. Because the photosynthetically fixed carbon is decomposed by bacterial activity, the ^{13}C of planktonic foraminifera reflect the nutrient concentrations and ventilation of the surface water.

The isotopic composition of foraminiferal shells in the water column often show a deviation from ^{18}O and ^{13}C which will be expected for inorganic calcite in thermodynamic equilibrium with seawater. This species-specific vital effect (Urey et al., 1951), caused by both ontogenetic development and hydrographic parameters, has been documented several times already for *N. pachyderma* (s.) and *T. quinqueloba* in the high latitude North Atlantic and Arctic Ocean (Kohfeld et al., 1996; Kohfeld, 1998; Bauch et al., 1997, 1999; Simstich, 1999; Volkmann, 2000b). The survey of the ontogenetic component of this vital effect for *N. pachyderma* (s.) and *T. quinqueloba* grouped by size, weight and degree of calcite encrustation is another emphasis of this study.

1.1 Oceanography of the Study Area

This work presents the results of plankton net samples from the Labrador Sea, central Greenland Sea and the Fram Strait. Figure 1 shows the most important surface currents in the study area and the geographic location of the multinet stations.

The surface current system in the survey area is characterized by the thermohaline circulation from the North Atlantic into the Nordic and Labrador Seas. The relatively warm and saline Atlantic water masses are being transported via the North Atlantic Current and the Norwegian Current ($T \sim 6-10^{\circ}C$, $S \sim 35.2$ psu) into the Iceland and Norwegian Seas and via the West Spitzbergen Current ($T \sim 3^{\circ}C$, $S \sim 35.0$ psu) into the Greenland Sea and Fram Strait. A part of the West Spitzbergen Current, which divides into two branches off the Spitzbergen coast, enters the Arctic Ocean as Subpolar Intermediate Water. The second part cools upon meeting the cold and less saline Arctic East Greenland Current ($T \sim -1.5^{\circ}C$, $S \sim 32.0$ psu) and forms a layer beneath the East Greenland Current only to flow back south as the Return Atlantic Current (Quadfasel et al., 1987; Koltermann, 1987).

The East Greenland Current, which flows south along the Greenland shelf, constitutes the western boundary current of an anticyclonic current system dominating the Greenland Sea circulation. A new water mass is the result of the mixing of Atlantic and Polar water masses in the Greenland Sea gyre, named Arctic Intermediate Water ($T < 2^{\circ}C$, $S \sim 34.7-34.9$ psu) due to their location. The differences in temperature and salinity between the Greenland and Norwegian Seas result in the formation of hydrographic fronts in these regions. The blending areas restricted by these fronts are known as domains (Swift, 1986).

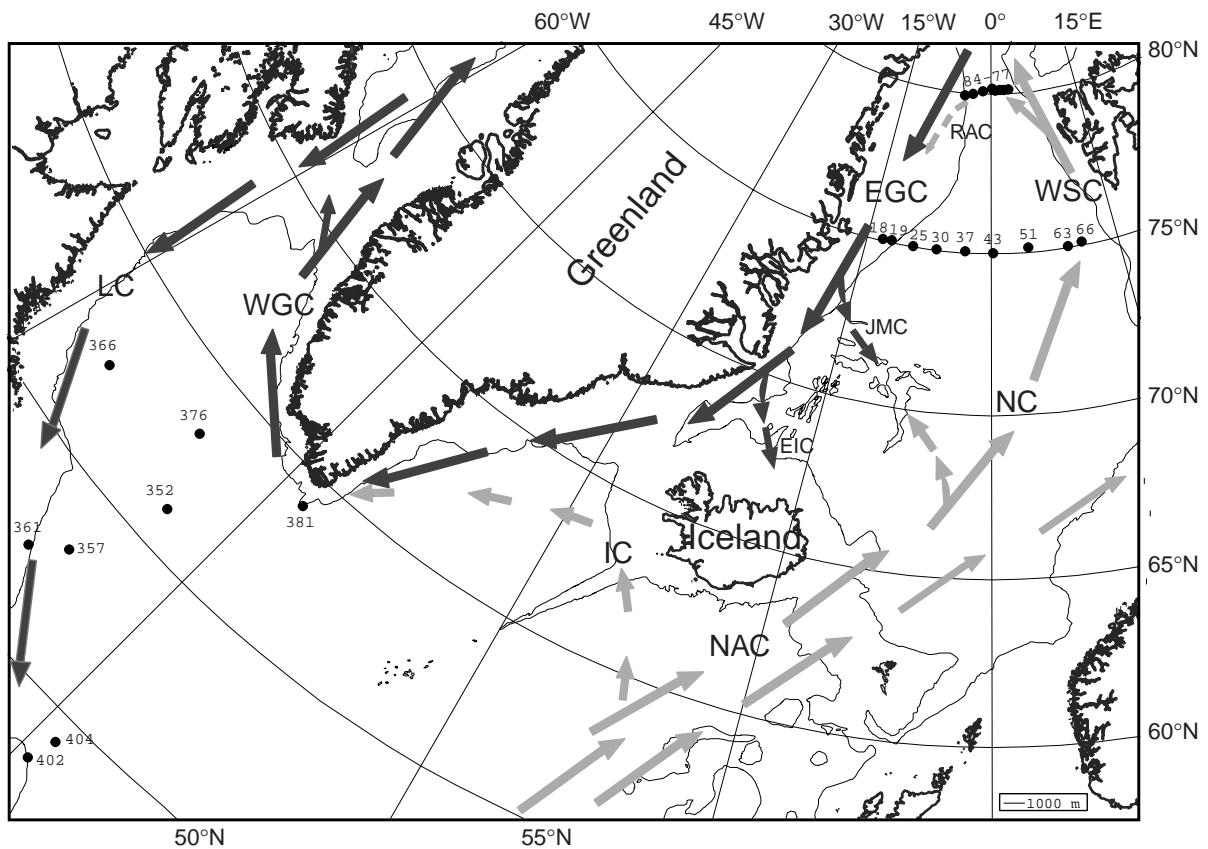


Figure 1: Schematic presentation of the shallow circulation of the investigations area. (●) Locations of the multinets. Dark arrows denote the cold low-salinity currents, light arrows: warm and saline currents. NAC: North Atlantic Current, NC: Norwegian Current, WSC: West Spitzbergen Current, RAC: Return Atlantic Current, EGC: East Greenland Current; JMC: Jan Mayen Current, EIC: East Icelandic Current; IC: Irminger Current; WGC: West Greenland Current; LC: Labrador Current. Modified from Dietrich et al. (1975).

The East Greenland Current turns to a northwesterly direction at the southern tip of the Greenland coast, mixing with the Irminger Current ($T > 5^{\circ}\text{C}$, $S > 35.0$ psu), which is the second branch of the North Atlantic Drift to transport warm and more saline water to the northwest. These two currents form the West Greenland Current ($T \sim 2^{\circ}\text{C}$, $S \sim 31\text{-}34$ psu), reaching into the Davis Strait and Baffin Bay. The West Greenland Current is being compensated in the west of the Labrador Sea by the Labrador Current ($T \sim 0^{\circ}\text{C}$, $S \sim 30\text{-}34$ psu), which flows southward off the Labrador coast. The Labrador Current transports cold and less saline water as far as the Newfoundland area, blending at the Grand Banks with the warm and highly saline waters of the Gulf Current (Lazier, 1973; Lazier & Wright, 1992).

2. Material and Methods

2.1 Multinet Samples and Hydrographic Measurements

The investigated plankton samples were collected using a Hydrobios multinet tow (63 μm mesh size) with depth intervals of 0-50, 50-100, 100-200, 200-300 and 300-500 m. Table 1 lists the positions of the multinet stations taken during the summer months in the course of the following expeditions:

Cruise	Area	Year
Meteor M 39/4	Labrador Sea	1997
Polarstern ARK XV/1	Greenland Sea (75°N)	1999
Polarstern ARK XV/2	Fram Strait (80°N)	1999

During the Polarstern cruise ARK XV/1+2, in addition to the multinet stations, water samples were taken using the CTD rosette from depths of 0, 25, 50, 100, 200, 300, 400 and 500 m for the ^{18}O , ^{13}C and nutrient measurements. The SiO_4 concentrations were determined on board using the photometer (model UV 150-01) according to Koroleff (1976) and were expressed in $\mu\text{M/l}$. In order to determine the chlorophyll *a* concentrations (*chl a*), 1 to 2 litres of water from depths of 0, 25, 50, 75, 100, 130, 160 and 200 m were filtered using a GF/F filter (\varnothing 25 mm) at < 0.3 bar pressure. The filters were stored until the extraction with 90% acetone (8-10 ml) at -20°C . The *chl a* concentrations were measured fluorometrically (fluorometer model AU-10) and expressed in $\mu\text{g/l}$.

The multinet samples were conserved on board using denaturalized 90% ethanol and kept cool (4°C). Before further treatment, the > 500 μm fraction was removed from the samples using a sieve. As a rule, the foraminifera were picked out of the sample by using a glass pipette. Samples with a lot of material were split using a plankton splitter prior to the foraminifera removal process. In order to distinguish between "living" (cytoplasm-full shells) and "dead" (cytoplasm-empty) individuals after drying the samples, the foraminiferal shells were dyed isotope neutral using rose-bengal-seawater solution (1g/100 ml). The samples were then rinsed using distilled water and dried at room temperature for about 24 hours.

The counting and dividing into size classes were done using a ZEISS binocular with an ocular scale at magnification $\times 100$ (interval = 23.2 μm). The species identification was done using the concepts of Kennett & Srinivasan (1983) and Hemleben et al. (1989). The abundance of planktonic foraminifera was calculated as individuals per cubic metre ($\text{Ind}\cdot\text{m}^{-3}$). For this, the number of foraminifera at each depth interval is divided by the filtered water volume.

In order to calculate the filtered water volume, the size of the multinet opening (0.5×0.5 m) was multiplied with the length of the sample interval (m).

Table.1: Multinet sampling locations (Fig.1).

Cruise	Station	Date	Time (UTC)	Latitude	Longitude	Water depth (m)
M 39/4	352	12.07.97	08:30	56°16.5'N	48°41.9'W	3716
	357	14.07.97	04:30	53°26.1'N	50°04.0'W	3533
	361	15.07.97	00:30	52°52.4'N	51°31.8'W	1691
	366	19.07.97	06:40	57°40.1'N	56°32.0'W	3019
	376	23.07.97	18:00	58°30.2'N	50°34.5'W	3552
	381	25.07.97	22:00	59°03.1'N	43°30.1'W	1707
	402	30.07.97	23:45	48°51.4'N	44°38.7'W	1573
	404	31.07.97	07:00	49°27.8'N	44°03.0'W	3845
ARK XV/1	18	11.07.99	07:10	74°59.7'N	12°43.9'W	647
	19	11.07.99	10:00	74°59.9'N	12°33.5'W	647
	25	11.07.99	22:20	75°00.0'N	10°36.0'W	3082
	30	12.07.99	13:20	75°00.1'N	07°23.8'W	3426
	37	13.07.99	13:00	75°00.3'N	03°33.2'W	3353
	43	14.07.99	05:05	75°00.0'N	00°21.4'E	3793
	51	15.07.99	04:50	75°00.9'N	05°08.9'E	3314
	63	16.07.99	09:05	74°59.9'N	10°37.7'E	2545
66	16.07.99	17:15	75°00.4'N	12°33.6'E	2190	
ARK XV/2	77	25.07.99	22:45	80°10.1'N	03°48.3'E	1441
	78	26.07.99	05:35	80°08.7'N	02°53.2'E	1992
	79	26.07.99	10:35	80°09.6'N	02°00.8'E	2016
	80	26.07.99	15:10	80°08.5'N	01°05.7'E	2854
	81	26.07.99	21:35	80°11.9'N	00°19.6'E	3000
	82	27.07.99	05:00	80°06.4'N	01°28.8'W	2848
	83	27.07.99	16:05	79°59.5'N	03°31.3'W	2290
	84	27.07.99	22:55	79°56.0'N	05°06.1'W	1150

Biometric analyses of the species *N. pachyderma* (s.) and *T. quinqueloba* were done with a ZEISS binocular at max. $\times 200$ magnification (interval = 11.4 μm), measuring in each case the longest diameter on the umbilical side of the shells. For each specimen the existence of a kummerform chamber and the degree of calcification was noted. The results are presented as the relative frequency. In order to describe the size distribution, the arithmetic mean, the standard deviation and the standard error are presented as well. The deviation from the Gaussian distribution and significance of the results was carried out through a variance ranking analysis by the Kruskal-Wallis method using the statistic program Stat View 4.5.

2.1.2 Foraminiferal Shell Mass and Stable Isotope Analysis

The weight of *N. pachyderma* (s.) sampled in the Labrador Sea was determined using an ultra precision scale (Sartorius Supermicro S4, precision: +/- 0.1 µm). At stations with sufficient material (st. 361, 402 (0-50 m)), the shells were divided into different degrees of calcification: nonencrusted, encrusted and heavily encrusted and classified according to size. Several shells of one calcification and size class were weighed together in order to calculate the average weight per shell. Specimens >250 µm were weighed individually.

Following the biometric analyses, *N. pachyderma* (s.) and *T. quinqueloba* were examined with regard to stable oxygen and carbon isotopes. Prior to isotope analyses, the foraminiferal shells were roasted under vacuum at 200°C for one hour in order to oxidize of organic substance. Dependent on the shell size, 2-50 specimens per size class were picked for the isotope measurement. The stable oxygen and carbon isotopes were measured using a MAT 251 Finnigan mass spectrometer (Dr. H. Erlenkeuser, Leibniz Labor, University of Kiel) and are given in the conventional notation (‰ PDB). The analytical precision for ¹⁸O was 0.08 ‰ and 0.05 ‰ for ¹³C. This was achieved at a carbonate mass of 7 µg CaCO₃ (Dr. H. Erlenkeuser, pers. communication).

The stable isotope analysis of water samples (¹⁸O_w and ¹³C_{DIC}) for the expedition ARK XV/2 was carried out at the Leibniz Labor (Dr. H. Erlenkeuser). The analysis of water samples was done using a MAT 251 mass spectrometer. For a detailed method description, see Erlenkeuser et al. (1999). The accuracy was at 0.07 ‰ for ¹⁸O_w and 0.05 ‰ for ¹³C_{DIC}.

For the Labrador Sea data (M 39/4), the ¹⁸O values of the sea water were predicted using the ¹⁸O_w/salinity relationship of Wu & Hillaire-Marcel (1994):

$$^{18}\text{O}_{\text{w (V-SMOW)}} = -17.8 + 0.51 * \text{S}; r^2 = 0.96 \quad (1)$$

In order to predict the ¹³C_{DIC} values of the examined stations, the relationship between PO₄ concentrations and ¹³C_{DIC} was used:

$$^{13}\text{C}_{\text{DIC}} = 1.93 - 1.02 * (\text{PO}_4); r^2 = 0.91, n = 30 \quad (2)$$

This relationship was determined for several stations in the Labrador Sea using the measured ¹³C_{DIC} (Dr. H. Erlenkeuser, Leibniz Labor) and PO₄ concentrations.

2.1.3. Water Column δ¹⁸O_{Eq} and δ¹³C_{Eq}

The oxygen equilibrium calcite values were calculated according to O'Neil et al. (1969) and

Shackleton (1974):

$$^{18}\text{O}_{\text{Eq}} = [21.9 - 3.16 * (31.061 + T)^{0.5}] + ^{18}\text{O}_{\text{w}} \quad (3)$$

The conversion factor between $^{18}\text{O}_{\text{w}}$ from the V-SMOW to the V-PDB scale is according to Bemis et al. (1998):

$$^{18}\text{O}_{\text{w(PDB)}} = 0.9998 * ^{18}\text{O}_{\text{w(V-SMOW)}} - 0.2 \text{‰} \quad (4)$$

The ^{13}C of planktonic foraminifera was compared with the ^{13}C of inorganic calcite formed in equilibrium with seawater. According to Romanek et al. (1992), the inorganic calcite in equilibrium to the seawater ($^{13}\text{C}_{\text{Eq}}$) is 1‰ heavier than $^{13}\text{C}_{\text{DIC}}$:

$$^{13}\text{C}_{\text{Eq}} = ^{13}\text{C}_{\text{DIC}} + 1.0 \text{‰} (\pm 0.2 \text{‰}) \quad (5)$$

3. Results

The following chapters will give an overview of the hydrographic setting as well as the foraminiferal composition in different current regimes. Afterwards, the horizontal, vertical and size distribution of *N. pachyderma* (s.) and *T. quinqueloba* will be presented, before the results of the examination of stable isotopes will be portrayed.

3.1. Labrador Sea: Hydrographic Setting and Total Foraminiferal Distribution

The examined eight stations (Table 1) were located in different current regimes of the Labrador Sea (Figure 1), which were ice free during the sampling period. Despite different locations, most of the stations showed slight differences regarding temperature and salinity in 0 to 500 m (Figure 2a).

Stations located in the Labrador Current (st. 361, 366, 402) showed low salinities, ranged from 33.8 to 34.8 psu and the lowest temperatures (3.2-7.6°C), except for the surface temperature at station 402 (9.8°C), which was due to summer warming. Higher salinities (34.5-34.9 psu) and temperatures (3.1-8.6°C) than in the Labrador Current were found in the Convection Area of the Labrador Sea (st. 352, 376) and at station 357 (S=34.3-34.9 psu, T=3.2-9.5°C), which is a transitional station. The highest salinities (34.8-35.0 psu) and relatively high temperatures (4.3-8.5°C) were found at station 381, which was located in an area where the East Greenland Current mixes with the Irminger Current, showing the properties of the Atlantic water. The highest temperatures (5.5-12.7°C) were found at station 404. This station was located in the North Atlantic Current and was characterized by large vertical gradients in temperature and salinity. The salinity, which was very low at the surface (33.5 psu), varied between 34.8-35.4 psu below 50 m depth.

The base of the thermocline (according to Hastenrath & Merle, 1987) was usually located at 100 m depth. At stations 352 and 402 the base was already at 50 m depth (Figure 2a).

The nutrient concentrations (Figure 2b) showed relatively large vertical gradients and ranged from 0.1 to 1.2 $\mu\text{MPO}_4/\text{l}$, from 0 to 17 $\mu\text{MNO}_3/\text{l}$ and from 0.3 to 11.3 $\mu\text{MSiO}_4/\text{l}$ in 0-500 m. Stations 352, 357, 381 and 402 showed higher NO_3 concentrations in the upper 0-50 m (6.9-8.0 $\mu\text{M}/\text{l}$), than stations 361, 366, 376 and 404 with a maximum of 4.6 $\mu\text{MNO}_3/\text{l}$. Higher SiO_4 concentrations were found at stations 352, 357 (4.2 and 4.8 $\mu\text{M}/\text{l}$), while the silicate concentrations at other stations ranged from 1.4 to 2.5 $\mu\text{M}/\text{l}$.

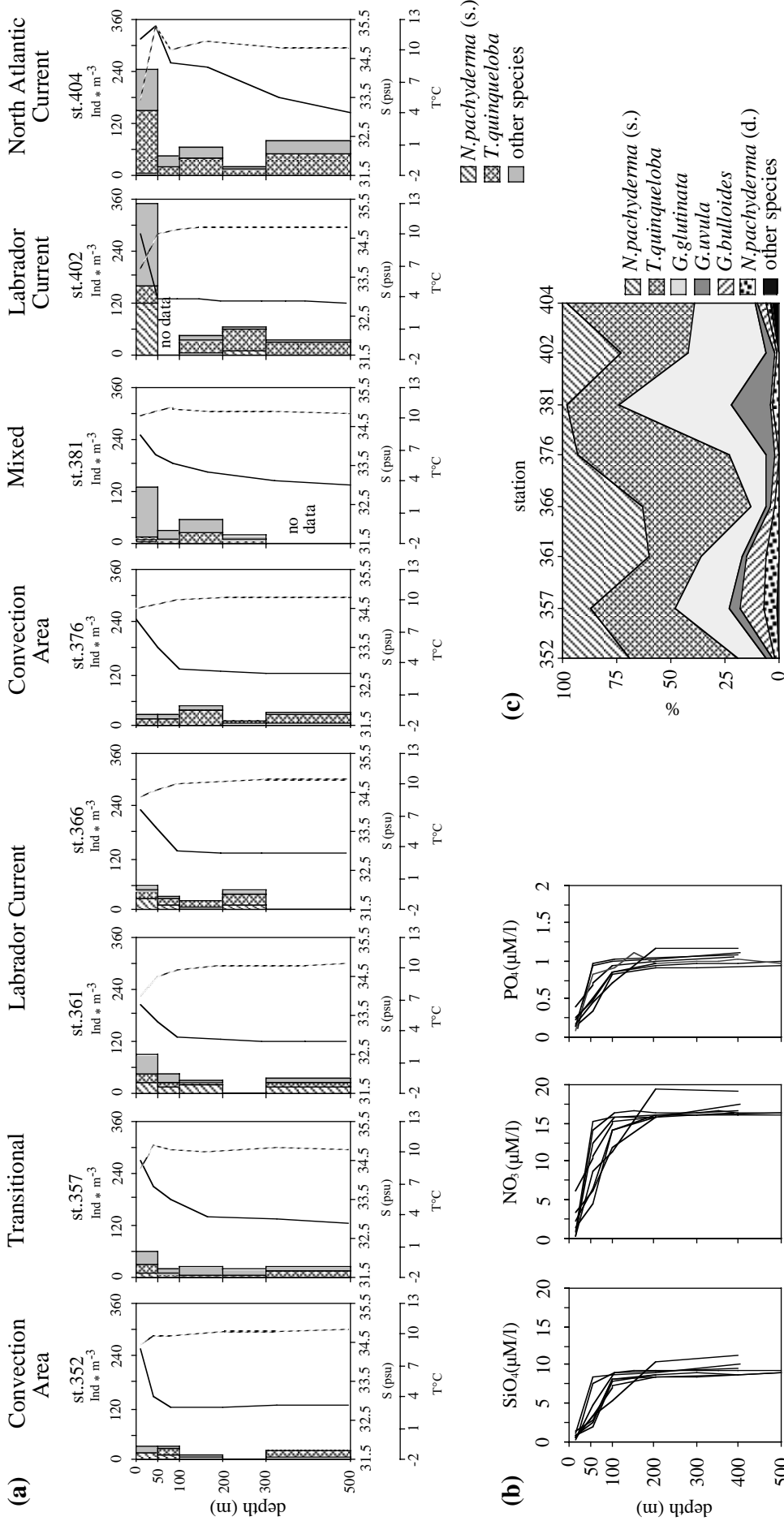


Figure 2: (a) Depth distribution of absolute foraminiferal abundance (bars), temperature (solid line) and salinity (dotted line) in the Labrador Sea (cruise M 39/4). (b) Concentrations of SiO_4 , NO_3 and PO_4 (Maiten, 1997) for the multinet stations used in this study. (c) Average foraminiferal composition in the 0 to 500 m of the water column.

Results

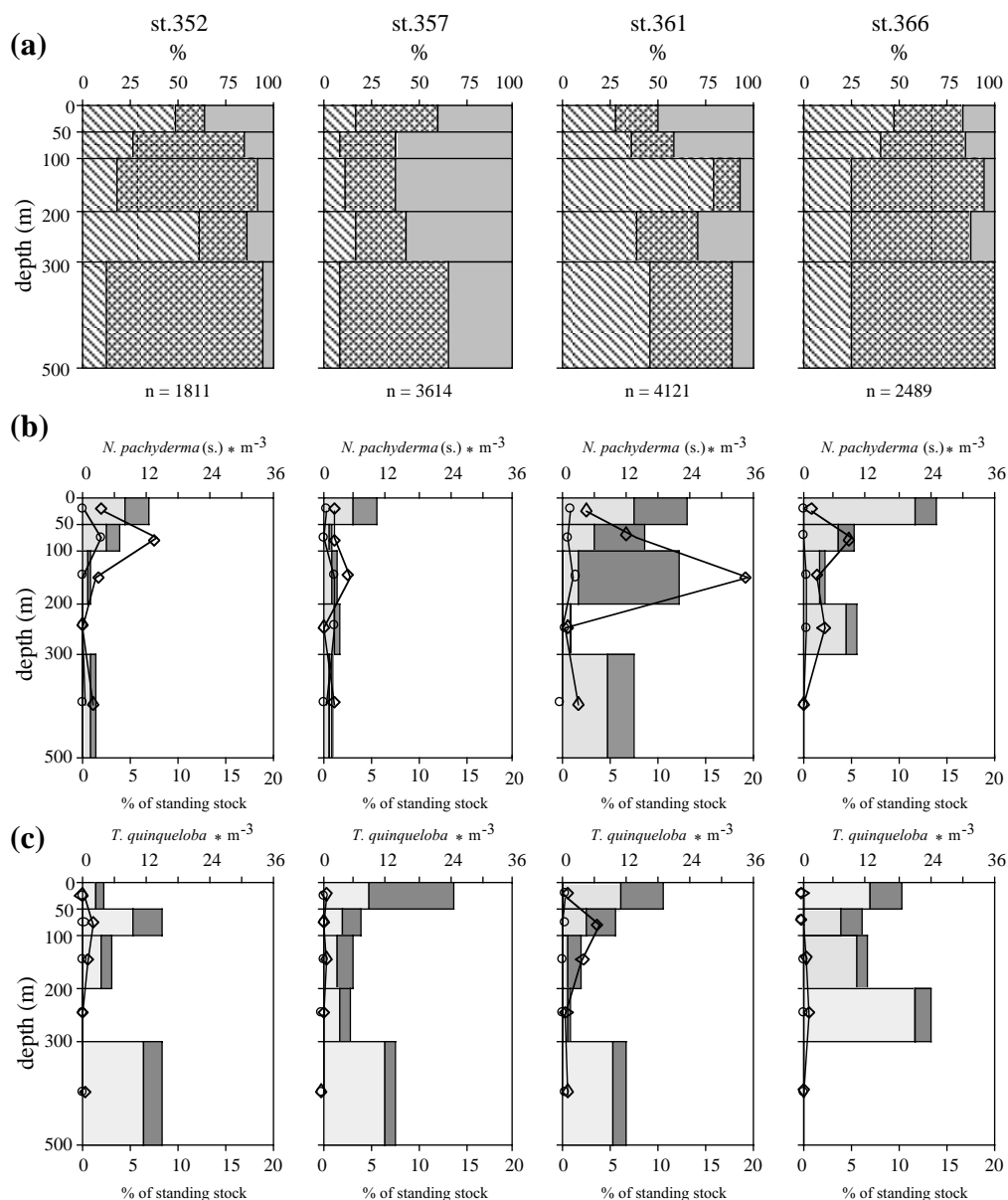


Figure 3: Depth distribution: (a) relative abundance of *N. pachyderma* (s.), *T. quinqueloba* and other species of planktonic foraminifera (per depth interval) in 0-500 m of the water column. (b-c) absolute abundance of *N. pachyderma* (s.) and *T. quinqueloba* (note different scales) and proportion of individuals with reproductive characteristics, given as % of standing stock. For further explanations see legend (page 11).

The total foraminiferal abundance ranges from 0.2 to 356 $\text{Ind} \cdot \text{m}^{-3}$ in 0-500 m (Figure 2a), showing maximum abundances between 123 and 356 $\text{Ind} \cdot \text{m}^{-3}$ in upper 0-50 m at stations 381, 402 and 404. Out of the ten identified foraminiferal taxa: left and right-coiling *N. pachyderma*, *T. quinqueloba*, *G. bulloides*, *G. glutinata*, *G. uvula*, *G. inflata*, *O. riedeli*, *G. scitula* and *G. ruber*, only six species are present at all stations (Figure 2c). Most of the stations (352, 357, 366, 376 and 404) were dominated by *T. quinqueloba* with a relative abundance between 38-70%. *G. glutinata* was relatively abundant at stations 402 and 381 with 37 and 52%, respectively. *N. pachyderma* (s.) was the dominant species at station 361 and accounted for 40% of the

Results

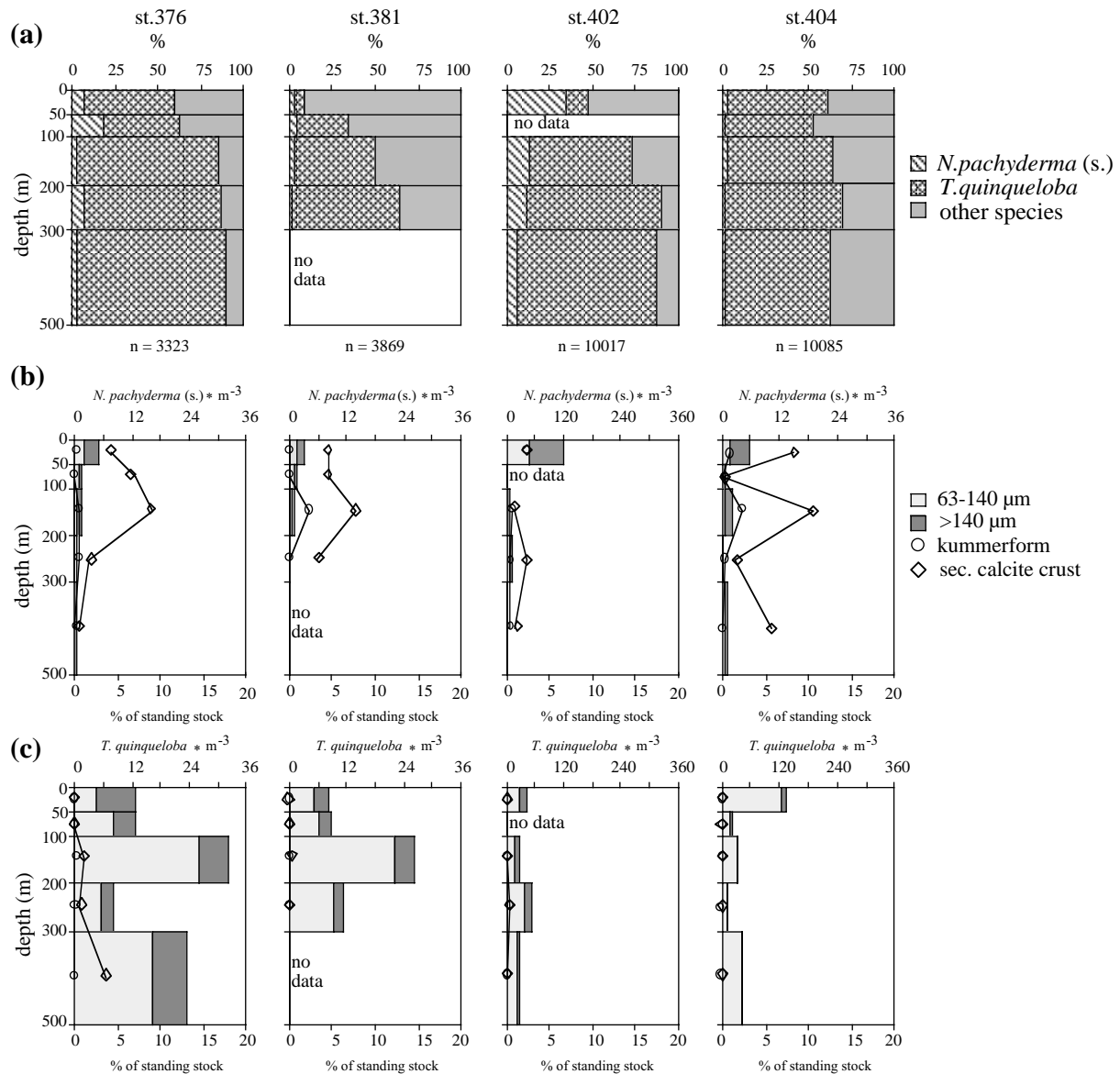


Figure 3: Continued.

foraminiferal abundance. The highest relative abundance of *N. pachyderma* (d.) ~6 % and *G. bulloides* (9 and 11 %) was found at stations 361 and 357, at the other stations both species showed lower abundances between 2 and 4 %. *G. uvula* accounted for a maximum of 18 % at station 381 and showed relatively low abundances (1-5 %) at other stations.

3.1.1 Abundance and Shell Size Distribution of *N. pachyderma* (s.) and *T. quinqueloba*

It is obvious from Figure 3 that *N. pachyderma* (s.) and *T. quinqueloba* each showed the different depth distribution patterns. In order to be able to compare the distribution of both species better, their abundance in 0 to 200 m was viewed. The abundance of *N. pachyderma* (s.) varied between 0.7 and 121 Ind*m⁻³ in 0-200 m (Figure 3b). This species occurred most abun-

dantly in the upper 0-50 m. Compared to *N. pachyderma* (s.), *T. quinqueloba* had a more variable depth distribution with maxima in 0-200 m (Figure 3c) and showed slightly higher abundances between 3.6 and 131 Ind*m⁻³. At stations 366 and 402 the abundance maximum of this species was found below 200 m depth.

The changes in abundance of *N. pachyderma* (s.) were inversely correlated with increasing salinity ($r^2 = 0.5$, $n = 38$), showing the maxima at stations 361, 366 and 402. The best correlations between the abundance of *N. pachyderma* (s.) and average salinity were found in the 0-50 m and 50-100 m depth intervals. In contrast, the increasing abundance of *T. quinqueloba* was positively correlated with temperature ($r^2 = 0.4$, $n = 38$). The highest abundance of this species was found at station 404 (0-50 m) at an average temperature of ~12°C. The abundance of dead *T. quinqueloba* (empty shells) rose however with increasing total abundance ($r^2 = 0.9$).

The highest abundances of *N. pachyderma* (s.) with reproductive characteristics (secondary calcite crust and kummerform chamber) were found between 0 and 300 m (Figure 3b). Most encrusted individuals of this species occurred at stations 361 (19 %) and 404 (11 %), while the abundance of kummerforms increased with increasing total abundance ($r^2 = 0.9$, $n = 38$), showing the maximum of 3 % at station 402. The maximum proportion of encrusted *T. quinqueloba* (4 %) was found at stations 361 (100-200 m) and 376 (300-500 m), whereas the abundance of kummerforms reached a maximum of 0.4 % at station 402 (200-300 m). The maxima of *T. quinqueloba* with reproductive characteristics varied irregularly over the 0 to 500 m at other stations (Figure 3c).

Changes in the shell size of *N. pachyderma* (s.) and *T. quinqueloba* are uncorrelated with each other or with variations in the total abundance of each species. The mean shell size of *N. pachyderma* (s.) varied between 110 and 230 µm (Figure 4a). In comparison to stations 352 and 357, where shell size was approximately 140-150 µm, a strong increase in shell size (180-230 µm) occurred at station 361 in 50-100 m depth. After three days at station 366, the size of *N. pachyderma* (s.) strongly decreased and reached the minimum of < 130 µm. At stations 376 and 381, the larger shells were found in 100-200 m depth, ranging from 180 to 190 µm. At the last two stations 402 and 404, relatively large specimens (160-180 µm) were found throughout the water column (exception: station 404, 300-500 m).

The mean shell size of *T. quinqueloba* was between 90 and 150 µm (Figure 4b), showing less variations compared to *N. pachyderma* (s.). The largest shells of about 150 µm were found at stations 357, 376 (0-50 m) and 361 (100-200 m). At stations 352, 366, 376, 381 and 402 the specimens size varied between 100 and 130 µm, while at the last station 404, the smallest individuals of *T. quinqueloba* were established, having a maximum diameter of 110 µm.

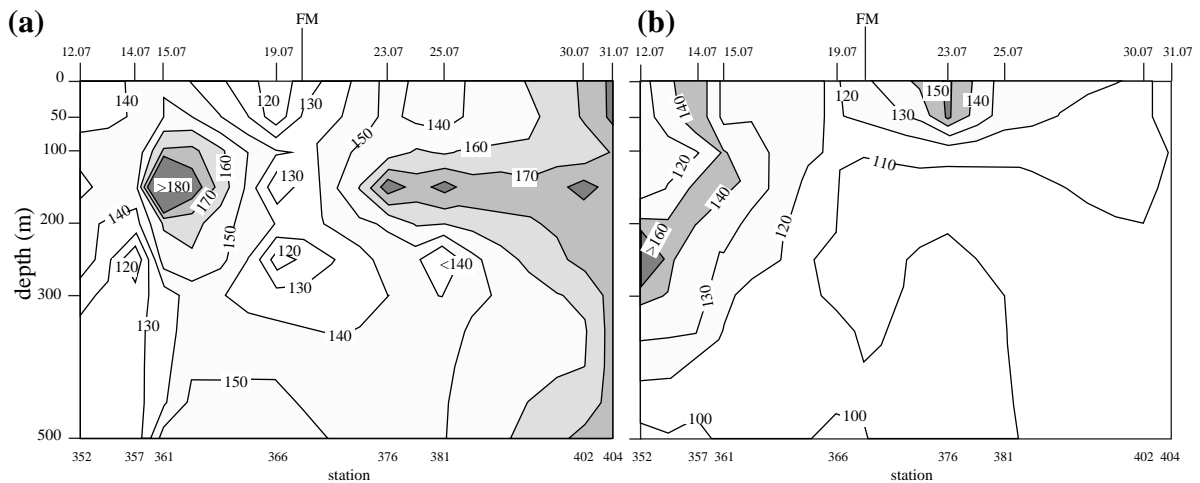


Figure 4: Mean shell size distribution of (a) *N. pachyderma* (s.) and (b) *T. quinqueloba* versus depth. Upper axis denotes the sampling date, FM: full moon; lower axis gives the station numbers. For sampling time see Table 1.

3.1.2. Shell Size, Mass and Stable Isotope Composition of *N. pachyderma* (s.)

At the examined stations 361 and 402 (0-50 m) (Chapter 2.1.2), the relationship between shell size and weight (Table 2) of the three different calcification groups of *N. pachyderma* (s.) can be described as follows:

$$\text{nonencrusted:} \quad \text{shell mass } (\mu\text{g}) = 0.0001 * (\text{size})^2 - 0.0221 * \text{size} + 1.66 \quad (6)$$

$$\text{encrusted:} \quad \text{shell mass } (\mu\text{g}) = 0.0001 * (\text{size})^2 + 0.0007 * \text{size} - 1.16 \quad (7)$$

$$\text{heavily encrusted:} \quad \text{shell mass } (\mu\text{g}) = 0.056 * \text{size} - 7.53 \quad (8)$$

The shell mass of the nonencrusted individuals does not change significantly with depth (Figure 5).

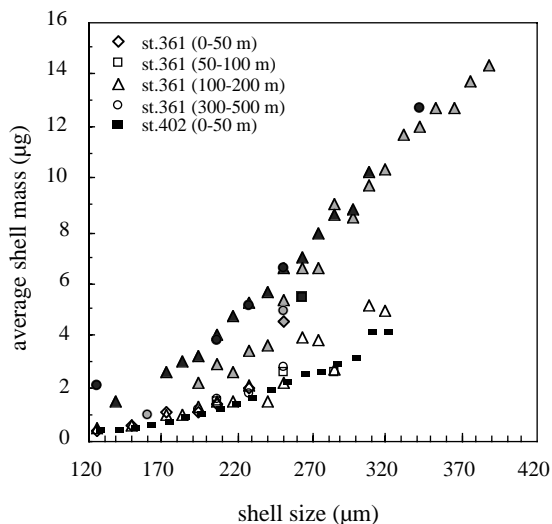


Figure 5: Shell size versus average shell mass at different degrees of calcification (Table 2); Station 361: non-filled symbols represent non-encrusted, gray-filled: encrusted and black-filled: heavily encrusted shells; At station 402, nonencrusted shells were measured. For further explanations see legend.

Results

Table 2: Shell size and mass of nonencrusted, encrusted and heavily encrusted *N. pachyderma* (s.) measured on samples from stations 361 and 402 (0-50 m) in the Labrador Sea.

shell size (μm)	shell mass (μg)												
	nonencrusted					encrusted				heavily encrusted			
	st. 402		st. 361			st. 402		st. 361		st. 402		st. 361	
	0-50 m	0-50 m	50-100 m	100-200 m	300-500 m	0-50 m	50-100 m	100-200 m	300-500 m	0-50 m	50-100 m	100-200 m	300-500 m
125	0.4	0.4	-	0.5	-	-	-	-	-	-	-	-	2.1
137	0.4	-	-	-	-	-	-	-	-	-	-	1.5	-
148	0.5	0.6	-	0.6	-	-	-	-	-	-	-	-	-
160	0.6	-	-	-	-	-	0.6	-	1.0	-	-	-	-
171	0.7	1.1	-	1	-	1.2	-	-	-	-	-	2.6	-
182	0.9	-	-	1	-	-	-	1.5	-	-	-	3.1	-
194	1.0	1.1	-	1.3	1.2	-	2.0	2.2	-	-	-	3.3	-
205	1.2	1.4	1.5	1.5	1.6	-	-	3.0	1.6	-	-	4.1	3.9
217	1.5	-	-	1.5	-	-	-	2.7	-	-	3.0	4.8	-
228	1.7	2	-	2.1	1.8	1.8	-	3.5	-	-	-	5.3	5.2
239	1.9	-	-	1.5	-	2.7	-	3.7	2.5	4.2	3.0	5.7	-
251	2.2	-	2.6	2.2	2.9	4.6	-	5.4	5.0	-	-	6.6	6.6
262	2.5	-	-	4	-	-	-	6.6	-	-	5.5	7.0	-
274	2.6	-	-	3.9	-	-	-	6.6	-	-	-	7.9	-
285	3.0	-	2.7	2.8	-	-	-	9.1	-	-	-	8.7	-
296	3.2	-	-	-	-	-	-	8.6	-	-	-	8.9	-
308	4.2	-	-	5.2	-	-	-	9.8	-	-	-	10.3	-
319	4.2	-	-	5	-	-	-	10.4	-	-	-	-	-
331	-	-	-	-	-	-	-	11.7	-	-	-	-	-
342	-	-	-	-	-	-	-	12.0	-	-	-	-	-
353	-	-	-	-	-	-	-	12.7	-	-	-	-	-
365	-	-	-	-	-	-	-	12.7	-	-	-	-	-
376	-	-	-	-	-	-	-	13.8	-	-	-	-	-
388	-	-	-	-	-	-	-	14.4	-	-	-	-	-

The mass of nonencrusted shells (considered as primary calcite) accounted for 37 % of the total shell mass of heavily encrusted specimens. No significant differences in weight were found between encrusted and heavily encrusted shells $>280 \mu\text{m}$, while in the size fraction $<280 \mu\text{m}$, the mass of encrusted specimens accounted for ~ 35 % of the heavily encrusted shells. In spite of these differences between both calcification groups ($<280 \mu\text{m}$), no significant variations in ^{18}O and ^{13}C were found as a function of the shell mass (Figure 5 and 6). The findings concerning encrusted and heavily encrusted *N. pachyderma* (s.) will therefore be jointly presented under the term "encrusted".

The ^{18}O values of encrusted shells showed no significant changes as a function of the shell size (Figure 6b-c, Table 3) and mass. In contrast, the ^{18}O values of nonencrusted shells showed a slight increase with increasing shell size and mass (Figure 6a). The ^{18}O rose with increasing size on average by 0.26 ‰ (station 361, 0-200 m) and 0.41 ‰ (station 402, 0-50 m). Between 300 and 500 m (station 361) however no shell size and mass dependent changes in ^{18}O were found. At both stations, the ^{18}O of encrusted *N. pachyderma* (s.) was within the range of $^{18}\text{O}_{\text{Eq}}$ values predicted for the upper 0-50 m (Equation 3). In the upper 0-200 m, the ^{18}O values of nonencrusted and encrusted *N. pachyderma* (s.) increased slightly with depth at station 361 (Figure 7). At this station, the nonencrusted and encrusted *N. pachyderma* (s.) in

Results

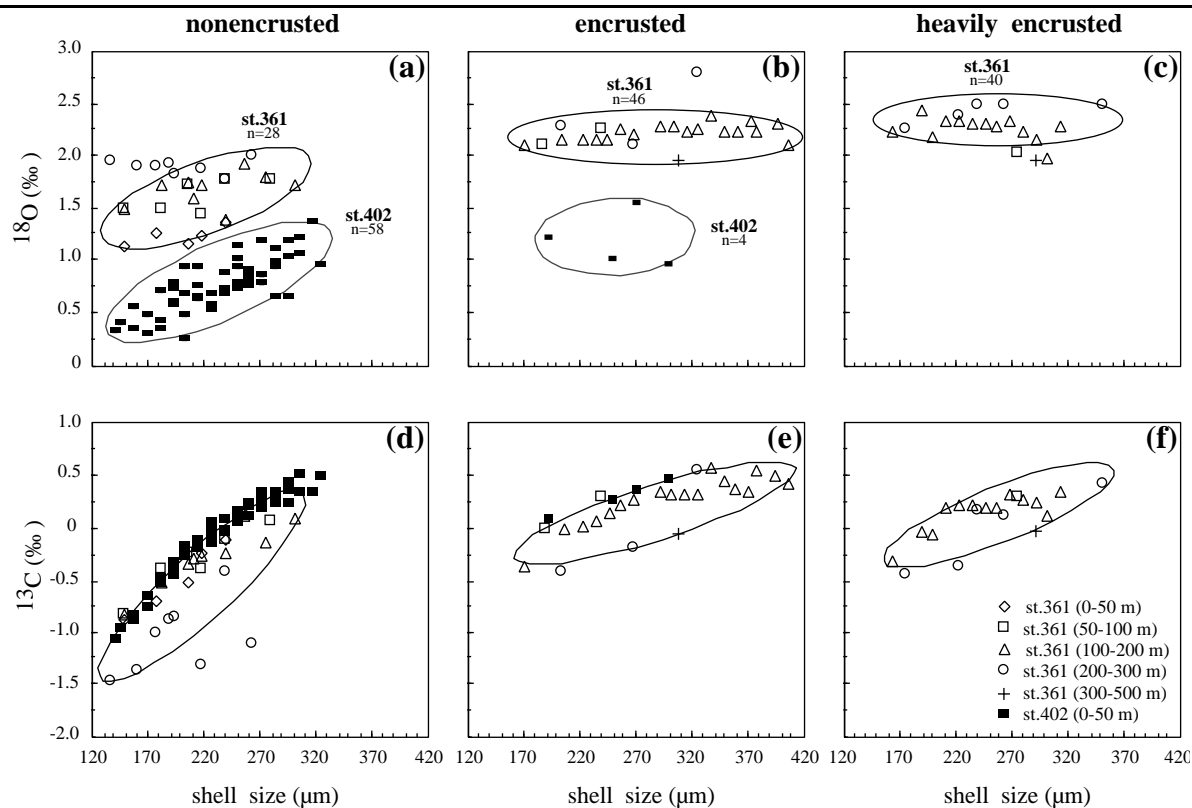


Figure 6: Size effect on the ^{18}O (a-c) and ^{13}C (d-f) at different degrees of calcite encrustation of *N. pachyderma* (s.). Note different scales. Station 361: mean values of encrusted and heavily encrusted are presented.

the upper 200 m were on average 1.1 ± 0.2 and 0.7 ± 0.1 ‰, respectively, depleted in ^{18}O compared to predicted $^{18}\text{O}_{\text{Eq}}$ (Figure 7). The difference between encrusted and nonencrusted shells below 50 m was approximately 0.6 ± 0.1 ‰. Similar to station 361, the mean ^{18}O values of nonencrusted and encrusted shells at station 402 (0-50 m) were lighter than $^{18}\text{O}_{\text{Eq}}$ values by 1.1 ± 0.3 ‰ and 0.7 ± 0.3 ‰. The ^{18}O between nonencrusted and encrusted shells was at ~ 0.4 ‰ there.

The ^{13}C values of the three examined calcification groups rose with increasing shell size and mass (Figure 6d-f). Nonencrusted shells at stations 402 (0-50 m) and 361 (0-200 m) increased in ^{13}C with increasing size on average by 1.54 ‰ and 0.86 ‰, respectively. At station 361, the encrusted *N. pachyderma* (s.) varied in ^{13}C approximately by 0.83 ‰ as a function of size. For station 361, the size/ ^{13}C relationship of all examined calcification groups can be described as follows:

$$^{13}\text{C} = - 7.58 + 3.15 * \text{Log}(\text{size}); r^2 = 0.6, n = 113 \quad (9)$$

In the upper 0-200 m, the ^{13}C values of *N. pachyderma* (s.) at station 361 showed a slight variation with depth. The mean ^{13}C values of nonencrusted and encrusted shells were lighter than the predicted $^{13}\text{C}_{\text{DIC}}$ by 1.7 ± 0.3 ‰ (~ 200 μm) and 1.0 ± 0.02 ‰ (~ 230 μm) (Figure 7).

Results

Table 3: Shell size and stable isotope data of *N. pachyderma* (s.) measured at stations 361 (all depth intervals) and 402 (0-50 m). Mean value \pm standard deviation (*n*);

station	depth (m)	shell size (μm)	^{18}O (‰)			^{13}C (‰)			
			nonencrusted	encrusted	heavily encrusted	nonencrusted	encrusted	heavily encrusted	
361	0-50	148	1.14	-	-	-0.88	-	-	
		177	1.28	-	-	-0.70	-	-	
		205	1.18	-	-	-0.53	-	-	
		217	1.24	-	-	-0.25	-	-	
		239	1.38	-	-	-0.12	-	-	
	50-100	148	1.49	-	-	-0.83	-	-	
		182	1.49	-	-	-0.40	-	-	
		188	-	2.12	-	-	-0.02	-	
		205	1.74	-	-	-0.24	-	-	
		217	1.45	-	-	-0.41	-	-	
		239	1.77	2.26	-	-0.12	0.29	-	
		274	-	-	2.04	-	-	0.30	
		280	1.78	-	-	0.07	-	-	
		100-200	148	1.50	-	-	-0.84	-	-
			162	-	-	2.24	-	-	-0.33
			171	-	2.11	-	-	-0.37	-
			182	1.72	-	-	-0.52	-	-
			188	-	-	2.45	-	-	-0.03
	200		-	-	2.19	-	-	-0.08	
	205		1.75	2.17	-	-0.36	-0.02	-	
	211		1.61	-	2.35 \pm 0.11 (2)	-0.30	-	0.18 \pm 0.03	
	217		1.72	-	-	-0.28	-	-	
	222		-	2.17	2.35 \pm 0.12 (5)	-	0.02	0.20 \pm 0.12	
	234		-	2.16	2.31 \pm 0.11 (5)	-	0.05	0.21 \pm 0.15	
	239		1.41	-	-	-0.24	-	-	
	245		-	2.17 \pm 0.08 (2)	2.31 \pm 0.06 (4)	-	0.14 \pm 0.02	0.20 \pm 0.11	
	257		1.93	2.26	2.28 \pm 0.02 (3)	0.11	0.21	0.20 \pm 0.07	
	268		-	2.21 \pm 0.14 (2)	2.35 \pm 0.05 (3)	-	0.28 \pm 0.01	0.31 \pm 0.11	
	274		1.80	-	-	-0.15	-	-	
	279		-	-	2.25 \pm 0.07 (2)	-	-	0.26 \pm 0.01	
	291		-	2.30 \pm 0.05 (2)	2.17 \pm 0.01 (3)	-	0.33 \pm 0.04	0.24 \pm 0.15	
	302		1.74	2.28 \pm 0.11 (5)	1.99 \pm 0.21 (2)	0.09	0.31 \pm 0.06	0.11 \pm 0.07	
	314		-	2.24 \pm 0.08 (5)	2.29	-	0.32 \pm 0.11	0.34	
	325		-	2.27 \pm 0.07 (2)	-	-	0.31 \pm 0.14	-	
	336		-	2.38	-	-	0.56	-	
	348		-	2.25 \pm 0.11 (2)	-	-	0.44 \pm 0.01	-	
	359		-	2.24 \pm 0.23 (4)	-	-	0.35 \pm 0.06	-	
	371		-	2.35 \pm 0.27 (5)	-	-	0.33 \pm 0.15	-	
	376		-	2.25	-	-	0.55	-	
	393		-	2.31 \pm 0.12 (3)	-	-	0.48 \pm 0.03	-	
	405	-	2.12	-	-	0.42	-		
	200-300	291	-	-	1.97	-	-	-0.05	
		308	-	1.95	-	-	-0.07	-	
	300-500	137	1.97	-	-	-1.46	-	-	
		160	1.91	-	-	-1.36	-	-	
		174	-	-	2.26	-	-	-0.45	
		177	1.90	-	-	-1.00	-	-	
		188	1.94	-	-	-0.89	-	-	
		194	1.84	-	-	-0.86	-	-	
		204	-	2.28	-	-	-0.43	-	
217		1.88	-	-	-1.32	-	-		
222		-	-	2.39	-	-	-0.37		
239		1.77	-	2.49	-0.43	-	0.15		
262		2.00	-	2.48	-1.11	-	0.12		
268		-	2.12	-	-	-0.19	-		
325		-	2.79	-	-	0.55	-		
351		-	-	2.48	-	-	0.41		
402		0-50	137	0.32	-	-	-1.05	-	-
	143		0.40	-	-	-0.96	-	-	
	154		0.46 \pm 0.16 (2)	-	-	-0.85 \pm 0.04	-	-	
	165		0.39 \pm 0.13	-	-	-0.71 \pm 0.07	-	-	
	177		0.50 \pm 0.18 (3)	-	-	-0.49 \pm 0.03	-	-	
	188		0.68 \pm 0.10 (4)	1.21	-	-0.38 \pm 0.06	0.08	-	
	200		0.60 \pm 0.29 (4)	-	-	-0.23 \pm 0.05	-	-	
	211		0.76 \pm 0.14 (4)	-	-	-0.16 \pm 0.03	-	-	
	222		0.59 \pm 0.05 (5)	-	-	-0.04 \pm 0.08	-	-	
	234		0.75 \pm 0.08 (5)	-	-	0 \pm 0.05	-	-	
	245		0.93 \pm 0.16 (5)	1.02	-	0.12 \pm 0.04	0.27	-	
	257		0.84 \pm 0.07 (5)	-	-	0.17 \pm 0.06	-	-	
	268		0.90 \pm 0.17 (5)	1.55	-	0.27 \pm 0.06	0.37	-	
	279		0.88 \pm 0.20 (5)	-	-	0.27 \pm 0.04	-	-	
	291		0.96 \pm 0.28 (3)	-	-	0.35 \pm 0.10	-	-	
	296		-	0.97	-	-	0.46	-	
	302		1.14 \pm 0.10 (2)	-	-	0.42 \pm 0.13	-	-	
	314		1.38	-	-	0.35	-	-	
319	0.96	-	-	0.49	-	-			

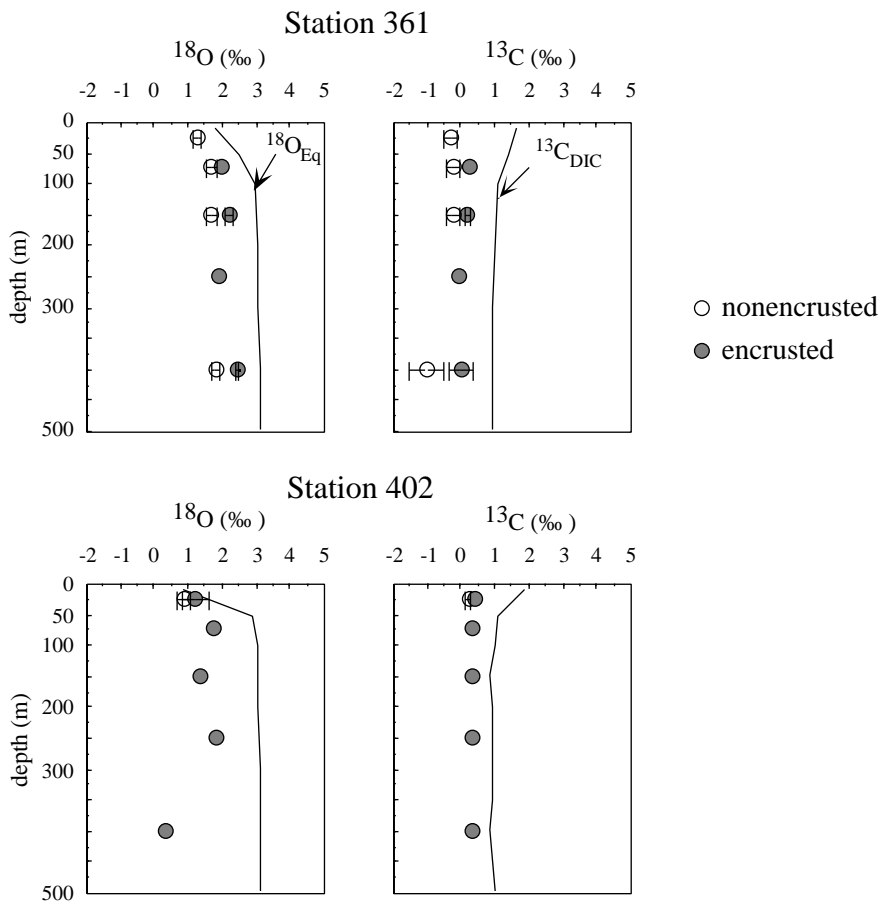


Figure 7: Depth distribution of ^{18}O , ^{13}C (circles) of *N. pachyderma* (s.) and $^{18}\text{O}_{\text{Eq}}$, $^{13}\text{C}_{\text{DIC}}$ (solid line) Station 402: below 50 m depth isotope data from Bauch 1999.

Nonencrusted shells between 50 and 200 m depth were depleted in ^{13}C by 0.6 ± 0.1 ‰ compared to encrusted shells. At station 402 (0-50 m), the nonencrusted specimens with an average diameter of 228 ± 60 μm were 1.6 ± 0.5 ‰ lighter than predicted $^{13}\text{C}_{\text{DIC}}$, whereas the encrusted shells (250 ± 45 μm) were 1.2 ± 0.2 ‰ lower in ^{13}C in comparison to $^{13}\text{C}_{\text{DIC}}$. The observed ^{13}C between nonencrusted and encrusted shells was ~ 0.4 ‰.

3.2. Greenland Sea: Hydrographic Setting and Total Foraminiferal Distribution along the 75°N-Transect

In the Greenland Sea, which was ice free in the sampling period, three surface water masses can be subdivided: Polar Water (East Greenland Current), Arctic Water (Greenland Arctic Intermediate Water) und Atlantic Water (West Spitzbergen Current) (Figure 1).

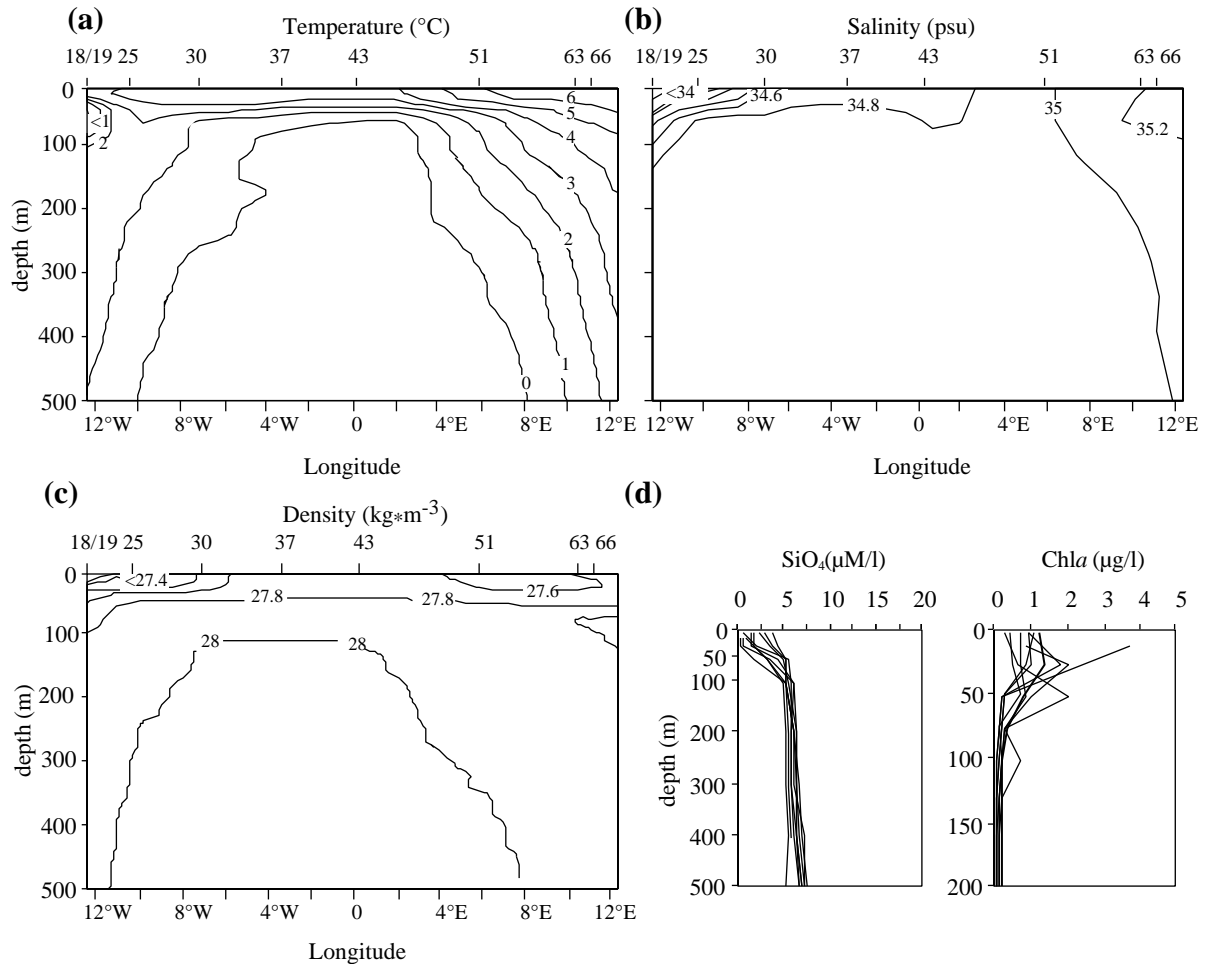


Figure 8: Hydrographic parameters along the 75°N transect in the Greenland Sea: (a) temperature; (b) salinity; (c) density () data (*Budeus, 1999*); (d) silicate and chl_a concentrations. Upper axis gives station numbers.

In the western part of the transect (stations 18-19), above 100 m depth, relatively cold and less saline Polar water (T=-1.5 to 0.6°C, S=32.7-34.7 psu) of the East Greenland Current (Figure 8a-c) was determined. As a result of summer warming, the shallow surface layer (< 3°C) was located above 25 m. The established SiO₄ concentrations between 0.4 and 5.8 μM/l were relatively high (Figure 8d). Accordingly, the chl_a concentrations < 2 μg/l were rather low with maximum values in 50 m depth. Below 100 m depth, the warmer and saltier Return Atlantic Current (T=0.9-2°C, S=34.8-35.0 psu) is situated. Despite the polar origins of the sur-

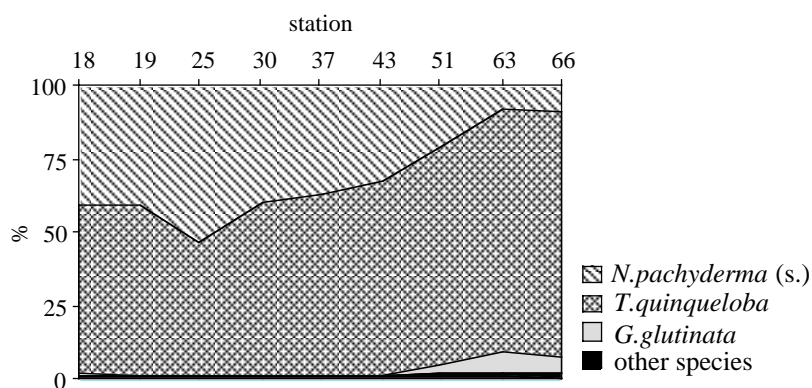


Figure 9: Average foraminiferal composition in the 0 to 500 m of the water column.

face water mass, both stations were dominated by *T. quinqueloba* with a relative abundance of 57 %, whereas the abundance of *N. pachyderma* (s.) was on average at 41 % (Figure 9).

Stations 25 to 43 were located in the Arctic water. The warmed layer of Arctic Surface Water (T=1.8-4°C, S=33.5-34.9 psu) was determined in the upper 35-55 m and a colder Arctic Intermediate Water (T=-1.4 to 2°C, S=34.8-35.0 psu) underneath (Figure 8a-c). Higher SiO₄ concentrations between 2.0 and 4.7 μM/l occurred at station 25, while stations 30-43 showed the lowest silicate (< 3 μM/l) and the highest chl_a (0.8-3.7 μg/l) concentrations in the upper 0-50 m along the transect (Figure 8d). The relative abundance of *N. pachyderma* (s.) at these transect stations continuously decreased from 53 to 32 %, whereas the abundance of *T. quinqueloba* increased from 46 to 68 % (Figure 9).

In the east of the Greenland Sea, the West Spitzbergen Current (stations 51-66) transports warm and saline Atlantic water northward (Figure 8a-c). The warm surface layer (T=3.7-6.5°C, S=35.0-35.6 psu) at these stations is located in the upper 45-55 m depth, underneath is the colder (T=0-5°C) and less saline (S=34.9-35.1 psu) Intermediate water. Higher SiO₄ concentrations (1.5-5.1 μM/l), which were found in the WSC compared to the Arctic water (Figure 8d), implied lower chl_a concentrations (< 1 μg/l). The relative abundance of *T. quinqueloba* reached the maximum of 80±5 % in this part of the transect, while the abundance of *N. pachyderma* (s.) strongly decreased to an average of 13±7 %. Additionally, the abundance of *G. glutinata* (5±2 %) and *G. uvula* (2±1 %) increased compared to other transect stations (max. 0.1 %). The abundance of *O. riedeli* rose as well, but was still very low at 0.1 % (Figure 9).

The relative abundance of *N. pachyderma* (d.) and *G. bulloides* decreased in easterly direction. Stations 18 and 19 showed the highest abundance of *N. pachyderma* (d.) with ~1 %. In the Arctic water (stations 25-43) the abundance of this species decreased to 0.6±0.2 %, before reaching the minimum of 0.3±0.2 % in the Atlantic water.

Results

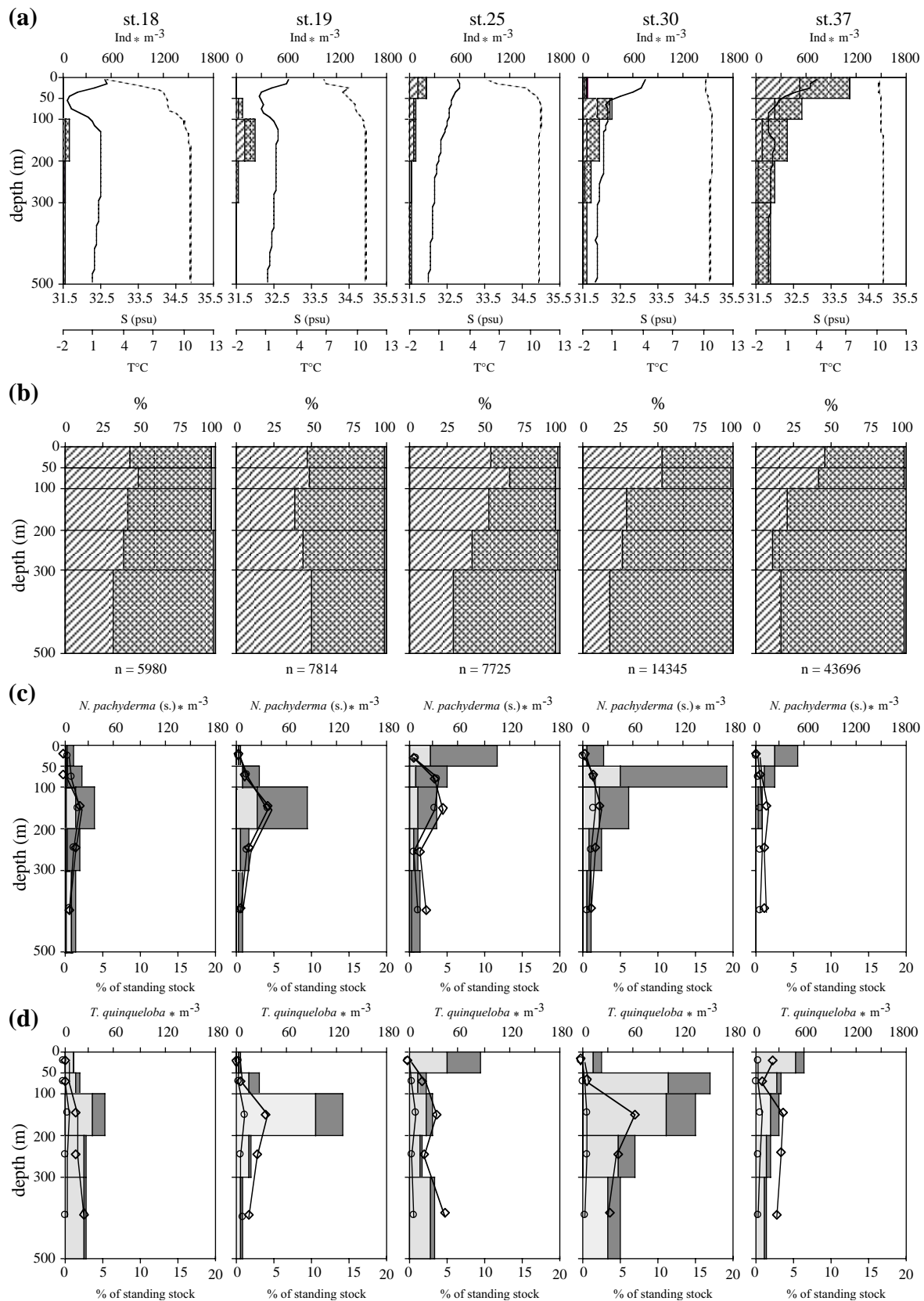


Figure 10: Depth distribution: (a) absolute abundances of planktonic foraminifera (bars), temperature (solid line) and salinity (dotted line); (b) relative abundance of *N. pachyderma* (s.), *T. quinqueloba* and other species (per depth interval); (c-d) absolute abundance of *N. pachyderma* (s.) and *T. quinqueloba* (note different scales) and proportion of individuals with reproductive characteristics. For further explanations see legend (page 21).

Results

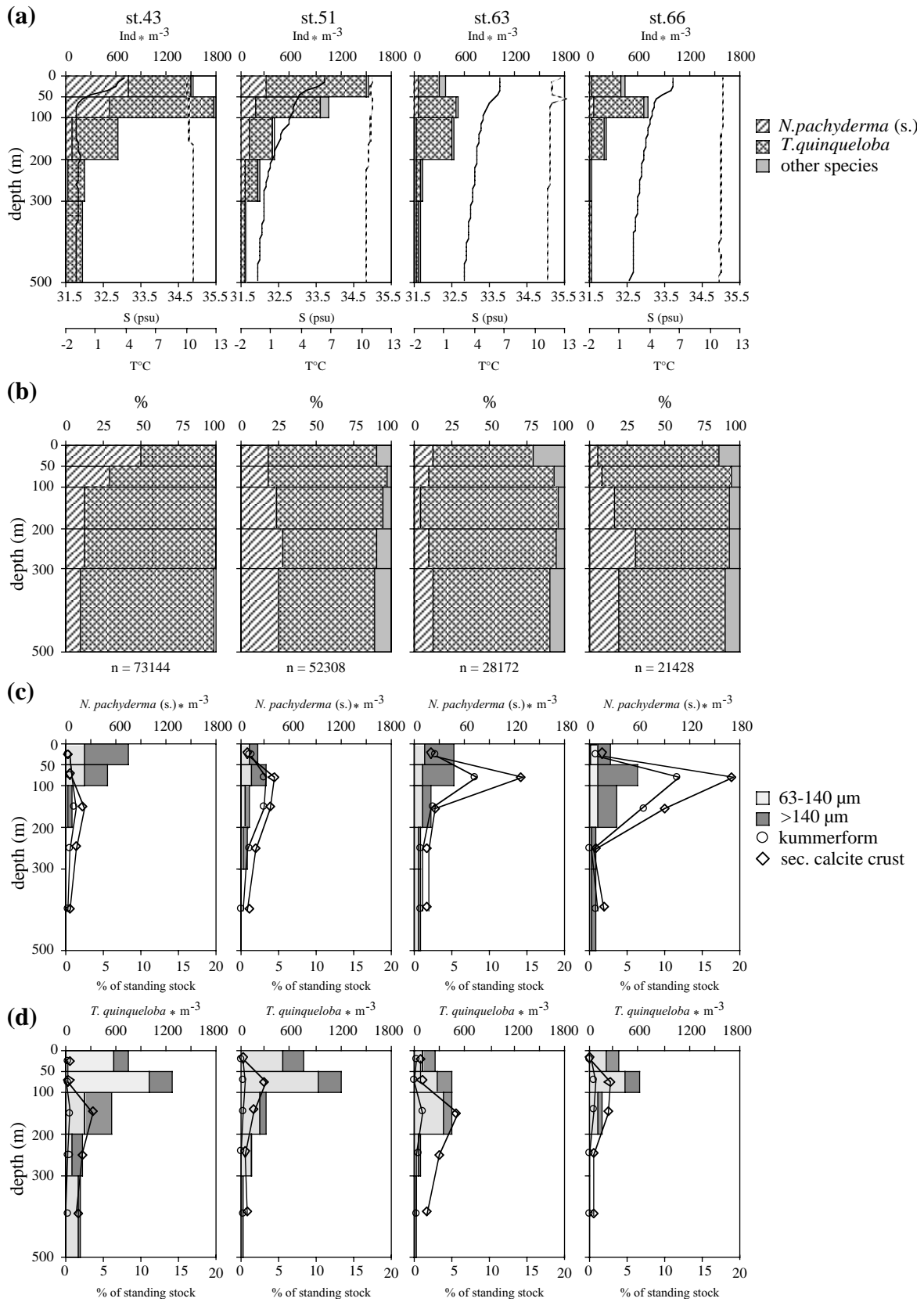


Figure 10: Continued.

The relative abundance of *G. bulloides* at stations 18 to 30 ranged between 0.2 and 0.4 % and further decreased to max. 0.2 % at stations 37 to 66.

The nine multinet tows, which were collected along the 75°N transect, indicate very high abundances of planktonic foraminifera with a maximum of 1802 Ind*m⁻³ (Figure 10a). The foraminiferal assemblage comprises of seven species: left and right-coiling *N. pachyderma*, *T. quinqueloba*, *G. bulloides*, *G. glutinata*, *G. uvula* and *O. riedeli*, while single specimens of *G. scitula* and *G. inflata* were found in the Atlantic water. The sampled 0 to 500 m were however dominated by the two species: *N. pachyderma* (s.) and *T. quinqueloba* (Figure 10b), whereas the relative abundance of *T. quinqueloba* increased strongly in the easterly direction.

3.2.1 Abundance and Shell Size Distribution of *N. pachyderma* (s.) and *T. quinqueloba*

The dominant species *N. pachyderma* (s.) and *T. quinqueloba* show a good match in their depth distribution along the transect, with the highest abundances in the upper 0-200 m (Figure 10c-d). At Stations 18 and 19, relatively low abundances between 4-83 Ind*m⁻³ for *N. pachyderma* (s.) and 4-129 Ind*m⁻³ for *T. quinqueloba* were found, reaching a maximum in the 100-200 m depth interval. In contrast, stations 25 to 66 showed the abundance maxima in the upper 0-100 m. Compared to stations 18 and 19, the abundance of both species strongly increased in the Arctic water (stations 25 to 43). There the abundance of *N. pachyderma* (s.) and *T. quinqueloba* in 0-200 m ranged between 24-754 Ind*m⁻³ and 20-1280 Ind*m⁻³, respectively, reaching the maximum at station 43. In the Atlantic water (stations 51-66), the abundance of *N. pachyderma* (s.) strongly decreased (18-298 Ind*m⁻³), while the abundance of *T. quinqueloba* showed only a slight decrease, ranging between 151 and 1222 Ind*m⁻³. The changes in the depth and horizontal distribution of both species were not correlated with variations in temperature, salinity, silicate and chl_a concentrations.

N. pachyderma (s.) was the only species to demonstrate a significant change in the distribution of individuals with reproductive characteristics along the transect (Figure 10c). The percentage of encrusted individuals and kummerforms decreased from 4 % (stations 18-25, maximum in 50-200 m) to max. 2 % encrusted and 1 % kummerform on the next stations 30 to 43 (maxima between 50 and 300 m). Further to the East (stations 51 to 66), the percentage of encrusted specimens (max. 19 %) and kummerforms (max. 12 %) increased compared to stations 30-43, whereas most of these individuals were found between 50 and 100 m depth.

The proportion of encrusted (max. 7 %) and kummerform (max. 1 %) individuals of *T. quinqueloba* varied irregularly along a transect (Figure 10d). While the reproductive features of this species were found below 100 m at stations 30 to 43, the most individuals with reproduc-

tive characteristics occurred between 50 and 200 m at stations 51 to 66.

The mean shell size of *N. pachyderma* (s.) and *T. quinqueloba* ranged from 130 to 200 μm and from 90 to 150 μm , respectively and showed similar distribution patterns along the transect (Figure 11a,b).

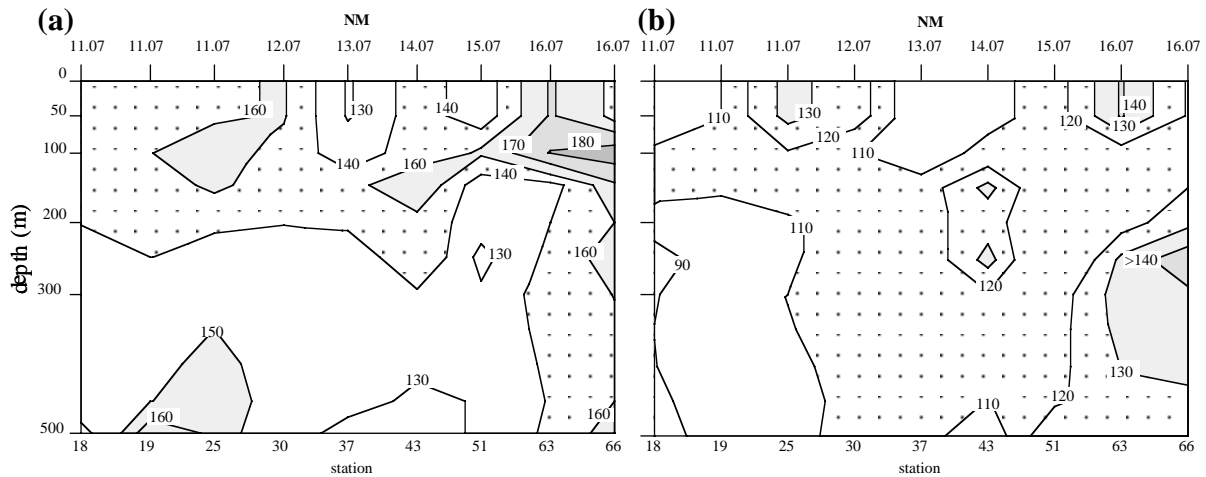


Figure 11: Mean shell size distribution of (a) *N. pachyderma* (s.) and (b) *T. quinqueloba* along the transect at 75°N. Upper axis denotes the sampling date, NM: new moon; lower axis gives the station numbers.

At the western stations 18 and 19, *N. pachyderma* (s.) and *T. quinqueloba* reached a maximum diameter of 160 μm and 120 μm , respectively. Compared to these stations, the mean shell size of both species slightly increased in the upper 100 m at stations 25 to 30, reaching a diameter between 160-170 μm for *N. pachyderma* (s.) and 120-130 μm for *T. quinqueloba*. At the next three stations (37-51) the shells size of both species decreased sharply, the specimens were small in 0-100 m with a maximum diameter of 150 μm for *N. pachyderma* (s.) and 110 μm for *T. quinqueloba*. During this time, larger shells of *N. pachyderma* (s.) between 160-170 μm were found at stations 37 and 43 in 100-300 m. Larger specimens of *T. quinqueloba* (~130 μm) were found at stations 43 and 51 in 100-300 m and 300-500 m, respectively. The largest shells were found at stations 63 and 66 in 0-100 m, where the mean shell size of *N. pachyderma* (s.) was between 160-200 μm and ranged from 110 to 140 μm for *T. quinqueloba*.

3.3. Fram Strait: Hydrographic Setting and Total Foraminiferal Distribution along the 80°N-Transect

Two dominant surface water masses are distinguished in the Fram Strait (80°N): Atlantic water of the West Spitzbergen Current (WSC) and Polar water of the East Greenland Current (EGC). A recirculated part of the WSC flows back south underneath the EGC as the Return Atlantic Current (Figure 1). The examined eight multinet stations were sampled during two days.

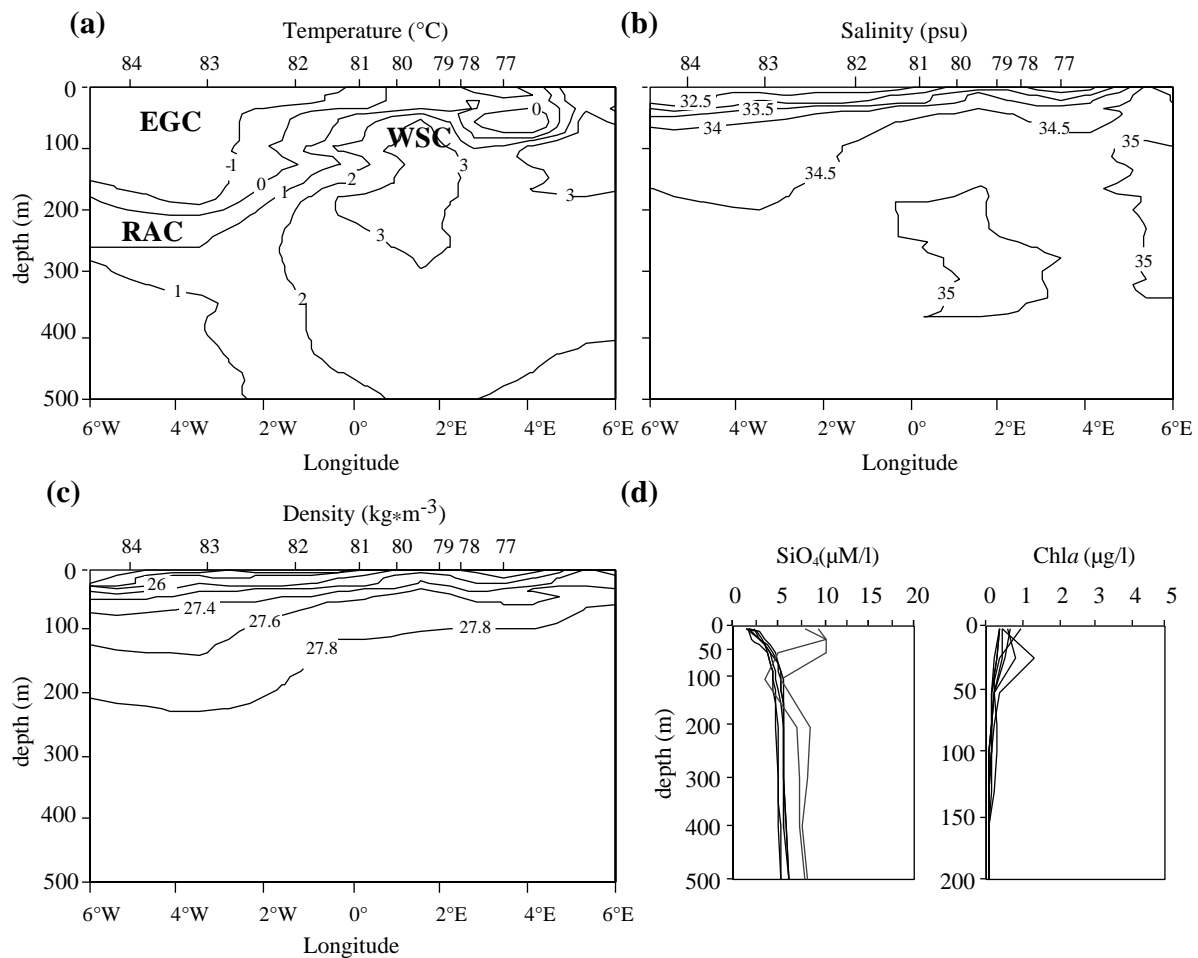


Figure 12: Hydrographic parameters along the 80°N-transect in the Fram Strait: (a) temperature; (b) salinity; (c) density (ρ_{σ_t}) data; (d) silicate and chl a concentrations, dotted line denotes stations 83 and 84 (see text). EGC: East Greenland Current, WSC: West Spitzbergen Current, RAC: Return Atlantic Current. Upper axis gives station numbers.

In the West Spitzbergen Current (st. 77-82), which in the eastern and central part of the Fram Strait transports warm and saline Atlantic water ($T=1.5-3^{\circ}\text{C}$, $S=35.0$ psu) into the Arctic ocean (Figure 12a-c), relatively low SiO_4 concentrations of maximum $2 \mu\text{M/l}$ were measured. The chl a concentrations varied between 0.3 and $1.2 \mu\text{g/l}$, with the maximal values in the upper

0-25 m (Figure 12d). At these stations, the foraminiferal assemblage was dominated by *T. quinqueloba* with a relative abundance between 74 and 95 % (Figure 13). The abundance of *N. pachyderma* (s.) ranged from 4 to 24 % (Figure 13).

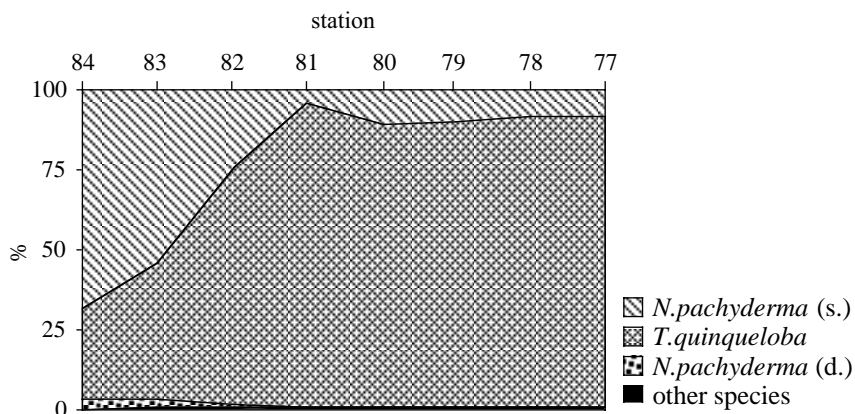


Figure 13: Average foraminiferal composition in the 0 to 500 m of the water column.

In the western part of the Fram Strait, where the East Greenland Current (stations 83-84) transports cold and less saline Polar water ($T=-0.8$ to -1.5°C , $S=33.7-34.4$ psu) southwards in a depth of 150 to 180 m (Figure 12a-c), higher SiO_4 concentrations ($8-10 \mu\text{M/l}$, Figure 12d) were measured compared to the eastern stations 77 to 82. Despite the high silicate concentrations, low chl *a* concentrations of $< 0.3 \mu\text{g/l}$ were measured at the surface (Figure 12d). Below, the warmer and more saline Return Atlantic Current ($T=0-1^{\circ}\text{C}$, $S=35$ psu) contains lower silicate concentrations compared to the EGC. *N. pachyderma* (s.) was found to be the dominant species at both stations with an average abundance of $61\pm 9\%$, while the proportion of *T. quinqueloba* ($36\pm 9\%$) strongly decreased relative to other stations (Figure 13).

Despite heavy ice-coverage at the sampling period, the abundances of planktonic foraminifera were relatively high in the Atlantic water (stations 77-82) with a maximum of $1096 \text{ Ind}\cdot\text{m}^{-3}$ at station 81, while in Polar water (stations 83-84) a maximum abundance of $52 \text{ Ind}\cdot\text{m}^{-3}$ was found (Figure 14a). Out of seven identified species: left and right-coiling *N. pachyderma*, *T. quinqueloba*, *G. bulloides*, *G. glutinata*, *G. uvula* and *O. riedeli*, the foraminiferal composition in the 0 to 500 m was dominated by only two species: *N. pachyderma* (s.) and *T. quinqueloba*. From east to west a dominance change from *T. quinqueloba* to *N. pachyderma* (s.) was found along the transect (Figure 14b).

The relative abundance of *N. pachyderma* (d.) and *G. bulloides* was very low in Atlantic water (max. 0.6 %), increasing slightly in the Polar water to 2.5 % and 0.9 %, respectively. The proportion of *G. glutinata* (max. 0.8 %, st. 77), *G. uvula* (max. 0.2 %, st. 77, 79) and *O. riedeli* (max. 0.3 %, st. 81) decreased in the western direction along the transect.

Results

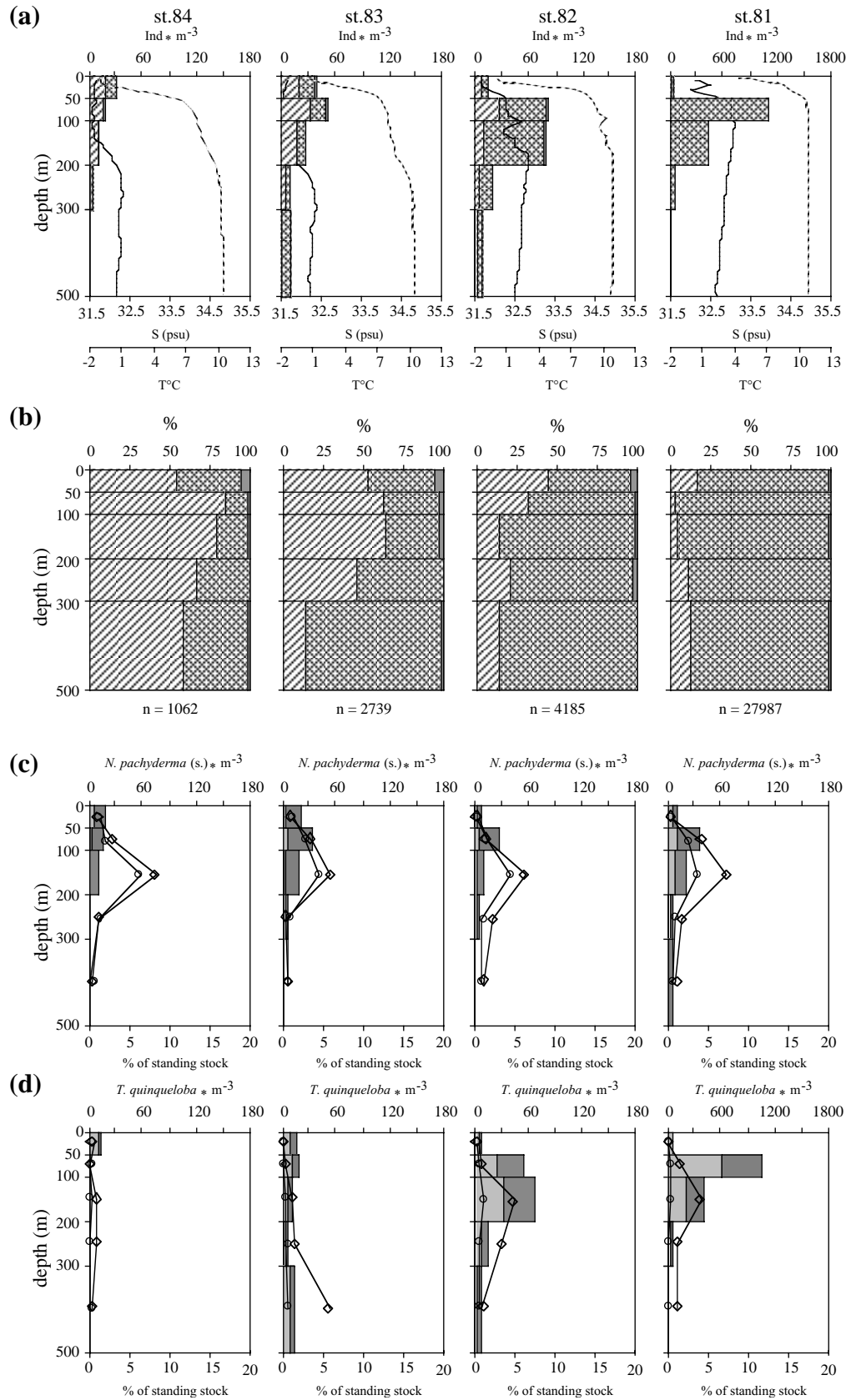


Figure 14: Depth distribution: (a) absolute abundances of planktonic foraminifera (bars), temperature (solid line) and salinity (dotted line); (b) relative abundance of *N. pachyderma* (s.), *T. quinqueloba* and other species (per depth interval); (c-d) absolute abundance of *N. pachyderma* (s.) and *T. quinqueloba* (note different scales) and proportion of individuals with reproductive characteristics. For further explanations see legend (page 27).

Results

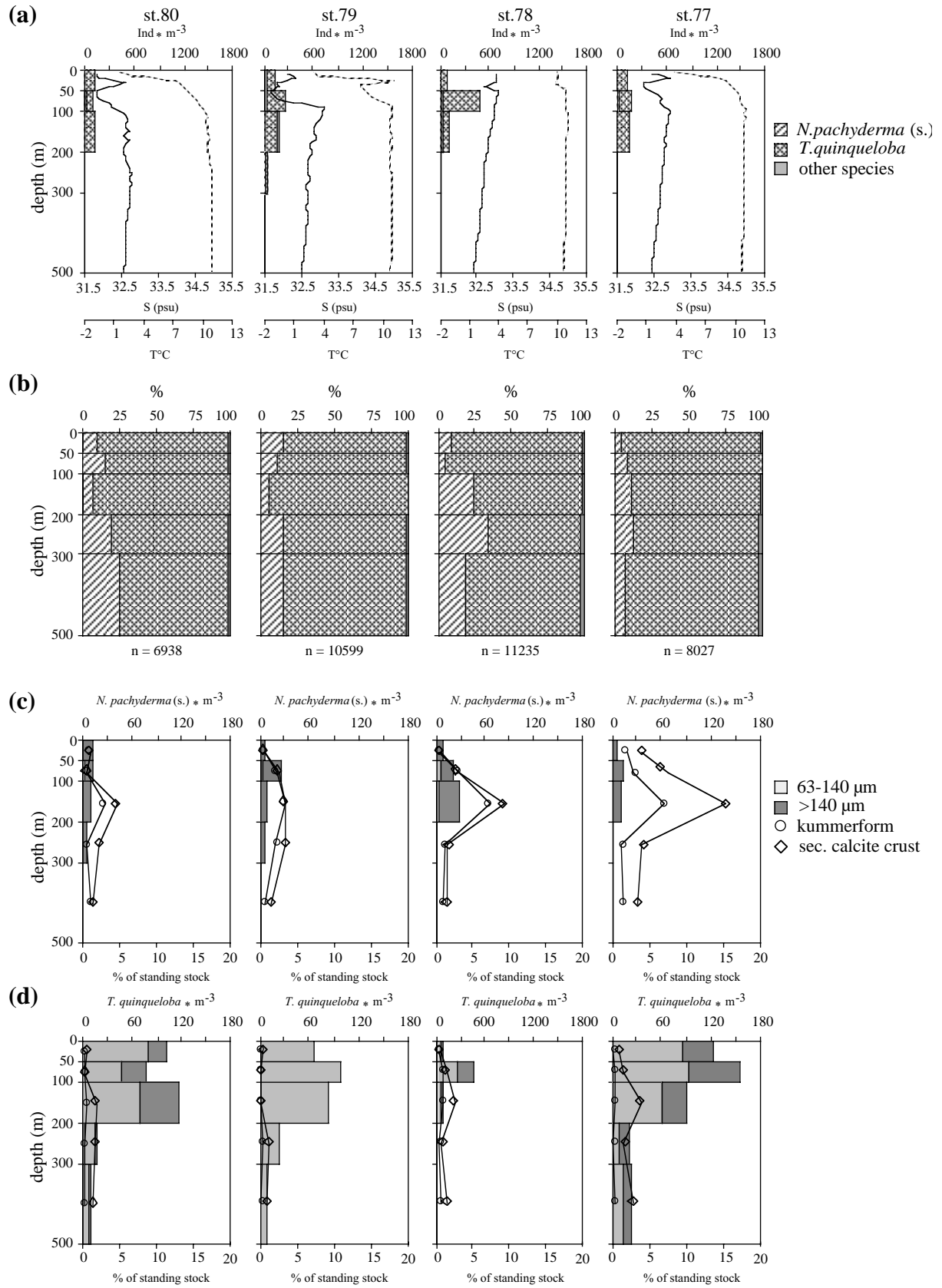


Figure 14: Continued.

3.3.1 Abundance and Shell Size Distribution of *N. pachyderma* (s.) and *T. quinqueloba*

The maximum abundances of *N. pachyderma* (s.) and *T. quinqueloba* were found in 0 to 200 m (Figure 14c,d). In the upper 0-50 m, *N. pachyderma* (s.) showed higher abundances in Polar water relative to Atlantic water. Over the 0 to 200 m depth interval the abundance of *N. pachyderma* (s.) however, showed no significant changes between both water masses. Slightly higher numbers of this species (10-34 Ind*m⁻³) were found at stations 81 and 83, whereas other transect stations showed lower abundances between 7 and 27 Ind*m⁻³. As opposed to *N. pachyderma* (s.), the abundance of *T. quinqueloba* decreased sharply in Polar water (2-19 Ind*m⁻³) compared to Atlantic water (8-1056 Ind*m⁻³). The changes in the abundance of both species were only in the 0-50 m depth interval well correlated with variations in average temperature and salinity. Below 50 m, no correlation between the abundance of *N. pachyderma* (s.) and *T. quinqueloba* and hydrographic parameters were found.

The percentage of individuals with a secondary calcite crust and kummerform chamber show no regular distributions pattern along a transect (Figure 14c,d). The kummerform percentage of *N. pachyderma* (s.) (Figure 14c) accounted to a maximum of 7 % (stations 77-78), whereas the proportion of encrusted shells was higher with max. 15 % (station 77). The maximum proportion of encrusted (6 %) and kummerform (0.9 %) *T. quinqueloba* (Figure 14d) was found at station 82. Most of *N. pachyderma* (s.) with reproductive characteristics were found in the 100-200 m depth interval, while the reproductive depth of *T. quinqueloba* varied irregularly below 100 m. The highest proportion of dead *N. pachyderma* (s.) was found in the Atlantic water at station 77 (25 %). Most empty shells of *T. quinqueloba* (23 %) occurred in the Polar water at station 84.

The shell size was measured for the stations 77, 82, 83 and 84. In the upper 0-200 m, the mean shell size of *N. pachyderma* (s.) and *T. quinqueloba* increased significantly in the westerly direction (Figure 15). At station 77, the shell size of *N. pachyderma* (s.) varied between 140 and 150 µm (Figure 15a), showing no significant variation throughout the water column. At stations 82 to 84, the species size increased in 0-200 m, reaching a maximum diameter between 180 and 200 µm in the upper 0-50 m at stations 82 and 83. At station 84, the shell size of *N. pachyderma* (s.) decreased in 0-50 m compared to stations 82-83, the largest individuals between 200 and 210 µm were found in 50-200 m.

The mean shell size of *T. quinqueloba* ranged from 100 to 140 µm (Figure 15b). At stations 77 to 82, larger shells (120-140 µm) were found only in the 300-500 m depth interval. At stations 83 and 84, the shell size between 130 and 140 µm was determined in 0-100 and 50-200 m.

Increasing size of *N. pachyderma* (s.) is inversely correlated with temperature ($r^2 = 0.5$, $n = 40$). Although the mean shell size of both species correlate well in the upper 0-200 m, no temperature dependent trend in the size distribution of *T. quinqueloba* was found.

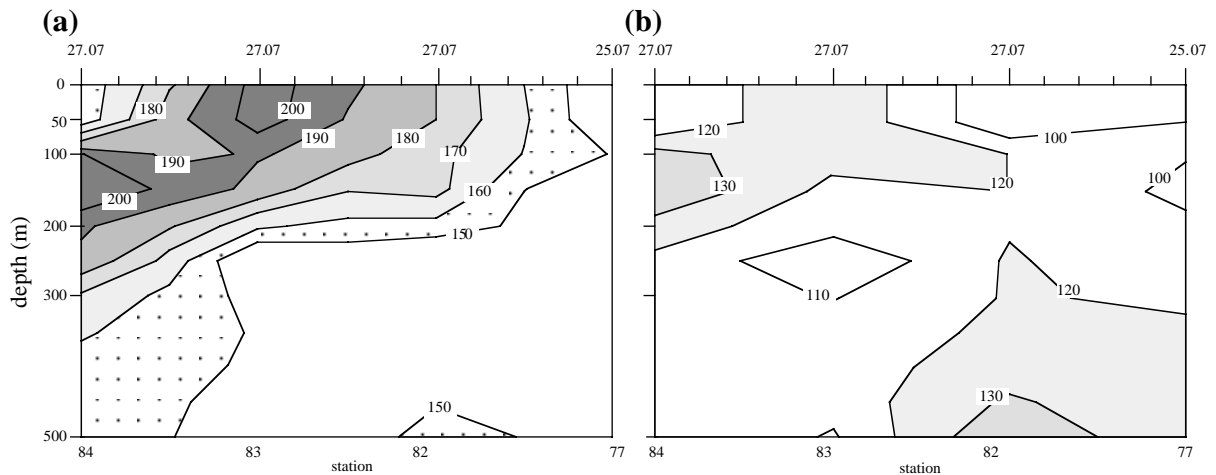


Figure 15: Mean shell size distribution of (a) *N. pachyderma* (s.) and (b) *T. quinqueloba* at stations 77, 82, 83 and 84. For sampling time see Table 1.

3.3.2 Stable Isotope Composition of *N. pachyderma* (s.) and *T. quinqueloba*

Due to the influence of sea-ice meltwater (Craig & Gordon, 1965), no linear relationship between $\delta^{18}\text{O}_w$ and salinity was found at stations 77 to 82 (Figure 16). In Polar water, salinity and $\delta^{18}\text{O}_w$ showed a linear correlation (stations 83 and 84).

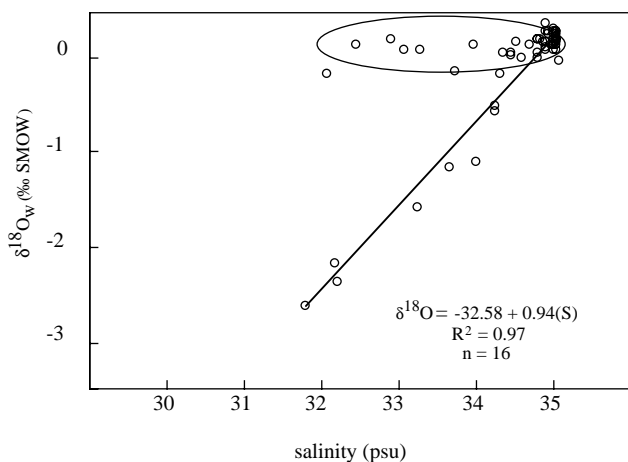


Figure 16: Relationship between salinity and $\delta^{18}\text{O}_w$ in the Fram Strait.

The isotopic analysis of nonencrusted foraminiferal shells was most possible in the upper 0-200 m, of encrusted shells usually below 100 m, wherever the largest numbers of either calcification group were found. The nonencrusted and encrusted shells showed no systematic variations in $\delta^{18}\text{O}$ as a function of shell size for examined size classes between 190-360 μm for *N. pachyderma* (s.) and 150-240 μm for *T. quinqueloba* (Figure 17).

The $\delta^{13}\text{C}$ of *N. pachyderma* (s.) varies clearly as a function of shell size:

$$\delta^{13}\text{C} = -6.91 + 2.94 * \text{Log}(\text{size}); r^2 = 0.41, n = 98 \quad (10)$$

In contrast, the $\delta^{13}\text{C}$ values of nonencrusted *T. quinqueloba* showed no correlation with shell size (Figure 17).

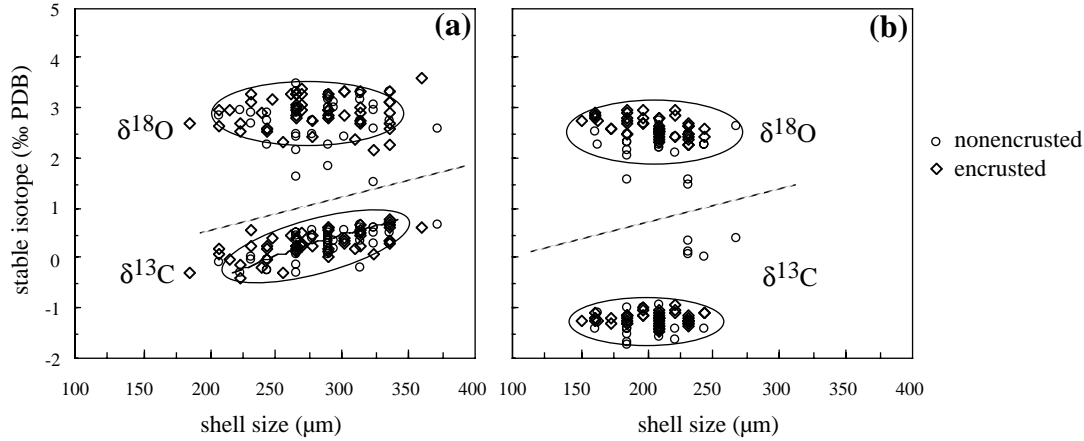


Figure 17: Stable isotope $\delta^{18}\text{O}$ and $\delta^{13}\text{C}$ versus shell size for (a) *N. pachyderma* (s.) and (b) *T. quinqueloba*.

The $\delta^{18}\text{O}_{\text{Eq}}$ values, calculated from $\delta^{18}\text{O}_{\text{w}}$ and temperature (Equation 3), varied along the transect between 1.9 and 4.3 ‰ (Figure 18). At stations 77 to 82, the vertical variations of $\delta^{18}\text{O}_{\text{Eq}}$ were inversely correlated with changes in temperature, resulting in relatively high $\delta^{18}\text{O}_{\text{Eq}}$ values between 3.1 and 4.5 ‰ in the upper 50 m. At stations 83 and 84, the $\delta^{18}\text{O}_{\text{Eq}}$ strongly decreased in upper 0-50 m (1.9-3.5 ‰), influenced by the salinity dependent $\delta^{18}\text{O}_{\text{w}}$ decrease.

The $\delta^{18}\text{O}$ values of *N. pachyderma* (s.) varied between 1.5 and 3.6 ‰ along the transect (Figure 18) and were slightly heavier than $\delta^{18}\text{O}$ of *T. quinqueloba* (1.5-3.0 ‰). With -0.3 ± 0.3 ‰ ($n = 3$), nonencrusted *T. quinqueloba* were not significantly lighter in $\delta^{18}\text{O}$ than encrusted shells, whereas *N. pachyderma* (s.) did not show a systematic difference between both calcification groups. In the upper 0-200 m, nonencrusted shells of *N. pachyderma* (s.) showed lighter $\delta^{18}\text{O}$ values (1.7-3.0 ‰) in Polar water than in Atlantic water (2.6-3.3 ‰). The $\delta^{18}\text{O}$ values of nonencrusted *T. quinqueloba* ranged between 1.5 and 2.7 ‰, showing no water masses dependent changes along the transect. The $\delta^{18}\text{O}$ values of nonencrusted shells of both species showed no systematic variations with depth in Atlantic water, whereas the $\delta^{18}\text{O}$ of foraminiferal shells increased correspondingly to $\delta^{18}\text{O}_{\text{Eq}}$ with increasing depth in Polar water. The $\delta^{18}\text{O}$ values of encrusted *N. pachyderma* (s.) and *T. quinqueloba* were between 2.4-3.3 ‰ and 2.3-2.9 ‰, respectively. In the upper 0-200 m, the $\delta^{18}\text{O}$ values of *N. pachyderma* (s.) and *T. quinqueloba* were on average 0.9 ± 0.4 ‰ ($n = 28$) and 1.2 ± 0.3 ‰ ($n = 23$) lighter than $\delta^{18}\text{O}_{\text{Eq}}$ (Figure 18).

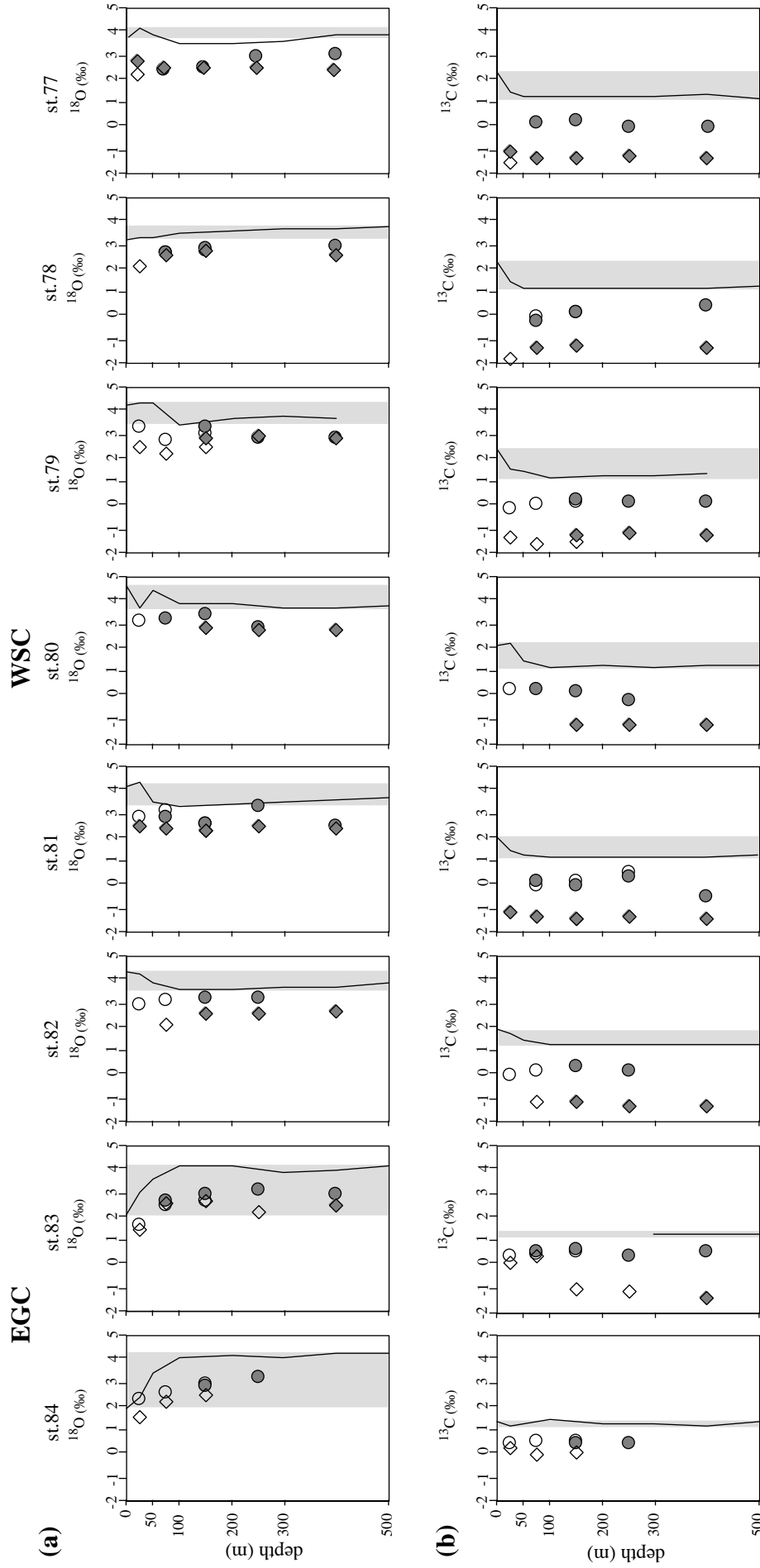


Figure 18: Depth distribution of (a) ^{18}O and (b) ^{13}C . Solid lines show depth distribution of $^{18}\text{O}_{\text{Eq}}$ and $^{13}\text{C}_{\text{DIC}}$ in the 0 to 500 m. The shaded areas denote the $^{18}\text{O}_{\text{Eq}}$ and $^{13}\text{C}_{\text{DIC}}$ range in 0-500 m. Station 83: no $^{13}\text{C}_{\text{DIC}}$ data in 0-300 m depth; for $^{13}\text{C}_{\text{DIC}}$ range, the $^{13}\text{C}_{\text{DIC}}$ values from station 84 are used. Symbols represent depth distribution of mean ^{18}O and ^{13}C values (standard deviations are given in Table 4): non-filled symbols: nonencrusted; filled: encrusted shells of *N. pachyderma* (s.) (*T. quinqueloba* (s.) (circles) and *T. pachyderma* (s.) (squares). EGC: East Greenland Current; WSC: West Spitzbergen Current.

Results

Table 4: Stable isotope composition and average shell size of nonencrusted and encrusted *N. pachyderma* (s.) and *T. quinqueloba* along the transect in the Fram Strait (80°N). Mean value ± standard deviation.

station	nonencrusted			encrusted			nonencrusted			encrusted		
	¹⁸ O	¹³ C	size	¹⁸ O	¹³ C	size	¹⁸ O	¹³ C	size	¹⁸ O	¹³ C	size
<u>st.77</u>												
0-50 m	-	-	-	-	-	-	2.24	-1.44	209	2.81	-1.01	197
50-100 m	-	-	-	2.39	0.21	309	-	-	-	2.54±0.08	-1.23±0.05	205±29
100-200 m	-	-	-	2.42±0.13	0.26±0.02	286±47	-	-	-	2.51±0.09	-1.28±0.19	209±35
200-300 m	-	-	-	2.93±0.29	-0.02±0.35	209±33	-	-	-	2.48±0.24	-1.14±0.17	205±41
300-500 m	-	-	-	2.96	-0.03	217	-	-	-	2.44±0.13	-1.26±0.06	209±23
<u>st.78</u>												
0-50 m	-	-	-	-	-	-	2.10±0.04	-1.69±0.10	204±25	-	-	-
50-100 m	2.66±0.54	0.05±0.41	267±33	2.68	-0.12	224	-	-	-	2.57±0.21	-1.28±0.13	221±16
100-200 m	2.76±0.01	0.19±0.29	261±25	2.84±0.03	0.24±0.09	284±25	-	-	-	2.75±0.11	-1.17±0.12	221±16
200-300 m	-	-	-	-	-	-	-	-	-	-	-	-
300-500 m	-	-	-	2.95	0.49	271	-	-	-	2.64±0.01	-1.23±0.10	284±47
<u>st.79</u>												
0-50 m	3.33±0.05	-0.06±0.16	290±23	-	-	-	2.54±0.23	-1.28±0.32	186±24	-	-	-
50-100 m	2.80±0.33	0.09±0.32	294±29	-	-	-	2.24±0.05	-1.54±0.13	213±29	-	-	-
100-200 m	3.02	0.18	294	3.34±0.22	0.31±0.21	307±40	2.47±0.02	-1.41±0.01	204±25	2.90±0.09	-1.15±0.04	198±16
200-300 m	-	-	-	2.85±0.30	0.24±0.09	240±44	-	-	-	2.93±0.06	-1.07±0.02	180±25
300-500 m	-	-	-	2.92±0.22	0.21±0.11	264±54	-	-	-	2.86±0.06	-1.15±0.10	190±30
<u>st.80</u>												
0-50 m	3.15±0.35	0.34±0.18	290±23	-	-	-	-	-	-	-	-	-
50-100 m	-	-	-	3.29±0.07	0.26±0.11	298±35	-	-	-	-	-	-
100-200 m	-	-	-	3.42	0.23	271	-	-	-	2.89±0.10	-1.16±0.07	190±30
200-300 m	-	-	-	2.91	-0.19	240	-	-	-	2.79±0.09	-1.19±0.04	180±25
300-500 m	-	-	-	-	-	-	-	-	-	2.78±0.02	-1.21±0.06	169±25
<u>st.81</u>												
0-50 m	2.91±0.04	-0.01±0.06	220±16	-	-	-	-	-	-	2.54	-1.06	209
50-100 m	3.20±0.21	0.25±0.11	298±35	2.84	0.24	284	-	-	-	2.40±0.18	-1.27±0.06	221±16
100-200 m	2.56±0.22	0.62±0.89	249±25	2.63±0.3	0.05±0.06	281±35	2.35±0.14	-1.38±0.11	209±23	2.35±0.05	-1.38±0.04	221±16
200-300 m	-	-	-	3.36	0.38	302	-	-	-	2.54±0.06	-1.24±0.10	209±23
300-500 m	-	-	-	2.52	-0.4	224	-	-	-	2.39±0.04	-1.33±0.13	221±16
<u>st.82</u>												
0-50 m	3.01±0.12	0.02±0.32	254±36	-	-	-	-	-	-	-	-	-
50-100 m	3.14±0.20	0.24±0.24	290±23	-	-	-	2.10±0.76	-1.08±0.13	198±16	-	-	-
100-200 m	-	-	-	3.26±0.11	0.43±0.21	302±35	-	-	-	2.65±0.09	-1.12±0.04	221±33
200-300 m	-	-	-	3.29	0.25	271	-	-	-	2.57	-1.25	209
300-500 m	-	-	-	-	-	-	-	-	-	2.67±0.07	-1.26±0.02	198±16
<u>st.83</u>												
0-50 m	1.68±0.16	0.44±0.09	294±16	-	-	-	1.49	0.10	232	-	-	-
50-100 m	2.47±0.22	0.50±0.11	290±23	2.68±0.06	0.56±0.13	309±29	2.64	0.39	267	-	-	-
100-200 m	2.73±0.10	0.58±0.12	325±39	2.96±0.03	0.63±0.10	307±22	2.68	-0.99	197	-	-	-
200-300 m	-	-	-	3.20	0.43	247	2.25	-1.07	163	-	-	-
300-500 m	-	-	-	2.93±0.25	0.61±0.05	293±45	-	-	-	2.53	-1.35	209
<u>st.84</u>												
0-50 m	2.33±0.19	0.51±0.07	284±25	-	-	-	1.57	0.34	232	-	-	-
50-100 m	2.56±0.07	0.59±0.07	302±33	-	-	-	2.26	0.01	244	-	-	-
100-200 m	3.00±0.03	0.56±0.04	294±29	2.91±0.12	0.47±0.08	290±23	2.51	0.16	232	-	-	-
200-300 m	-	-	-	3.28	0.45	263	-	-	-	-	-	-
300-500 m	-	-	-	-	-	-	-	-	-	-	-	-

The ¹³C_{DIC} varied in 0-500 m between 1.1-2.4 ‰, showing slight variations with increasing depth (Figure 16). Only at the surface (0 m) at stations 77-82 did ¹³C_{DIC} show higher values, while no depth dependent ¹³C_{DIC} variations were found in the Polar water. The ¹³C values of *N. pachyderma* (s.) varied from -0.4 to 0.6 ‰ along the transect, being much higher than the ¹³C values of *T. quinqueloba* at -1.7 and 0.4 ‰ (Table 4). In the upper 0-200 m, the ¹³C values of nonencrusted *N. pachyderma* (s.) increased with increasing depth (¹³C max. 0.4 ‰) and tended to have heavier ¹³C values in Polar water (0.5±0.1 ‰) than those found in Atlantic water (0.2±0.2 ‰). Encrusted *N. pachyderma* (s.), similarly to nonencrusted specimens, tended to heavier ¹³C values (0.5±0.1 ‰, n = 6) in Polar water than in Atlantic water

(0.1 ± 0.2 ‰, $n=19$), but varied irregularly with depth. Due to the low resolution, no statement concerning ^{13}C depth distribution of nonencrusted *T. quinqueloba* was possible. With an average of 0 ± 0.5 ‰, nonencrusted *T. quinqueloba* in the Polar water showed much heavier ^{13}C values than in Atlantic water (-1.4 ± 0.2 ‰). The ^{13}C of encrusted *T. quinqueloba* ranged from -1.4 to -1.0 ‰ and did not vary systematically with depth or location. Encrusted *T. quinqueloba* were with 0.3 ± 0.2 ‰, ($n = 3$) not significantly heavier in ^{13}C than nonencrusted shells. In the upper 0-200 m, the ^{13}C values of *N. pachyderma* (s.) and *T. quinqueloba* were on average 1.0 ± 0.3 ‰ and 2.2 ± 0.7 ‰ lighter than $^{13}\text{C}_{\text{DIC}}$.

4. Discussion

4.1 Distribution of Planktonic Foraminifera in the Study Area

4.1.1 Species Distribution Pattern

According to Bé & Tolderlund 1971, the assemblages of planktonic foraminifera in high latitude environments consist of the subpolar species: *T. quinqueloba*, right-coiling *N. pachyderma*, *G. bulloides*, *G. scitula*, *G. uvula* and a single polar species: left-coiling *N. pachyderma*. Using nets with 200- μm mesh size, their plankton tow surveys of the Atlantic Ocean showed the species distribution of planktonic foraminifera to be primarily controlled by sea surface temperature. The large vertical gradients in temperature and salinity in the survey area, due to summer warming and ice-melting, lead however to the conclusion that SST (Sea Surface Temperature) and SSS (Sea Surface Salinity) are not reliable indicators of different water masses, which justifies examining the average temperature and salinity in the 0 to 50 m. Corresponding to the main habitat (life depth) of *N. pachyderma* (s.) and *T. quinqueloba* and due to different residence times of both species in the water column (Arikawa, 1983), the following will present an average foraminiferal species composition in the upper 0-200 m (Table 5, Figure 19).

Table 5: Average foraminiferal composition (0-200 m), mean temperature and salinity (0-50 m) in different current regimes in the survey area.

	(%)									T(°C)	S(psu)
	<i>N.pach</i> (s.)	<i>T.quin</i>	<i>G.glu</i>	<i>N.pach</i> (d.)	<i>G.bul</i>	<i>G.uvu</i>	<i>O.ried</i>	<i>G.sci</i>	<i>G.infl</i>		
Labrador Sea											
Labrador Current	37.4	27.8	25.0	2.5	4.7	2.6	0	0	0	6.5 \pm 0.5	34.3 \pm 0.2
Convection Area	19.6	46.8	20.8	2.6	6.4	3.5	0.3	0	0.1	7.2 \pm 1.0	34.6 \pm 0.03
Atlantic Water	2.4	39.4	41.0	2.9	2.2	9.7	0.2	0.2	2.0	9.9 \pm 2.1	34.7 \pm 1.0
Greenland Sea (75°N)											
East Greenland Current	42.5	55.8	0.1	1.2	0.3	0	0	0	0	0.9 \pm 0.6	34.1 \pm 0.3
Arctic Water	43.9	55.1	0	0.6	0.3	0	0	0	0	2.5 \pm 0.4	34.7 \pm 0.5
West Spitzbergen Current	12.3	80.1	5.5	0.3	0.1	1.6	0.1	0	0	5.8 \pm 0.6	35.1 \pm 0.1
Fram Strait (80°N)											
East Greenland Current	63.4	33.0	0.1	2.4	0.5	0	0	0	0	-1.6 \pm 0.1	33.0 \pm 0.4
West Spitzbergen Current	10.7	88.2	0.4	0.2	0.2	0.1	0.1	0	0	1.0 \pm 1.6	34.1 \pm 0.5

N.pach (s.): *N. pachyderma* (s.); *T.quin*: *T. quinqueloba*; *G.glu*: *G. glutinata*; *N.pach* (d.): *N. pachyderma* (d.); *G.bul*: *G. bulloides*; *G.uvu*: *G. uvula*; *O.ried*: *O. riedeli*; *G.sci*: *G. scitula*; *G.infl*: *G. inflata*.

In the present study, established species composition in the Labrador Sea (49-59°N) was much more diverse than in the Greenland Sea (75°N) and Fram Strait (80°N), where a two species-assemblage was recorded (Table 5, Figure 19). This clearly reflects latitudinal and temperature influence on the species diversity and is in agreement with observations of Bé & Tolderlund (1971).

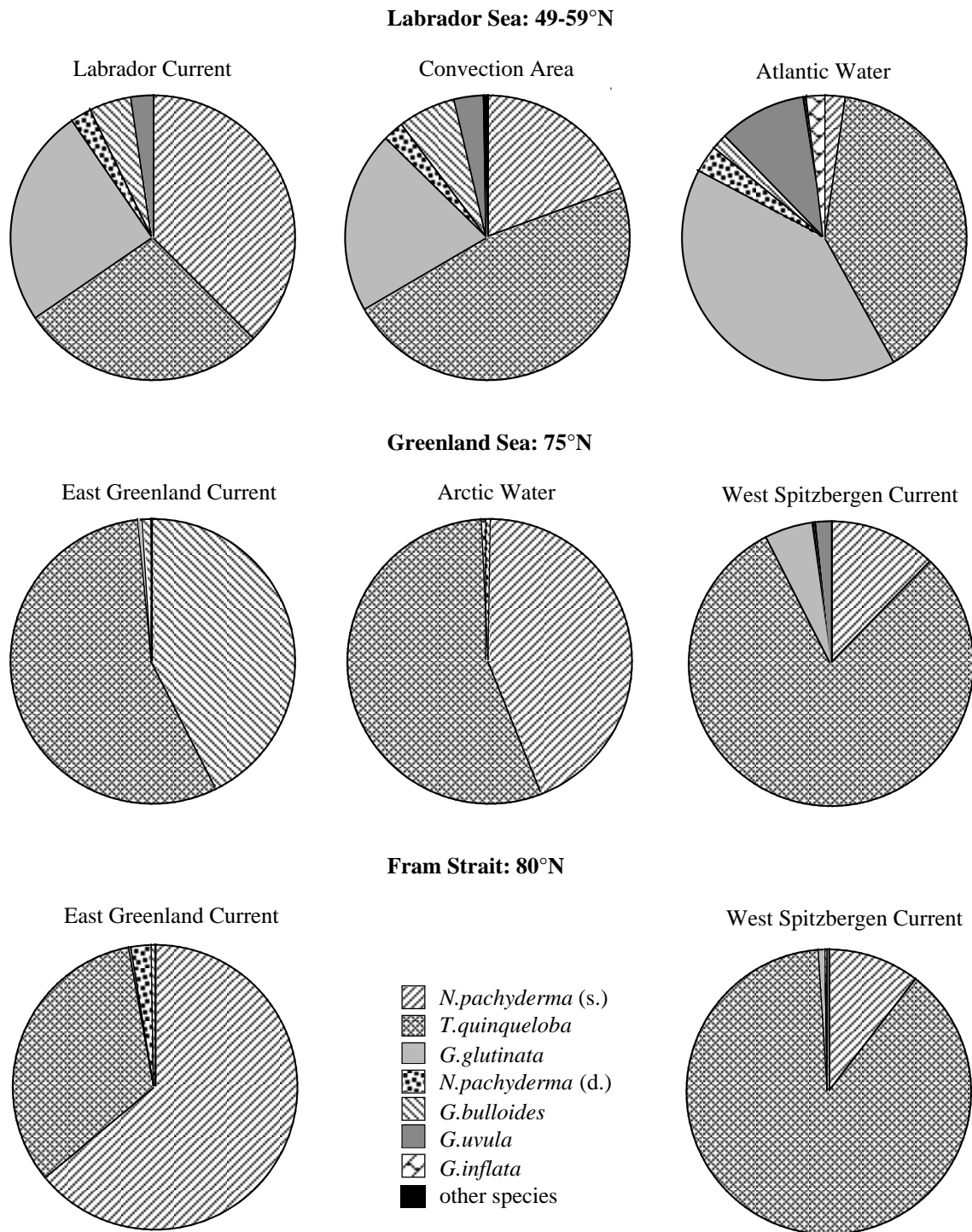


Figure 19: Proportion of foraminiferal species (0-200 m) in different water masses of the study area. Species percentage, average temperature and salinity are given in Table 5.

Similar foraminiferal communities to those presented in Figure 19 have been described already by previous plankton studies using smaller mesh size nets in the survey area: 63 μm in the Fram Strait at 80°N (Carstens et al., 1997) and Greenland Sea at 75°N (Jensen, 1998), 125 μm in the northern Fram Strait at 81-82°N (Volkman, 2000a). These and many other studies show the dramatic impact the net mesh size has on the abundance and species composition of plankto-

nic foraminifera. A summary of this problem is given e.g. by Berger (1969) and Carstens et al. (1997). In the present study, for example, *N. pachyderma* (s.) accounts for > 60 % of the foraminiferal abundance only in the East Greenland Current at 80°N ($T < -1$ °C) (Table 5, Figure 19). Opposed to this, Bé & Tolderlund (1971) described *N. pachyderma* (s.) as the single dominant species of the polar province (0-5°C). The main cause for this contrast might result from the higher proportion of *T. quinqueloba* found in the present study. Because *T. quinqueloba* is most abundant in the 63-125 µm size-class, the proportion of this species was underestimated in the >200 µm size fraction examined by Bé & Tolderlund (1971). This is confirmed by other surveys in the Fram Strait, which obtained similar proportion of *N. pachyderma* (s.) in the Polar water. Using 63-µm nets mesh, Carstens et al. (1997) found that the assemblage of planktonic foraminifera in the Polar water was dominated by *N. pachyderma* (s.) with a proportion of 60 %, whereas Volkmann (2000a) observed a proportion of 70 % upon analysing the >125 µm size fraction.

In the Labrador and Greenland Seas, at higher average temperatures, lower relative abundances of *N. pachyderma* (s.) were found in the polar province compared to the Fram Strait (Table 5, Figure 19). This abundance decrease within the polar province in the survey area seems dependent upon water temperature. This can also be seen from Greenland Sea data at 75°N published by Jensen (1998). He found in the East Greenland Current in October 1995, at similarly low temperatures (< -1 °C) as in the Fram Strait in July 1999 (this study), a correspondingly high proportion (61 %) of *N. pachyderma* (s.), whereas in the present study, a lower relative abundance of this species at higher temperatures in East Greenland Current (75°N) was found compared to Jensen (1998). No findings regarding the foraminiferal assemblage using small mesh nets in the Labrador Sea have been published yet. As opposed to the investigation of Stehmann (1972), who could only find two species: *N. pachyderma* (s.) and *G. bulloides* in the Labrador Sea, Baffin Bay and Davis Strait, using nets of 200 µm mesh size. In the present study however, two subpolar species: *T. quinqueloba* and *G. glutinata* were found to be dominant besides *N. pachyderma* (s.) in the Labrador Sea, further emphasizing the strong influence the mesh size has on species composition. Compared to the Labrador Sea, the proportion of *G. glutinata* sharply decreased in the polar province of the Greenland Sea and Fram Strait, leading the foraminiferal assemblage to be dominated by only two species, *N. pachyderma* (s.) and *T. quinqueloba*. The surveys using net mesh of 63 µm (Carstens et al., 1997; Jensen, 1998) show a similar species composition. The sediment trap studies carried out in Arctic water of the Greenland Sea (75°N), which obtained a proportion of 40 % *N. pachyderma* (s.) and 54 % *T. quinqueloba* in July 1994 (Jensen, 1998), also agreed well with species composition found in July 1999 in this study (Table 5).

In the Atlantic water of the Labrador Sea ($T=7-10$ °C), the foraminiferal assemblage was do-

minated by *T. quinqueloba* and *G. glutinata* with a higher proportion of other subpolar species (Table 5, Figure 19). Relative to the Labrador Sea, the species diversity sharply decreased in the Greenland Sea and Fram Strait ($T=1-6^{\circ}\text{C}$), where in the Fram Strait the least percentage of subpolar species (~4 %) were found. The assemblage of planktonic foraminifera in the Greenland Sea and Fram Strait was dominated almost exclusively by *T. quinqueloba* (>80 %). In contrast, based on multinet samples from the summer of 1985, Carstens et al. (1997) noted similar absolute abundances of planktonic foraminifera in the Fram Strait but a lower proportion (61 %) of *T. quinqueloba*. *N. pachyderma* (s.) and subpolar species account in their study for 35 % and 5 %, respectively. Volkmann (2000a), on the other hand, found similarly high proportions of *T. quinqueloba* (>80 %) and subpolar species at 5 % in the >125 μm size class, taken in 1997. This increase in relative abundance of *T. quinqueloba* in the years 1997 and 1999 compared to the year 1985 may possibly be explained by the warming of the Atlantic inflow into the Arctic ocean by 0.5 to 1°C , which has been observed since the 1950s (Macdonald, 1996).

The correlations between different hydrographic regimes and relative abundance of *N. pachyderma* (s.) and *T. quinqueloba* were used to calculate the optimum temperature and salinity ranges, according to Berger (1969):

$$T_{\text{av}} = \frac{\sum_{i=1}^n T_i \cdot P_i \cdot N_{fi}}{\sum_{i=1}^n P_i \cdot N_{fi}} \quad (11)$$

T_i : average temperature or salinity at the station i , P_i : species percentage at station i , N_{fi} : abundance of total foraminiferal population at the station i , n : number of stations.

Calculated temperature optima for *N. pachyderma* (s.) and *T. quinqueloba* between $0-7^{\circ}\text{C}$ and $1-9^{\circ}\text{C}$, respectively, were slightly lower than the species' characteristic temperature range of $0-9^{\circ}\text{C}$ and 12°C in the North Atlantic (Bé and Tolderlund, 1971). The calculated salinity optimum was about 34.3 ± 0.6 psu for *N. pachyderma* (s.) and 34.5 ± 0.3 psu for *T. quinqueloba*. The known salinity optima for *N. pachyderma* (s.) and *T. quinqueloba* were found by Bé (1977) at the surface of the Indian Ocean, having a similar range of 34.1 ± 2.9 and 34.5 ± 3.6 ‰, respectively. The size dependent shift of the species spectrum as well as lower spatial resolution of multinet tows as compared to surveys of Bé and Tolderlund (1971), leads to changes in the temperature optima of both dominant species in the survey area. Consistent with results of the present study, Reynolds & Thunell (1986) observed that *N. pachyderma* (s.) in the northeast Pacific prefers a habitat with temperatures of $< 8^{\circ}\text{C}$ in low stratified waters.

4.1.2 Absolute Abundance and Depth Distribution of *N. pachyderma* (s.) and *T. quinqueloba*

While the species composition allows conclusions as to the dominant water masses, weak or no correlation between the absolute abundance of planktonic foraminifera and hydrographic parameters were found in this study. The distribution of absolute foraminiferal abundance in the water column is the product of a complex interaction between physical-chemical and biological factors (Bé, 1977). The following chapter will discuss the relationships between some of these factors and foraminiferal abundance.

In the Labrador Sea, *N. pachyderma* (s.) and *T. quinqueloba* are most abundant in the upper 0 to 200 m (Table 6). A correlation between foraminiferal abundance and hydrographic parameters existed only in single depth intervals, leading the 0 to 200 m integrated abundances of both species varied irregularly with temperature and salinity (Figure 20).

Table 6: Abundance maxima of *N. pachyderma* (s.) and *T. quinqueloba* in the study area:

	<i>N. pachyderma</i> (s.)	<i>T. quinqueloba</i>	
Labrador Sea (ice-free)	0-200 m	0-200 m	
Greenland Sea (75°N) (ice-free)	50-200 m	50-200 m	East Greenland Current
	0-100 m	0-100 m	Arctic Water
	0-100 m	0-100 m	West Spitzbergen Current
Fram Strait (80°N) (ice-covered)	0-100 m	0-100 m	East Greenland Current
	50-200 m	50-200 m	West Spitzbergen Current

N. pachyderma (s.) was the only species to demonstrate a distribution trend as a function of salinity in the Labrador Sea, preferably occurring in the less saline Labrador Current (Figure 20a-b). The largest numbers of this species, as well as the best correlation between abundance and salinity ($r^2 = 0.52$, $n = 8$), were found in the upper 0-50 m. The highest abundance of 121 Ind*m⁻³ was reached at low salinity of 34.2±0.6 psu (Figure 3b, station 402), while at highest salinity of 34.9±0.02 psu, the lowest abundance of 2.7 Ind*m⁻³ in 0-50 m was found (Figure 3b, station 381). Bé & Tolderlund (1971) also observed that *N. pachyderma* (s.) is generally associated with low temperature and salinity. The salinity tolerance range of this species is however extremely wide. Laboratory experiments on individuals living in Antarctic sea ice demonstrated that *N. pachyderma* (s.) tolerates salinities higher than 60 psu (Spindler, 1996).

In contrast, a weak correlation was found between the abundance of *T. quinqueloba* and temperature (Figure 20c-d). Similarly to *N. pachyderma* (s.), the abundance of *T. quinqueloba* and temperature was better correlated in the upper 0-50 m ($r^2 = 0.8$, $n = 8$). This species reached the highest abundance of 143 Ind*m⁻³ in the North Atlantic Current, at the highest average

temperature of $12 \pm 1.4^\circ\text{C}$ (Figure 3c, station 404). The proportion of dead individuals rose however with increasing total abundance. The lowest numbers of *T. quinqueloba* ($3.8 \text{ Ind} \cdot \text{m}^{-3}$) were found at the lowest temperature of $6.3 \pm 0.1^\circ\text{C}$ in the convection area (Figure 3c, station 352).

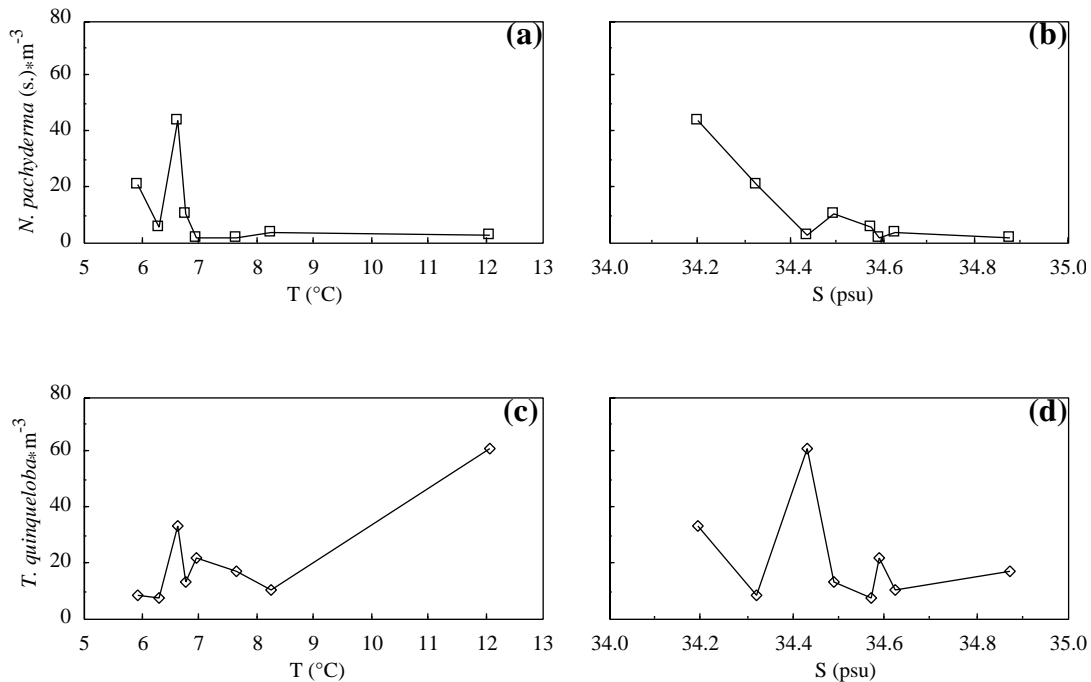


Figure 20: Absolute abundances of (a-b) *N. pachyderma* (s.) and (c-d) *T. quinqueloba* in the upper 0-200 m (integrated values) versus average temperature and salinity (0-50 m) in the Labrador Sea (M 39/4).

In the 50-100 m depth interval, the abundance of both species and hydrographic parameters already showed a weaker correlation compared to the upper 0-50 m. In 100-200 m, the differences in temperature and salinity between most stations were already slight, therefore no correlation between foraminiferal abundance, temperature and salinity existed. The abundance changes in 50-100 m and 100-200 m were not or just weakly correlated with variations in temperature and salinity in 0-50 m. This indicates that both species prefer a habitat above 50 m in the Labrador Sea and that a secondary abundance maximum below 50 m to be a result of active sinking and/or sedimentation. This assumption is consistent with ^{18}O data of *N. pachyderma* (s.) from surface sediments in the Labrador Sea, discussed by Wu & Hillaire-Marcel (1994). They found that *N. pachyderma* (s.) secretes its test in the surface layer (colder than 8°C , below the temperature tolerance limit) during summer. Similar to the conclusion of the present study, *T. quinqueloba* as a symbiont-bearing species is general accepted as adapted to the uppermost 50 m (Hemleben et al., 1989).

According to Bé (1977), *N. pachyderma* (s.) changes its preferred habitat below 100 m when the water temperature decreases, living closer to the surface. Despite relatively low tem-

peratures in the Greenland Sea and Fram Strait, *N. pachyderma* (s.) usually occurs in greater depths in these regions compared to the Labrador Sea. In the Greenland Sea and Fram Strait, *T. quinqueloba* shows a similar depth distribution as *N. pachyderma* (s.) (Table 6).

In the ice-covered Fram Strait, *N. pachyderma* (s.) and *T. quinqueloba* changed their habitat between the different water masses (Figure 14c-d). Both species were most abundant in 0-100 m in Polar water and between 50 and 200 m (exception: st. 77) in Atlantic water (Table 6). This deepening of the main habitat along the transect seems to depend on the subsidence of Atlantic water below Polar water and sea ice meltwater. Only in the 0-50 m depth interval did the abundance of *N. pachyderma* (s.) significantly increase in Polar water compared to Atlantic water (Figure 21c), while no significant changes in abundance were found below 50 m. Since low salinity and temperature are associated with each other, the abundance of *N. pachyderma* (s.) in upper 0-50 m was inversely correlated with both parameters (Figure 21a, c).

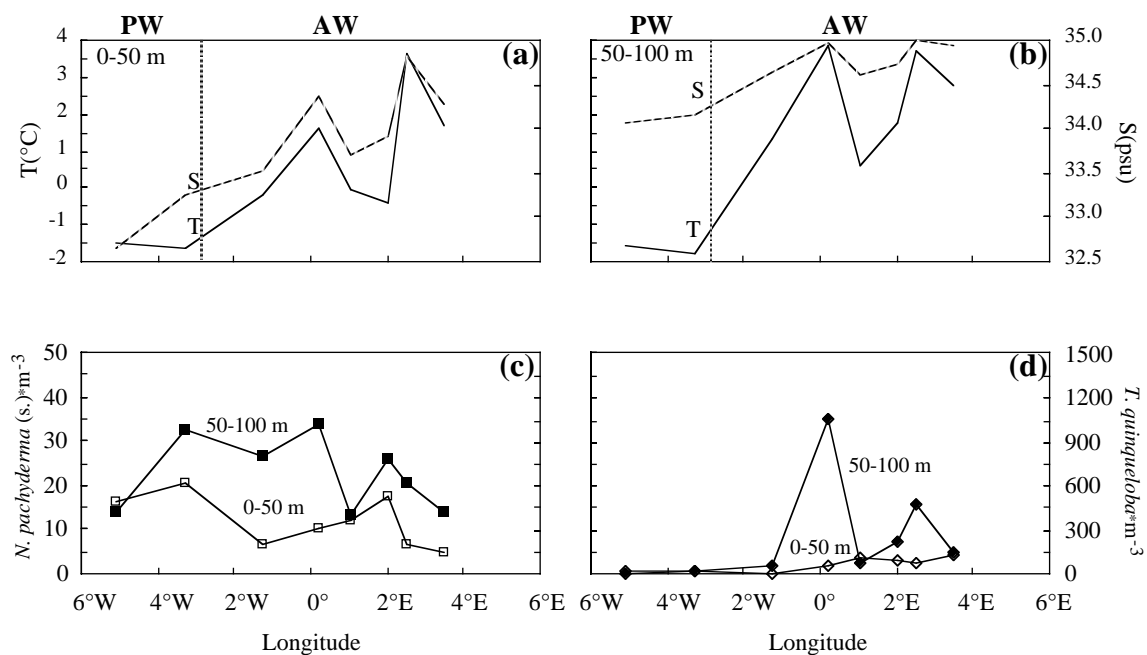


Figure 21: Distribution of (a-b) temperature (solid line) and salinity (dotted line), (c) *N. pachyderma* (s.), (d) *T. quinqueloba* in the 0-50 m (non-filled symbols) and 50-100 m (filled symbols) depth intervals along the 80°N-transect in the Fram Strait. Note different scales. PW: Polar water; AW: Atlantic water.

As opposed to *N. pachyderma* (s.), the abundance of *T. quinqueloba* drastically decreased in the cold and less saline Polar water (Figure 21b, d), showing the best positive correlation with average temperature and salinity in the upper 50-100 m.

The strong increase in absolute abundance of *N. pachyderma* (s.) and *T. quinqueloba* in the Arctic water (Greenland Sea at 75°N), as well as the variations in the main habitat of both species (Table 6) was however not correlated with variations in temperature and salinity (Figure 22

a-b). This suggests that temperature and salinity are not the dominant factors controlling the distribution of absolute foraminiferal abundance in the water column. Ortiz et al. (1995) reached a similar conclusion in the California Current, where out of seven examined species only *G. ruber* exhibited a temperature dependent distribution. Carstens & Wefer (1992) also did not believe distribution patterns of *N. pachyderma* (s.) and *T. quinqueloba* in the Nansen Basin to be controlled by temperature alone.

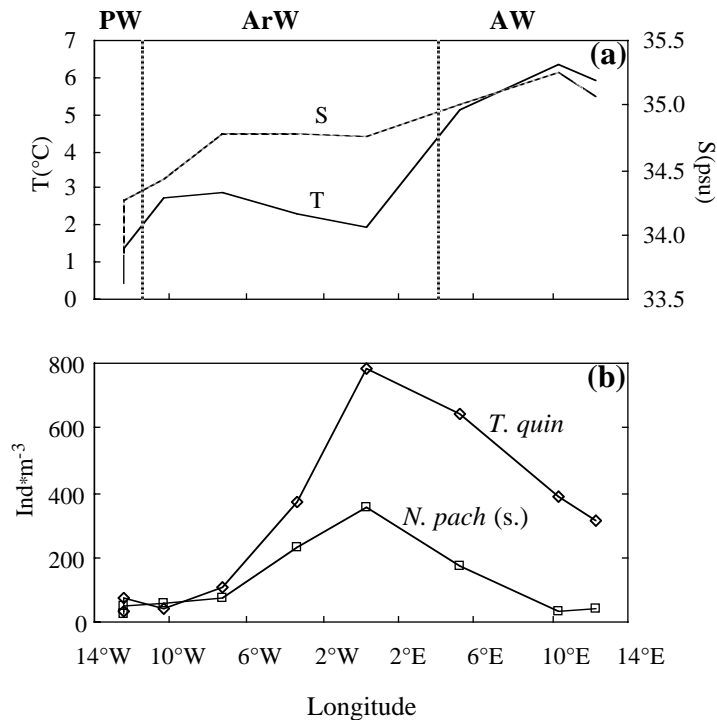


Figure 22: Greenland Sea (75°N): Distribution of (a) average temperature (solid line) and salinity (dotted line) in 0-50 m, (b) absolute abundances of *N. pachyderma* (s.) and *T. quinqueloba* in the 0-200 m (integrated values). PW: Polar water; ArW: Arctic water; AW: Atlantic water.

A comparison between the distribution of *N. pachyderma* (s.) and *T. quinqueloba* in the Polar and Atlantic water along the 75°N-transect (ice-free) and 80°N-transect (ice-covered) indicates the lower abundances of both species in the ice-covered Fram Strait can be attributed to the ice coverage only, but not the changes of their main habitat (Table 6). The maximum abundances were established in the ice-covered Polar water in 0-100 m and in the ice-free Polar water between 50 and 200 m. An inverse relationship was found in the Atlantic water: in ice-free and ice-covered conditions, the abundance maximum was found in 0-100 m and 50-200 m, respectively. The literature references on the influence of ice coverage on foraminiferal abundance are partly contradictory. In contrast to studies of Jensen (1998) and Volkmann (2000a) in the Fram Strait, Carstens et al. (1997) established that the abundance of planktonic foraminifera correlates with the degree of the ice-coverage. Volkmann (2000a) reported, *N. pachyderma* (s.) and *T. quinqueloba* prefer a shallow depth habitat (0-50 m) under the permanent ice cover and

migrated in ice-free areas below 100 m in the Laptev Sea, Fram Strait and Barents Sea.

Like all planktonic organisms, the distribution of planktonic foraminifera in the water column is usually non homogenous (patch-wise) (e.g. Boltovskoy, 1971; Hemleben & Spindler, 1983; Carstens & Wefer, 1992). The very high abundances of *T. quinqueloba* established at station 81 in the Fram Strait (Figure 14d) may be explained as a result of patchiness (small scale variations in abundance). The continuous increase in abundance of *N. pachyderma* (s.) and *T. quinqueloba* in the Arctic water relative to other water masses in the Greenland Sea (Figure 22a-b) can not be explained with patchiness, however.

Several authors report the increase of foraminiferal concentrations offshore (e.g. Vilks, 1973; Ortiz et al., 1995; Berberich, 1996). In the Greenland Sea, the abundance of *N. pachyderma* (s.) and *T. quinqueloba* rose at stations with the greatest water depth (see Table 1). The fact that partly higher abundances were established for some near coast stations than for offshore stations indicates however, that water depth was not the primary controlling factor for the detected increase in foraminiferal abundance.

Besides the parameters discussed above, the food supply (e.g. *chl a* concentrations) can lead to changes in foraminiferal abundance. Most planktonic species live in the euphotic zone, where they find the largest diet source of phytoplankton and zooplankton. The examination of the feeding vacuoles of planktonic foraminifera from the multinet tows and laboratory cultures has shown most foraminiferal species to be omnivorous (Anderson et al., 1979; Spindler et al., 1984). The spinose species (like *T. quinqueloba*) show a preference for zooplankton, while the non-spinose species (like *N. pachyderma* (s.)) are more herbivorous (Anderson et al., 1979; Hemleben & Auras, 1984; Hemleben et al., 1985). In the sampling period of this study (mid till end of July), the depth distribution of foraminiferal abundance and *chl a* concentrations were not correlated. The maximum abundances of *N. pachyderma* (s.) and *T. quinqueloba*, as a rule, were found below the *chl a* maximum (0-50 m) in the Greenland Sea and Fram Strait. This result is being confirmed by another study in the Fram Strait (Volkman, 2000a), which established an abundance maximum of *N. pachyderma* (s.) and *T. quinqueloba* below the *chl a* maximum as well. The highest concentrations of *N. pachyderma* (s.) in the summer months in Antarctica were also found below the maximum of the phytoplankton biomass (Berberich, 1996). In contrast, some authors established the highest abundances of asymbiotic species at the chlorophyll maximum in the North Atlantic (Fairbanks & Wiebe, 1980; Fairbanks et al., 1982). The maximal abundance of *N. pachyderma* (s.) coincided with the *chl a* maximum in the NEW-Polynya as well (Kohfeld et al., 1996).

Although *N. pachyderma* (s.) is regarded as a species feeding on phytoplankton (Hemleben et al., 1989), the horizontal distribution of this species in the Greenland Sea and the Fram Strait

was also not correlated with *chl a* concentrations. In the Greenland Sea at 75°N, a seasonal thermocline was established during the sampling period. Much higher *chl a* concentrations (0.6-3.7 µg/l) and foraminiferal abundances were found there when compared to the Fram Strait at 80°N (0.3-1.2 µgchl a /l), where sea-ice melting, which is highly variable in time and space, controls the stratification. The development of the phytoplankton bloom, which is dominated by diatoms (Bauerfeind et al., 1994; Kohly, 1998), occurs in the Greenland Sea in May-June (before Mid-July) and is dependent on the ice-coverage. The occurrence of phytoplankton bloom and the zooplankton biomass in the Greenland Sea are temporally not coupled with each other (v. Bodungen et al., 1995), which would explain the *chl a* independent distribution of *N. pachyderma* (s.) in this region.

The lack of correlation between the distribution of *N. pachyderma* (s.) and *chl a* concentrations established in this study suggests that the trophic strategy of this species does not only include algae. The electron microscope examination of the feeding vacuoles of this species substantiates, that *N. pachyderma* (s.) ingests mainly diatoms and other eukaryotic algae (Anderson et al., 1979; Kohfeld et al., 1996). Specimens kept in a laboratory culture feed on algae as well (Spindler, 1996). In the present study, the individuals of *N. pachyderma* (s.) in the multinet samples had a light-green, brown and "copepod-orange" cytoplasm, which might be an indication for the species' omnivorous diet. The feeding behaviour of *T. quinqueloba* under natural conditions is still unknown. According to Hemleben et al. (1989), *T. quinqueloba* is regarded as symbiont-bearing, which would explain its *chl a* independent distribution. The cytoplasm of this species in the multinet samples was usually of pale white, golden-green and light-brown colour.

4.1.3 Reproductive Cycles

The abundance and the shell size of planktonic foraminifera are above all influenced by the reproduction synchronized with the lunar periodic cycle (e.g. Spindler et al., 1979; Bijma et al., 1990a; Erez et al., 1991). In the lower latitudes, a synchronic reproduction of a large number of gametes was found in fixed water depths for some foraminiferal species (Hemleben et al., 1989). Erez et al. (1991) used the abundance, mean shell size and kummerforms percentage of the tropical species *G. sacculifer* to derive the lunar reproductive cycles. According to them, the population had grown in just a few days before the full moon and sinks below the euphotic zone in order to reproduce. A synchronic gamete release during the full moon initiates the reproduction there. After the gametes fusion (zygote formation) and a further development, the juveniles start to rise to the euphotic zone during the new moon. The foraminiferal development includes five stages before the lunar cycle begins anew (Brummer et al., 1987; Lee & Anderson, 1991). The reasons for the vertical migration might include the optimal nutrient con-

ditions in thermocline and chlorophyll-maximum (Murray, 1991) and better living conditions in non-influenced depths (no ice-coverage) as well as the lack of predators. Accordingly, the foraminiferal organisms must have a mechanism allowing for buoyancy. Besides the spines and pseudopodia net, Anderson and Bé (1976) suspect the existence of vacuolated fibrillar systems.

The influence of the moonlight (light/dark differences) was seen as a triggering mechanism of the synchronic reproduction in low latitude environments. The few studies with the timing of the lunar periodicity conducted in the polar regions (Carstens, unpublished data; Berberich, 1996; Volkmann, 2000a), indicate that the reproduction of *N. pachyderma* (s.) and *T. quinqueloba* is influenced by lunar cycles in these regions as well. The short or non-existent dark phases during the time of the new moon above 55°N, especially during the summer, lead to the assumption that not the moonlight itself, but rather the changes in the earth's magnetic field trigger a synchronic reproduction at these latitudes (Bijma et al., 1990a).

The samples being examined in this study were taken in different regions and at variable times, therefore the reproductive cycles are only partially discernible (Figure 23). The lunar periodicity may be masked due to the complex hydrographic regime in the survey area, as well as the different sampling period. Even so, the combination of all data sets led to the assumption that *N. pachyderma* (s.) and *T. quinqueloba* reproduce around the full moon in these regions.

In the Labrador Sea, the shell size of *N. pachyderma* (s.) and *T. quinqueloba* sharply increased between 50 and 200 m four days before the full moon (Figure 4). One day before the full moon, a decrease of the mean shell size evident in all depths occurred. At the same time, the proportion of dead individuals reached the maximum in 0-200 m (Figure 23c and 24). These results indicate that the gametogenesis of both species takes place two or three days before the full moon. Besides the shell size changes, *N. pachyderma* (s.) showed an increase of abundance below 50 m depth four and one day before the full moon (Figure 3b, stations 361 and 366). Since 50-61 % of living *N. pachyderma* (s.) in the 63-139 μm size-fraction were found in the 0-50 m depth interval in the Labrador Sea, whereas larger and mature individuals with a high proportion of reproductive characteristics occurred in 100-200 m, the vertical migration during the ontogenesis may be concluded. Arikawa (1983) and Berberich (1996) also assumed that the reproduction of *N. pachyderma* (s.) occurs in deeper water layers. In contrast, in the Panama Basin Bé et al. (1985) noted the similar depth distribution of the juvenile and adult population for *G. theyeri* and *G. dutertrei*, concluding that the reproduction of these species has to occur before the sinking of adults below the euphotic zone. They calculated the rising velocities of 0.5-2 m/d and 8-50 m/d for 5-10 μm large proloculi and multichambered individuals between 20-50 μm , respectively. Based on these calculations, the rising of juvenile *N. pachyderma* (s.), which in the Labrador Sea have to cross about 50 m of the water column does not seem improbable.

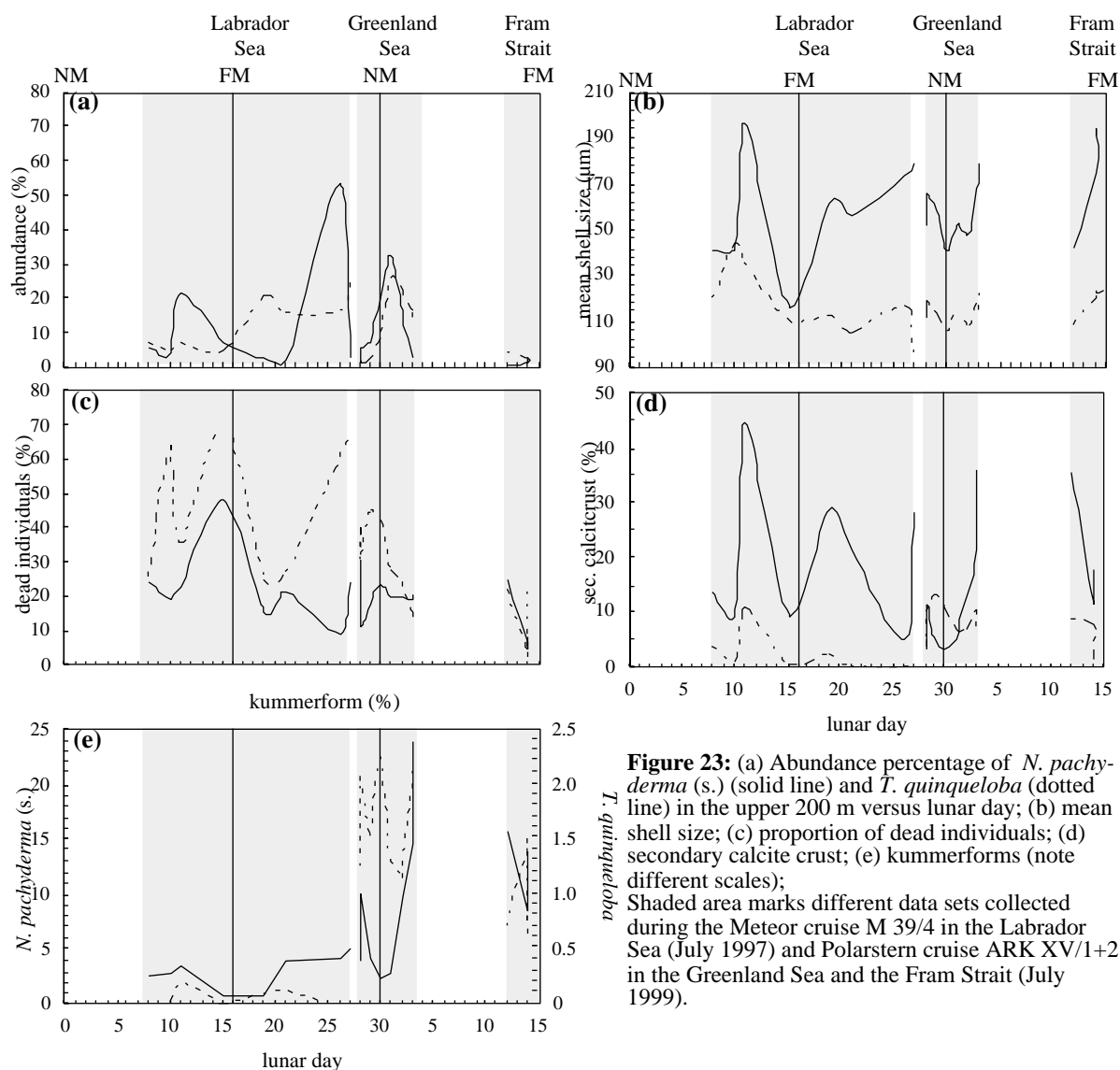


Figure 23: (a) Abundance percentage of *N. pachyderma* (s.) (solid line) and *T. quinqueloba* (dotted line) in the upper 200 m versus lunar day; (b) mean shell size; (c) proportion of dead individuals; (d) secondary calcite crust; (e) kummerforms (note different scales); Shaded area marks different data sets collected during the Meteor cruise M 39/4 in the Labrador Sea (July 1997) and Polarstern cruise ARK XV/1+2 in the Greenland Sea and the Fram Strait (July 1999).

Similar to *N. pachyderma* (s.), the abundance of *T. quinqueloba* in the Labrador Sea increases in 50-300 m one day before the full moon (Figure 3c, station 366). On the third and fifth day after the full moon, the abundance of this species was higher in 100-200 m compared to the upper 0-100 m (Figure 3c, stations 376 and 381). The maximum abundances and the smallest individuals of *T. quinqueloba* were found in 0-50 m three and four days before the new moon, which indicates a rising of juveniles into the surface water. As opposed to *T. quinqueloba*, the abundance of *N. pachyderma* (s.) on the third and fifth day after the full moon stays low in 0-200 m, while the shell size increases slightly (Figure 23a-b and 24). After fourteen days (four days before the new moon), the shell size of *N. pachyderma* (s.) slightly increases at strongly increasing abundance in 0-50 m. The shell size of this species increased again on the next day, the abundance however decreased dramatically, in all probability due to non-optimum conditions in the North Atlantic Current.

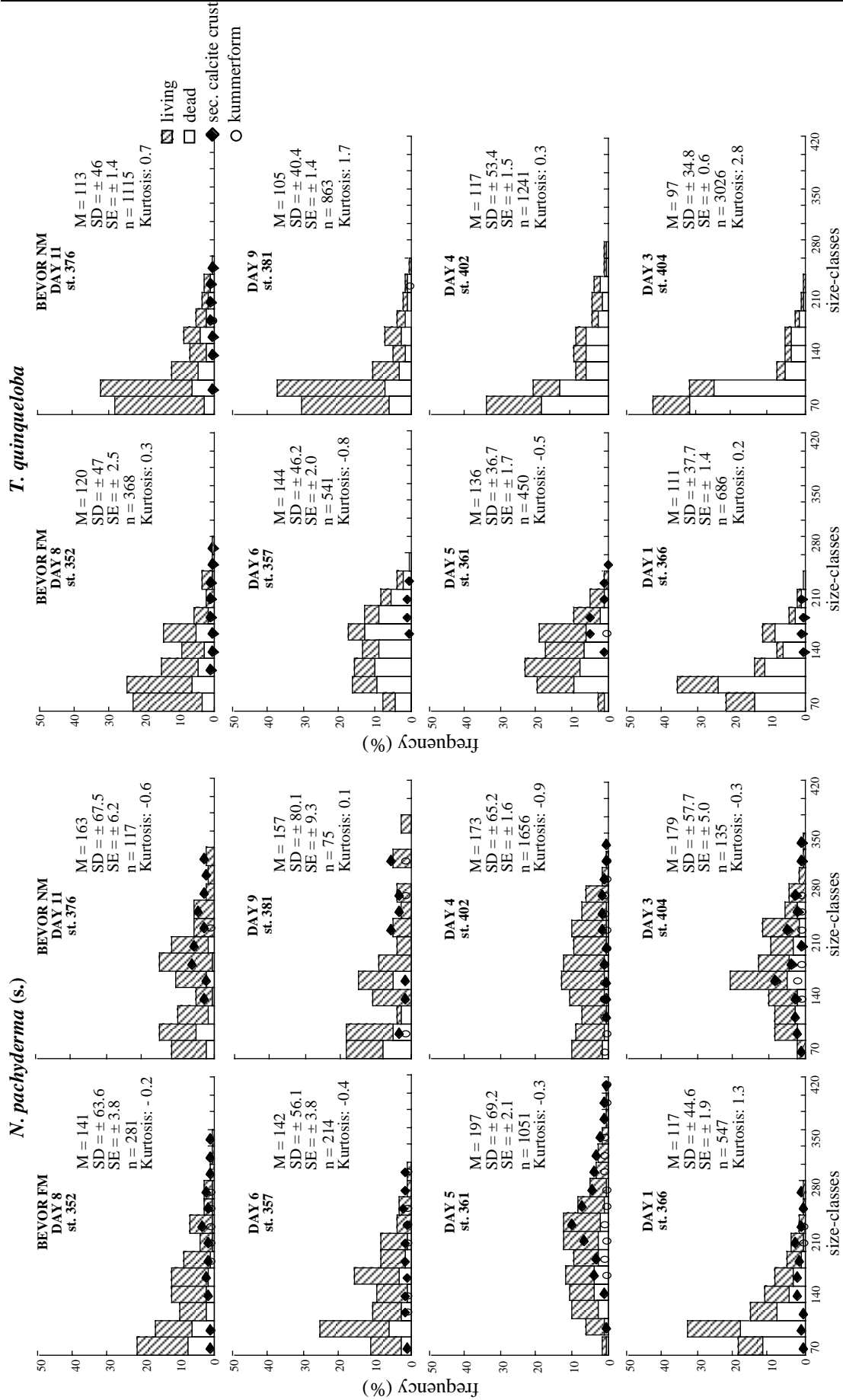


Figure 24: Frequency distribution of *N. pachyderma* (s.) and *T. quinqueloba* for 0-200 m in the Labrador Sea including the full moon (20.07.1997). The width of each size class is 23 μ m; M=mean, SD=standard deviation, SE=standard error, n=counts.

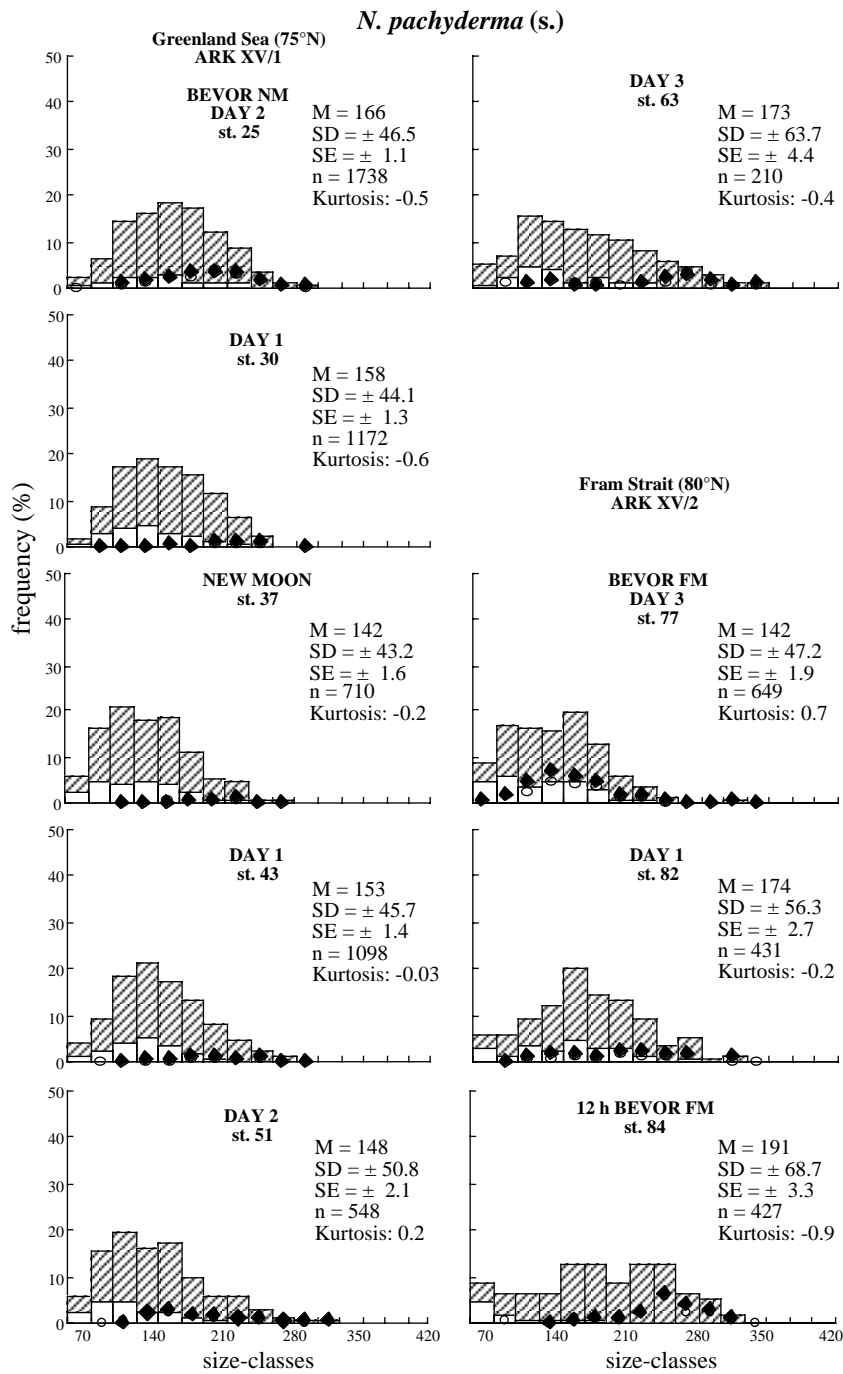


Figure 25: Frequency distribution of *N. pachyderma* (s.) and *T. quinqueloba* for 0-200 m in the Greenland Sea and Fram Strait including the new moon (13.07.1999). The width of each size class is 23 μ m. M-mean, SD-standard deviation, SE-standard error, n-counts. For further explanations see legend on page 48.

In the samples from Greenland Sea, which were taken around the new moon, both species show a strong increase in abundance at decreasing shell size (Figure 23a-b and 25). These variations in abundance and size can not be explained by either hydrographic conditions or chla concentrations (Chapter 4.1.2). The highest abundances and smallest shells of *N. pachyderma* (s.) and *T. quinqueloba* were found one day after the new moon in 0-50 m and 50-

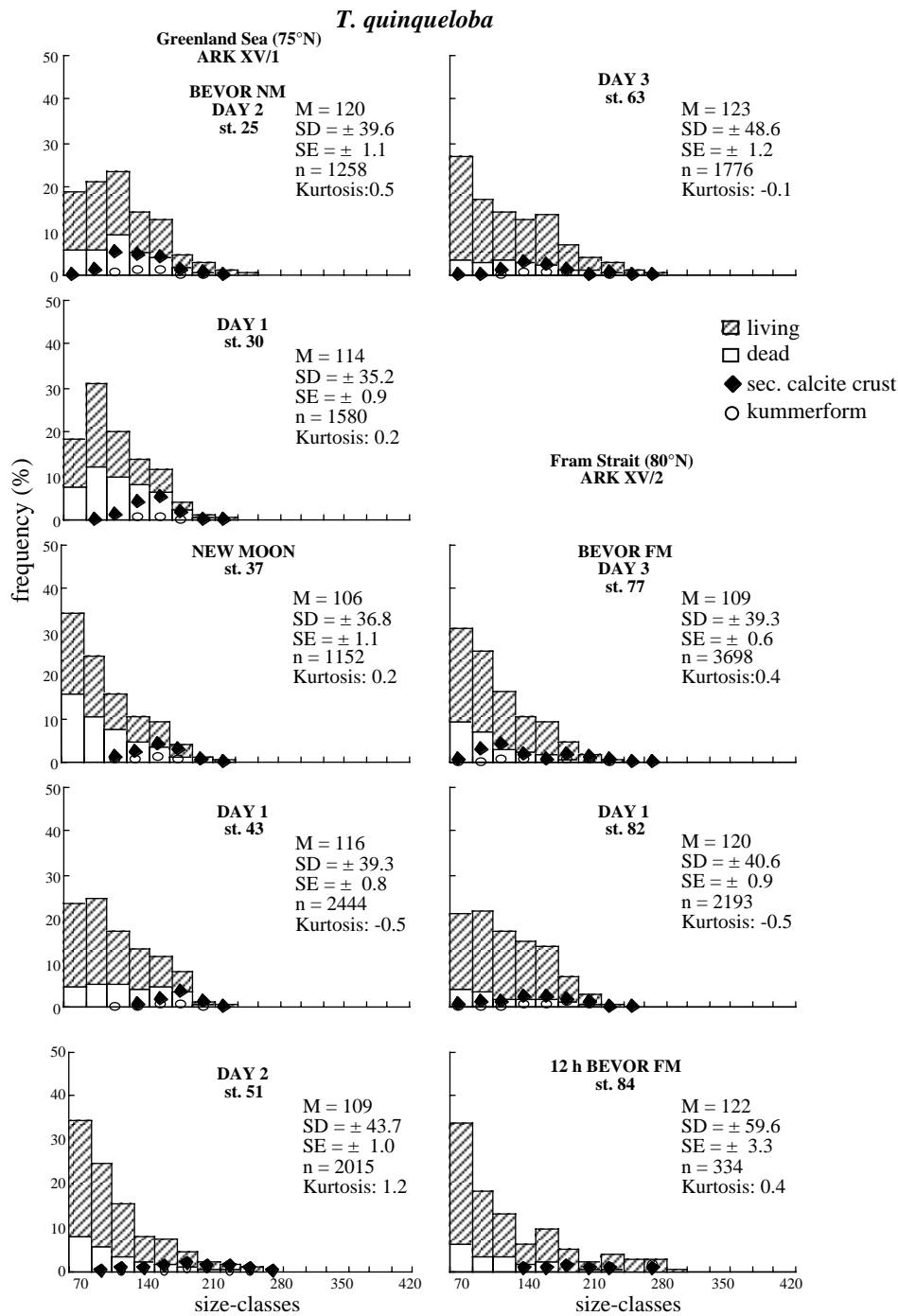


Figure: 25: Continued.

100 m depths, respectively (Figure 10c-d and 11, station 43). Three days after the new moon, a strong decrease in abundance of *N. pachyderma* (s.), coupled with an increase in shell size, occurred in the Atlantic water, while *T. quinqueloba* showed a slight decrease in abundance parallel to increasing shell size (Figure 10c-d and 11, stations 51-66).

In the samples taken after eight days in the Fram Strait, both species showed an increase in shell size one day before the full moon (Figure 23b and 25). The transect at 80°N was sampled

within two days (one and two days before the full moon), in this time, the mean shell size of *N. pachyderma* (s.) and *T. quinqueloba* increased on average by 51 and 14 μm , respectively (Figure 25). Beside the forthcoming reproduction, the optimal hydrographic conditions (Hemleben et al., 1989) and the higher light intensity in case of symbiont-bearing species (Spero & Lea, 1993) can lead to the formation of the larger shells. Only in the Fram Strait, however, a weak negative correlation between temperature and mean shell size of *N. pachyderma* (s.) was found in the present study (Figure 26).

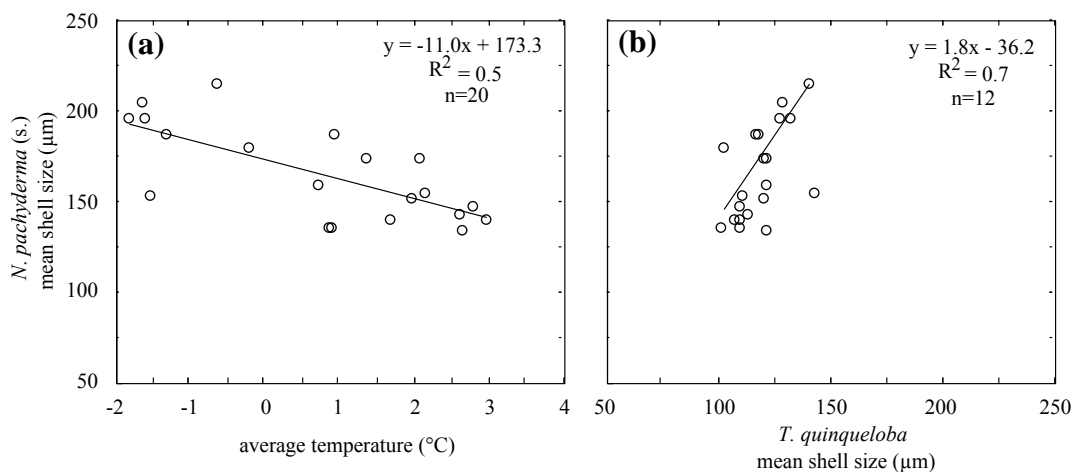


Figure 26: Relationships between mean shell size of *N. pachyderma* (s.) and (a) temperature, (b) mean shell size of *T. quinqueloba*, 0 to 200 m, in the Fram Strait (80°N).

Bijma et al. (1990b) noticed that larger shells of single species are more likely to result from optimal temperature and salinity than from extreme conditions. The very low temperatures and salinities in the East Greenland Current (80°N) rather indicate the rapid increase of *N. pachyderma* (s.) and *T. quinqueloba* in shell size to be attributed to the imminent reproduction around the full moon.

The assumption of the reproductive cycles for *N. pachyderma* (s.) and *T. quinqueloba* is further supported by the distribution of individuals with gametogenetic calcification and an atypical last chamber (kummerform chamber) (Figure 23d-e). In the last (terminal) stage of foraminiferal development, the ultrastructure of the shells is drastically altered with the resorption of the spines and chambers septa (Brummer et al., 1987), the formation of the kummerform and a gametogenetic calcite crust (Hemleben et al., 1989). The maximum percentage of kummerform *N. pachyderma* (s.) in 0-200 m (5 %) in the Labrador Sea was found three days before the new moon, while the most encrusted individuals (45 %) were detected four days before the full moon (Figure 23d-e). *T. quinqueloba*, on the other hand, showed a highest proportion of kummerforms (0.2 %) and secondary calcification (11 %) four days before the full moon (Figure 23d-e). The samples from the Greenland Sea and Fram Strait, due to a low temporal resolution, do not allow a reliable statement regarding the distribution of individuals

with reproductive characteristics with timing of the lunar cycle. The maximum proportion of encrusted *N. pachyderma* (s.) about 36 % and kummerforms (24 and 16 %) in the Atlantic water were each found on the third day after the new moon and two days before the full moon (Figure 23d-e). *T. quinqueloba* in the Greenland Sea showed the highest proportion of kummerforms (2 %) and secondary calcification (13 %) one day before the new moon (Figure 23d-e). In the Fram Strait, this species showed one and two days before the full moon a similar proportion of kummerforms and secondary calcite of 2 and 9 %, respectively. The changes in distribution of individuals with reproductive characteristics and absolute abundance in the Labrador Sea indicates a semi-lunar and lunar periodicity for *N. pachyderma* (s.) and *T. quinqueloba*, respectively. This conclusion is supported by the study of Arikawa (1983), who used the net tows and sediment trap data from the Northwest Pacific to calculate the turnover times of 14-15 and 22 days for *N. pachyderma* (s.) and *T. quinqueloba*, respectively. Hemleben et al. (1989) assumed a lunar cycle for *T. quinqueloba* as well.

According to Arikawa (1983), the gametogenetic calcite crust accounts for > 50 % of the total shell mass for *N. pachyderma* (s.), whereas *T. quinqueloba* just seals the pores with calcite after the shedding or resorption of the spines prior to gametogenesis (Hemleben et al., 1989). In contrast, other authors established for some non-spinose species, that the secondary calcification may be induced by low temperatures (Hemleben & Spindler, 1983; Hemleben et al., 1989; Srinivasan & Kennett, 1974). In this study however, no correlation between variations in temperature and secondary calcification was detected. The proportion of encrusted *N. pachyderma* (s.) and *T. quinqueloba* accounted for maximally 67 % and 32 % (per depth interval) in the upper 0-200 m, being in all samples higher than the proportion of kummerforms with maxima at 29 % and 5 %, respectively. The induction of kummerform phenotype occurrence are not sufficiently understood yet. While some authors (Berger 1969, 1970; Hecht, 1976; Berberich, 1996) interpret the existence of kummerform chambers as an indication of the environmental stress (e.g. slowing growth due to insufficient food supply), other authors established that the reproductive processes induced its formation (Olsson, 1973; Hemleben et al., 1989; Bijma et al., 1990a). In the present study, the abundance of kummerforms and temperature, salinity, chl_a concentrations are uncorrelated. Even with the extreme temperature and salinity in Polar water (Fram Strait), no significant increase of individuals with this characteristic was found. The variation in kummerform phenotypes for *N. pachyderma* (s.) and *T. quinqueloba* can therefore not be unambiguously interpreted as a result of environmental stress in this study. This is being confirmed by Bijma et al. (1990b), who in the laboratory culture of tropic and subtropic species only rarely detected the kummerform chamber formation at extreme temperature and salinities. Consistent with studies by Carstens (1988) and Berberich (1996), reproductive characteristics were however already found on individuals as small as 80 µm (Figure 24 and 25), indicating that both reproduction as well as environmental stress can re-

sult in the formation of kummerforms and secondary calcite crust.

4.2 Isotopic Composition of *N. pachyderma* (s.) and *T. quinqueloba*

4.2.1 Effect of Size, Weight and Encrustation on the Stable Isotope Composition of *N. pachyderma* (s.) and *T. quinqueloba*

An important question for paleoceanographic interpretations is, how accurately the ^{18}O and ^{13}C values of planktonic foraminifera reflect the conditions in the water column. The isotopic composition of foraminiferal tests is influenced by both environmental conditions (temperature, salinity, foraminiferal diet, $[\text{CO}_3^{2-}]$ and pH) and by the ontogenetic development of foraminiferal species (e.g. Epstein et al., 1951; Berger et al., 1978; Curry & Matthews, 1981; Bouvier-Soumagnac & Duplessy, 1985; Spero, 1992). The growth of planktonic foraminifera includes two processes: the formation of chambers (accretionary growth) and in later development stages the formation of a secondary calcite crust (Hemleben et al., 1989). While the accretion of chambers leads to an increase in shell size, the shell encrustation rather causes an increase of the shell density due to the increasing weight (Schweitzer & Lohmann, 1991; Lohmann, 1995).

The shell size is an important factor influencing the ^{18}O and ^{13}C incorporation into the foraminiferal shells. The isotopic composition of single species may vary by more than 1 ‰ as a function of shell size (Berger et al., 1978; Curry & Matthews, 1981). Detailed studies of the isotope signal on *N. pachyderma* (s.) in the Labrador Sea have established that the nonencrusted shells tend to heavier ^{18}O values with increasing size. For example, the ^{18}O value within the 150-240 μm size fraction at stations 361 (0-200 m) and 402 (0-50 m) increased by approximately 0.26 ‰ and 0.41 ‰, respectively (Figure 6a). One hypothesis to explain this ^{18}O increase in larger shells are the changes of metabolic rate during ontogeny. In culture experiments on the asymbiotic, spinose species *G. bulloides*, Spero & Lea (1996) detected a ^{18}O increase over the 180-500 μm size range. They suggest, that in earlier stages of foraminiferal development more of the isotopically light metabolic CO_2 is used for chamber formation than in later stages. In contrast, no significant differences in ^{18}O with increasing size were found for nonencrusted *N. pachyderma* (s.) in the Labrador Sea below 200 m depth (Figure 6a). This is in agreement with observations in the Fram Strait, where no variations in ^{18}O as a function of shell size (all depth intervals) in the examined size classes between 190-360 μm and 150-240 μm for *N. pachyderma* (s.) and *T. quinqueloba* were established (Figure 17).

Assuming that *N. pachyderma* (s.) secretes its shells in equilibrium with seawater, the depth at which the ^{18}O of foraminiferal shells is approximately equal to the ^{18}O predicted for inorga-

nic calcite formed in equilibrium with seawater ($^{18}\text{O}_{\text{Eq}}$, Equation 3) corresponds to the so called calcification depth. The deviation of measured ^{18}O from $^{18}\text{O}_{\text{Eq}}$, is the so called "vital effect" (Urey et al., 1951). The average ^{18}O value of nonencrusted *N. pachyderma* (s.) in 0-50 m reflected well the $^{18}\text{O}_{\text{Eq}}$ in 10 m depth at station 402 (Figure 7). At this station, the vital effect was reduced with increasing size as follows:

$$\text{vital effect} = -0.004 * (\text{size}) + 1.1; r^2 = 0.87, n = 17 \quad (13)$$

The ^{18}O value of shells in the 140-240 μm size fraction was lighter than $^{18}\text{O}_{\text{Eq}}$, whereas the ^{18}O of shells $> 240 \mu\text{m}$ were slightly heavier than $^{18}\text{O}_{\text{Eq}}$ in 10 m. This result, as well as a high noise of ^{18}O values detected at both examined stations (361 and 402) in the Labrador Sea, indicate that the established ^{18}O increase with increasing shell size of nonencrusted individuals mainly derives from the different distribution of larger and smaller individuals within the 0-50 m depth interval. This assumption is being supported by the study of Hemleben & Bijma (1994), who found the size dependent depth preferences for the distribution of *G.sacculifer* in the productive zone. In their study, the upper 20 m constituted the preferred habitat for specimens between 100-300 μm , whereas specimens $>300 \mu\text{m}$ were detected in the depth range from 20 to 40 m.

Besides the size dependent ^{18}O increase in nonencrusted *N. pachyderma* (s.), the ^{18}O increased with depth at station 361 (Figure 7). There, the ^{18}O of nonencrusted shell of the same size fraction (140-240 μm) and weight ($1.2 \pm 0.5 \mu\text{g}$) increased in the 50-100 m depth interval approximately by 0.34 ‰ relative to the upper 0-50 m (Figure 7). In contrast, the ^{18}O of nonencrusted shells in this size fraction do not vary between 50-100 m and 100-200 m depths. Since the weight of nonencrusted shells does not change throughout the water column, the ^{18}O increase between 0-50 m and 50-100 m is interpreted as depth dependent variation.

Neither the encrusted *N. pachyderma* (s.) in the Labrador Sea and Fram Strait nor the encrusted *T. quinqueloba* in the Fram Strait show a size dependent ^{18}O change in the present study (Figure 6 and 17). In contrast, several previous studies of different size fractions have demonstrated increasing ^{18}O with increasing size for *N. pachyderma* (s.) (Sautter & Thunell, 1989; Bauch et al., 1997; Volkmann, 2000b) and *T. quinqueloba* (Volkmann, 2000b). These studies have shown no consistent offset from $^{18}\text{O}_{\text{Eq}}$ in size dependent ^{18}O variability however. Alderman (1996) even detected an ^{18}O decrease with increasing shell size. This indicates the shell size to have no significant influence on the ^{18}O signal of encrusted shells, therefore the changes in ^{18}O with increasing size to be mainly the result of various depth distribution of different size classes (Sautter & Thunell, 1989; Alderman, 1996). Emiliani (1971) also concluded the variations in the isotopic composition of different shell sizes to result from the change of the habitat depth during ontogenetic development.

The secondary calcification of *N. pachyderma* (s.) is induced during the terminal stage and linked to the alteration of the shell ultrastructure. Continued encrustation turns the shell pores increasingly invisible. The secondary calcite crust, which consists of robust, euhedral calcite crystals (Kennett & Srinivasan, 1983), accounted on average for 63 % of the total weight for *N. pachyderma* (s.) (Chapter 3.1.2). Arikawa (1983) detected in the Northwest Pacific that the secondary calcite crust of *N. pachyderma* (s.) may amount to more than 50 % of the total weight. Even though the encrusted shells in the present study were on average ~35 % lighter in weight than heavily encrusted shells, no significant differences in isotopic composition between encrusted and heavily encrusted shells, as well as within each of the two encrustation groups, were found. In the sediments from the Sulu Sea, Sautter (1998) detected upon examination of dextral-coiled morphotypes from the genus *Neogloboquadrina* that the mass of secondary calcite, or the degree of encrustation, is not a significant variable controlling the oxygen isotope composition of the crystalline (heavily encrusted) and reticulate textural groups.

In contrast, the nonencrusted *N. pachyderma* (s.) from the Labrador Sea (station 361) were on average 0.6 ‰ depleted in ^{18}O relative to encrusted shells. At station 402 (0-50 m) in the Labrador Sea and in the Fram Strait however, no systematic ^{18}O differences between non-encrusted and encrusted *N. pachyderma* (s.) were found. The ^{18}O values of nonencrusted *T. quinqueloba* in the Fram Strait were not significantly lighter in ^{18}O than encrusted shells as well. These results indicate that the ^{18}O increase in encrusted shells is a result of ontogenetic migration of mature individuals in deeper and colder water. Due to a thermally rather homogeneous water column in the Fram Strait (in the main habitat of planktonic foraminifera), the influence of gametogenetic calcification on the oxygen isotope signal is less than in the more stratified water column in the Labrador Sea. Similar results for *N. pachyderma* (s.) have been documented by other studies (Kohfeld et al., 1996; Simstich, 1999) and were inferred to be caused by the addition of a secondary calcite in greater water depths. Duplessy et al. (1981) have shown as well the ^{18}O change in *G. sacculifer* during gametogenetic calcification to be correlated with the sinking into the deeper water layers.

The ^{13}C values in all examined calcification groups of *N. pachyderma* (s.) increased as a function of shell size (Figure 6d-f). In the Labrador Sea at station 361, only encrusted shells <300 μm showed clearly heavier ^{13}C values than the nonencrusted shells. The ^{13}C values of encrusted and nonencrusted shells are equalized with each other with increasing size, indicating the ^{13}C signal of *N. pachyderma* (s.) to be primarily controlled by the size. That agrees with the findings of Ravelo & Fairbanks (1995), who detected no weight dependent ^{13}C changes for asymbiotic species in the sediments of the tropical Atlantic.

The established relationship between ^{13}C and size for all examined calcification groups of *N. pachyderma* (s.) (Equation 9) is in good agreement with the ^{13}C progression versus size for

the symbiont-bearing species *G. sacculifer*, given by Hemleben & Bijma (1994) (Equation 13). The ^{13}C values of both species track the logarithmic growth curve typical for planktonic foraminifera:

$$^{13}\text{C} = -7.96 + 3.52 * \text{Log}(\text{size}) \quad (13)$$

Accordingly, the shells of *G. sacculifer* are being more enriched in ^{13}C (due to increasing symbiont activity) during the ontogenetic development than shells of *N. pachyderma* (s.), leading to larger ^{13}C difference between both species with increasing size. The symbiont activity is a possible explanation for the ^{13}C values of *T. quinqueloba* in the Fram Strait to be $\sim 1.2 \pm 0.4$ ‰ ($n = 30$) lighter than ^{13}C of *N. pachyderma* (s.). The ^{18}O values of both species however differ with ^{13}C of 0.4 ± 0.3 ‰ less severely, indicating the symbiont activity to only slightly influence the ^{18}O value of planktonic foraminifera. Spero et al. (1997) detected in culture experiments examining the symbiont-bearing species *O. universa*, that the symbiont activity cause the pH value in seawater to decrease due to increasing CO_3^{2-} concentration. On a $[\text{CO}_3^{2-}]$ increase of $100 \mu\text{mol/kg}$, this species shows a decrease in ^{13}C and ^{18}O of 0.7 ‰ and 0.2 ‰, respectively (Spero et al., 1997).

The ^{13}C values of planktonic foraminifera are mainly determined by the $^{13}\text{C}_{\text{DIC}}$ (Dissolved Inorganic Carbon) in the seawater (Berger et al., 1978; Bouvier-Soumagnac & Duplessy, 1985; Spero, 1992). In the present study however, the ^{13}C for all examined size-classes and calcification groups from both Labrador Sea as well as the Fram Strait was clearly lighter than the $^{13}\text{C}_{\text{DIC}}$ values (Figure 7 and 18). For the Labrador Sea predicted $^{13}\text{C}_{\text{DIC}}$ shows slightly vertical variations over the 0 to 50 m depth. At station 402 on average 0.7 ‰ higher $^{13}\text{C}_{\text{DIC}}$ values were calculated compared to station 361 (Figure 7). Despite of this difference, the ^{13}C of *N. pachyderma* (s.) shows no significant variation between the both stations. The magnitude of the ^{13}C increase as a function of size in *N. pachyderma* (s.) showed no station dependent variations as well. The ^{13}C difference between small and large shells (size effect) for non-encrusted *N. pachyderma* (s.) at station 402 (0-50 m) was with approximately 1.54 ‰ larger than the $^{13}\text{C}_{\text{DIC}}$ difference between 10 and 50 m depth (0.84 ‰). The size effect was reduced in encrusted shells (station 361) and amounted with increasing size to a minimum of 0.9 ‰ for shells $> 330 \mu\text{m}$. The ^{13}C variations in *N. pachyderma* (s.) can therefore not be explained with $^{13}\text{C}_{\text{DIC}}$ changes between both stations and are more likely influenced by metabolic processes in this species. These results are being confirmed by other investigations on *N. pachyderma* (s.), which have established this species to show lighter ^{13}C than $^{13}\text{C}_{\text{DIC}}$, or be completely out of equilibrium (Ortiz et al., 1996; Bauch et al., 1999; Simstich, 1999; Volkmann, 2000b). In contrast, some sediment trap studies have established that ^{13}C of left and right-coiling *N. pachyderma* show a clear seasonal signal and calcify in equilibrium with ^{13}C of ambient water

(Sautter & Thunell, 1989; Alderman, 1996). Ortiz et al. (1996) have suggested that carbon isotope disequilibrium of foraminiferal shells in the plankton tows may result from an increasing metabolic rate, related to temperature and/or food supply. The influence of temperature on ^{13}C of planktonic foraminifera results from a change in isotopic fractionation that is caused by the change of the metabolic rate. The calibration studies of *N. pachyderma* (s.) in the South Atlantic reached the conclusion that carbon isotope disequilibrium is caused by several factors, including a combination of diet, calcification temperature and carbonate ion chemistry (Kohfeld et al., 1998, 2000). The change of the habitat depth is able to influence the ^{13}C values of planktonic foraminifera. The study of Kroon (1988) shows that the deep dwelling species prefer to incorporate the isotopically lighter ^{12}C .

4.2.2 The Estimation of Disequilibrium in ^{18}O and ^{13}C

In the view of isotopic composition of *N. pachyderma* (s.) up to now, the oxygen isotopic equilibrium has been assumed. At the examined stations in the Labrador Sea, the ^{18}O values of *N. pachyderma* (s.) reflect the predicted $^{18}\text{O}_{\text{Eq}}$ in the upper 50 m. Since no equilibrium shell calcite precipitation has been experimentally demonstrated for this species, this assumption is not necessarily correct. In order to be better able to compare results from this study with other studies, the deviation from isotopic equilibrium was at first calculated as the difference from the average $^{18}\text{O}_{\text{Eq}}$ or $^{13}\text{C}_{\text{DIC}}$ and isotopic composition of *N. pachyderma* (s.) and *T. quinqueloba* per depth interval:

$$^{18}\text{O}(\text{vital effect}) = ^{18}\text{O}_{\text{Eq}} - ^{18}\text{O}_{\text{shell}} \quad (14)$$

$$^{13}\text{C}(\text{vital effect}) = ^{13}\text{C}_{\text{DIC}} - ^{13}\text{C}_{\text{shell}} \quad (15)$$

Vital effects calculated correspondingly to the main habitat for the upper 0-200 m show a good agreement with the references from literature (Table 7).

Based on the concept of McConnaughey (1989), Ortiz et al. (1996) in the California Current used the slope of the ^{18}O to ^{13}C disequilibrium relationship of 0.37 to estimate the equilibrium points for several planktonic species. For biogene calcite, realistic ^{18}O : ^{13}C slopes of 0.32 and 0.29-0.41 (~0.34) were established for encrusted and nonencrusted *N. pachyderma* (s.) at the surface (0-50 m) in the Labrador Sea. The equilibrium points for both calcification groups were calculated using the slope of 0.32 (Figure 27). Accordingly, the average isotopic composition of encrusted and nonencrusted shells was lower than the equilibrium by 0.7 and 1.0 ‰ for ^{18}O and 2.1 and 2.8 ‰ for ^{13}C . A similar vital effect for this species was established by Ortiz et al. (1996) (Table 7). The equilibrium points for encrusted shells collected below 50 m (station 361) were between 50 and 75 m (Figure 27), whereas the equilibrium poi-

nts of nonencrusted shells, as well as for encrusted *N. pachyderma* (s.) collected at station 402, were in the upper 0-50 m. This result agrees well with the sediment surface study of Wu & Hillaire-Marcel (1994), who found in the Labrador Sea that *N. pachyderma* (s.) secretes its test in the surface layer during summer.

Table 7: Compilation of the vital effects calculated in this study and literature references.

Reference	<i>N. pachyderma</i> (s.)		<i>T. quinqueloba</i>		Area
	$\delta^{18}\text{O}$	$\delta^{13}\text{C}$	$\delta^{18}\text{O}$	$\delta^{13}\text{C}$	
Kohfeld et al. (1996)	1.0	-			NEW-Polynya
Ortiz et al. (1996)	0.7	2.4**			California Current
Bauch et al. (1997)	1.0				Arctic Ocean
Simstich (1999)	0.9	0.85	1.1	2.0	Greenland and Norwegian Seas
Volkman (2000)	1.0	1.3	1.3	2.6	Fram Strait (82°N)
this study*	0.7	1.1	-	-	Labrador Current
this study*	0.9	1.0	1.2	2.2	Fram Strait (80°N)
mean	0.9	1.0	1.1	2.3	

* Vital effects are given correspondingly to the main habitat for the upper 0-200 m.

For a better comparison with other studies, the vital effect for $\delta^{13}\text{C}$ is given with respect to $\delta^{13}\text{C}_{\text{DIC}}$.

** $\delta^{13}\text{C}$ difference with respect to $\delta^{13}\text{C}_{\text{Eq}}$

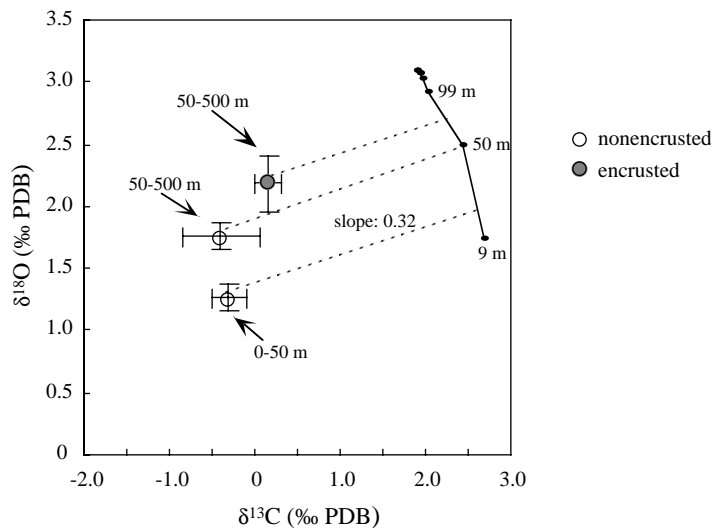


Figure 27: Carbon isotopes versus oxygen isotopes at station 361 in the Labrador Sea. Solid curve represents isotopic composition of equilibrium calcite (Equations 3, 5). Symbols denote measured $\delta^{13}\text{C}$ and $\delta^{18}\text{O}$ of *N. pachyderma* (s.). Dotted lines show used slope of 0.32 to estimate of equilibrium points.

In the Fram Strait, the ^{18}O values of *N. pachyderma* (s.) and *T. quinqueloba* were approximately equal to average $^{18}\text{O}_{\text{Eq}}$ in the upper 0-50 m only in the East Greenland Current (Figure 18, stations 83 and 84; Figure 28).

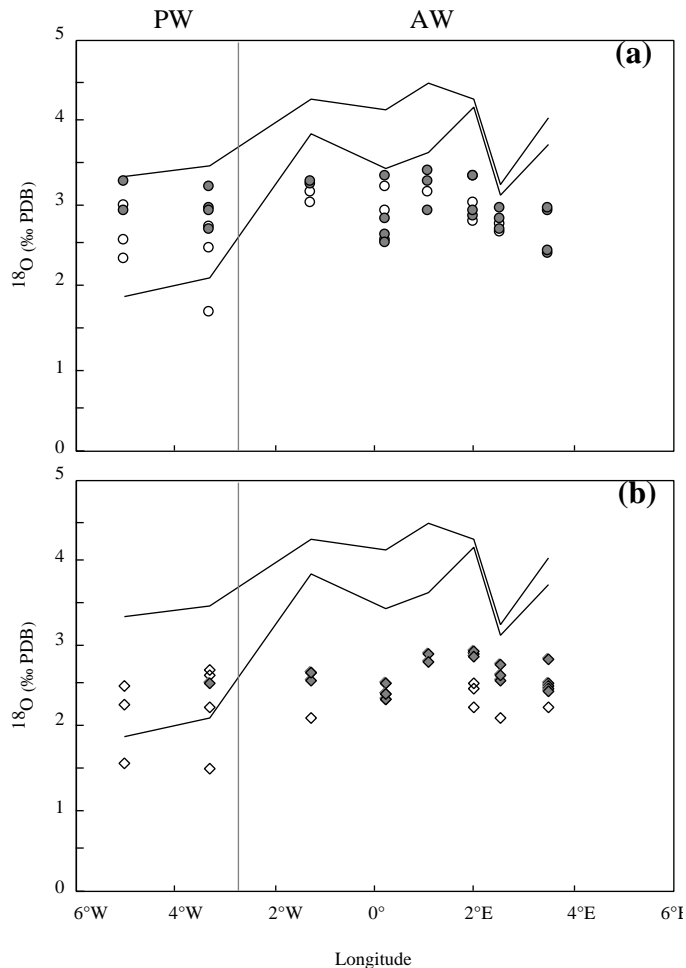


Figure 28: Distribution of ^{18}O along the 80°N -transect in the Fram Strait: (a) *N. pachyderma* (s.) and (b) *T. quinqueloba* in 0-500 m. Non-filled symbols: nonencrusted; filled: encrusted shells. Solid lines represent the $^{18}\text{O}_{\text{Eq}}$ range in the upper 0-50 m. PW: Polar water, AW: Atlantic water.

Using a slope of 0.32 in order to estimate the equilibrium points, the ^{18}O of *N. pachyderma* (s.) and *T. quinqueloba* were lower than $^{18}\text{O}_{\text{Eq}}$ by 0.5 ± 0.03 ‰ ($n = 6$) and 0.8 ± 0.2 ‰ ($n = 5$), consistent with equilibrium calcification at depths of 50 to 75 m. The ^{13}C of both species was 1.7 ± 0.09 ‰ and 2.5 ± 0.7 ‰ lighter than $^{13}\text{C}_{\text{Eq}}$. Nonencrusted and encrusted shells showed a similar vital effect for both isotopes in this part of the transect. Other observations of *N. pachyderma* (s.) established calcification depths in the upper water layers: between 20 and 40 m in the Sea of Okhotsk (Alderman, 1996), around 60 m in the San Pedro Basin (Sautter & Thunell, 1989) in the 5 to 35 m in the California Current (Ortiz et al., 1996) and at the surface (8 m) in the Arabian Sea (Ivanova et al., 1999). These references, as well as the results of the present study, indicate that *N. pachyderma* (s.) and *T. quinqueloba* spend only a part of their life cycle below 100 m, where most of the encrusted species were found. The migration into deeper water layers only takes place in the later development stages, whereas the secondary calcite crust is formed in a narrow temperature range before the sinking. This assumption is consi-

stent with the study of Simstich (1999), who uses a model exercise to derive that *N. pachyderma* (s.) calcifies within a narrow depth interval as opposed to a gradual calcite forming during the descent.

As a result of this calcifications behaviour, the magnitude of ^{18}O and ^{13}C between foraminiferal shells and predicted $^{18}\text{O}_{\text{Eq}}$ and $^{13}\text{C}_{\text{Eq}}$ in the present study may be influenced (among other factors) by the choice of sampled depth intervals. The magnitude of ^{18}O may furthermore be influenced by the used paleotemperature equation (Figure 29). In the present study, the equation of O'Neil et al. (1969) and Shackleton (1974) (Equation 3) were used in order to be better able to compare results from this study with other studies in the survey area. Figure 29 shows the offsets between predicted values ($^{18}\text{O}_{\text{Eq}}$) and plankton tows data. The paleotemperature equation of Erez and Luz (1983), which was calibrated with cultured *G. sacculifer* between 14°C and 30°C, is better fit with the ^{18}O values measured in the Fram Strait than the equation of O'Neil et al. (1969) and Shackleton (1974) calibrated for inorganic calcite. Zahn & Mix (1991) used core-top data from the Northeast Atlantic to test seven paleotemperature equations, establishing different equations to strongly diverge at temperatures below 5°C. Similar to the present study, the best fit to the ^{18}O of benthic genera *Uvigerina* in the study of Zahn & Mix (1991) was found using the equation of Erez and Luz (1983).

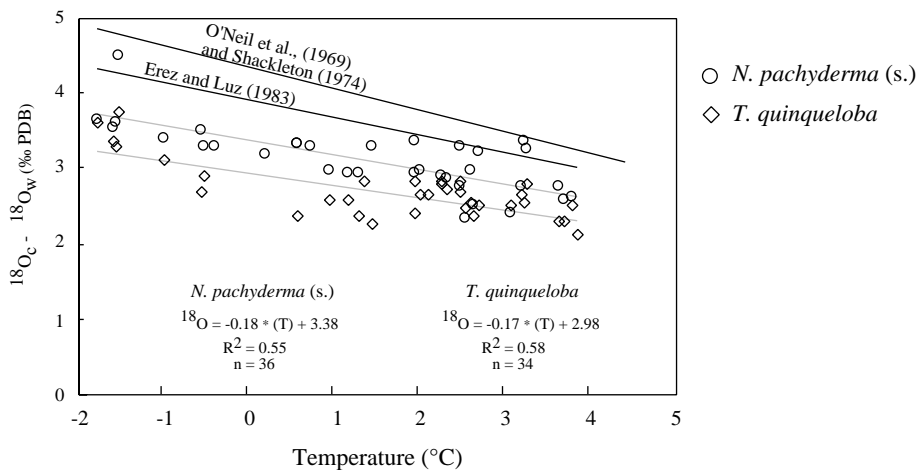


Figure 29: Relationship between ^{18}O of *N. pachyderma* (s.) and *T. quinqueloba* and temperature along the 80°N-transect in the Fram Strait.

The ^{18}O values of *N. pachyderma* (s.) and *T. quinqueloba* in the West Spitzbergen Current (WSC), however, are completely out of equilibrium (Figure 18, stations 77-82; Figure 28). The first possible explanation for that could be the non-linearity between salinity and $^{18}\text{O}_w$ observed in the WSC (Figure 16). The $^{18}\text{O}_w$ of the sea water is usually linearly correlated with salinity. Due to the influence of sea-ice meltwater (Craig & Gordon, 1965), the water ^{18}O values changed irregularly with salinity in this part of the transect. This non-linearity can affect the

^{18}O of foraminiferal shells. It can furthermore be assumed that *N. pachyderma* (s.) and *T. quinqueloba* have been advected out of warmer areas and reflect isotopically lighter (warmer) water. Using a linear relationship between $^{18}\text{O}_{\text{Eq}}$ and temperature established for this part of the transect: $T = -4.28 * (^{18}\text{O}_{\text{Eq}}) + 17.87$, ($r^2 = 0.95$, $n = 48$), the calcification temperature can be estimated from ^{18}O of foraminiferal shells. If ^{18}O of *N. pachyderma* (s.) from upper 0-50 m would be corrected by +0.5 ‰, the shell ^{18}O would reflect approximately 2.5°C higher temperature than those measured during the sampling period in the Fram Strait. This points to the lateral advection. Carstens & Wefer (1992) also assumed most of the subpolar foraminifera to be advected by branches of the Spitsbergen Current into the Nansen Basin. Bauch et al. (1997) also believe that the differences between the vital effect of *N. pachyderma* (s.) in the southern and northern region of the Nansen Basin may result from partial advection of this species in the southern regime.

4.2.3 Comparison between the Isotope Signal of *N. pachyderma* (s.) from Plankton Tows and from Surface Sediments in the Fram Strait

In the surface sediments of a transect across the Fram Strait (80°N), Spielhagen & Erlenkeuser (1994) reported lower ^{18}O values (2.4-2.6 ‰) in the eastern part and higher ^{18}O values in the central and western part (2.9-3.2 ‰) for *N. pachyderma* (s.). The comparison of the average isotopic composition from plankton tow (100-500 m) and core-top data generally resulted in a good match (Figure 30), whereas the cores located in the area of the plankton tows

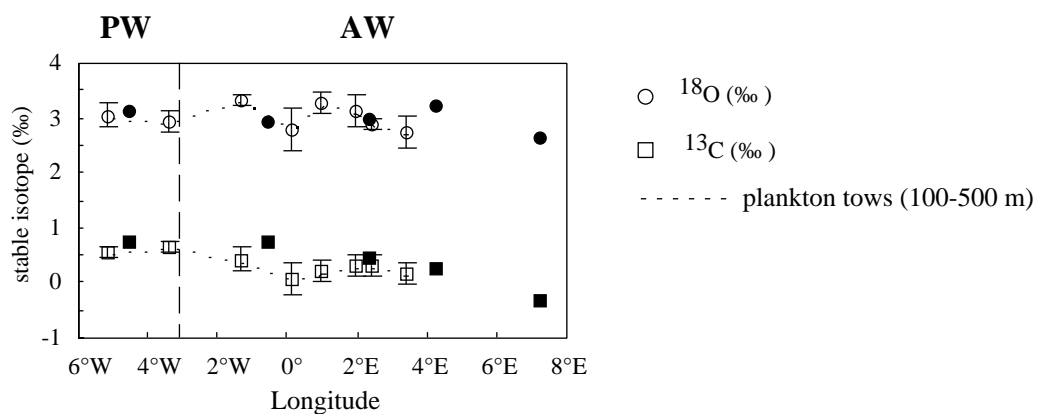


Figure 30: Mean isotopic composition of *N. pachyderma* (s.) from plankton tows and from surface sediments (Spielhagen & Erlenkeuser, 1994) along the 80°N-transect in the Fram Strait. Non-filled symbols represent plankton tows; filled: surface sediments. PW: Polar water, AW: Atlantic water.

and the multinet data did not let the ^{18}O trend described by Spielhagen & Erlenkeuser (1994) to be detected. This may be due to the spatial resolution of the multinet tows being not sufficient and the sampling being mainly in the central and western Fram Strait.

The ^{18}O values increase in the surface sediments by $0.2\pm 0.2\text{‰}$, while ^{13}C values in the sediments are $0.3\pm 0.3\text{‰}$ higher than from the multinet samples. Figure 30 demonstrates however, that the isotope values from the core-tops are within standard deviations of the plankton tows and reflect well the summer signal of *N. pachyderma* (s.) in the Fram Strait. Besides, the surface sediments present the mean isotope composition of several centuries, whereas the plankton samples are only a "snapshot". Furthermore, an alteration of isotopic values due to calcite dissolution and bioturbation in the surface sediments can not be discounted.

5. Conclusions

1. The community of the planktonic foraminifera, which in the study area mainly consists of six species: left and right-coiling *N. pachyderma*, *T. quinqueloba*, *G. bulloides*, *G. glutinata* and *G. uvula*, is primarily controlled by the temperature in the different current regimes. Other parameters such as ice-coverage, salinity, nutrients and food supply (chl_a concentrations) have no significant influence on the species composition in these regions.

2. The use of the 63-mesh nets leads to the establishment of lower temperature optima for the dominant species *N. pachyderma* (s.) and *T. quinqueloba* compared to Bé & Tolderlund (1971). This is due to the increase of relative abundance of *T. quinqueloba*, compared to the abundances described for the size classes > 200 µm.

3. The changes in the absolute abundance and size distribution of *N. pachyderma* (s.) and *T. quinqueloba* is influenced as well by hydrographic parameters, but primarily by the synchronic reproduction, which follows the lunar cycle. The occurrence of kummerform phenotypes and secondary calcification in the later development stages are linked to the reproductive cycles as well. The Labrador Sea data, with sufficient temporal resolution, indicates *N. pachyderma* (s.) and *T. quinqueloba* to respectively show the semi-lunar and lunar periodicity. For a better understanding of the reproductive behaviour of these species, further investigations (e.g. drifter experiments with parallel multinet sampling) are however required.

4. The detailed studies of the isotope signal on *N. pachyderma* (s.) grouped by size and degree of calcification showed in the Labrador Current that size and weight (or degree of calcification) are not significant variables in controlling the oxygen isotope composition of non-encrusted and encrusted *N. pachyderma* (s.) >140 µm, but changes of the life horizon during ontogeny.

5. The ¹⁸O vital effect is primarily caused by the thermal stratification of the water column, whereas the ¹³C vital effect mainly resulted from the ontogenetic development. The ¹³C values of *N. pachyderma* (s.) follow the typical logarithmic growth curve of planktonic foraminifera. Investigations conducted in the Fram Strait on *T. quinqueloba* established an additional influence of the symbiont activity on the ¹³C signal of this species.

6. Estimates of the ¹⁸O and ¹³C disequilibria resulted in a ¹⁸O vital effect of -0.5 to -0.7 ‰ for *N. pachyderma* (s.) and -0.8 ‰ for *T. quinqueloba* relative to equilibrium precipitation of inorganic calcite. The ¹³C vital effect relative to ¹³C_{Eq} was at -1.7 to -2.1 ‰ for *N. pachyderma* (s.) and at -2.5 ‰ for *T. quinqueloba*.

7. Both examined species calcify within a narrow temperature range. The secondary calcification occurs before the sinking into the deeper water layers (as a rule into 100-200 m depth) and may vary between the upper 0-50 m and 50-75 m in response to the reproductive cycles. The accurate calcification depths should be examined in more detail, using multinet tows with a higher depth resolution within the reproductive depth.

8. In the West Spitzbergen Current (80°N) measured isotope values of *N. pachyderma* (s.) and *T. quinqueloba* were out of equilibrium with the surrounding water. The reasons for this finding could be the non-linearity between salinity and $^{18}\text{O}_w$ in the WSC and/or advection of planktonic foraminifera out of warmer areas (ca. 2.5°C higher water temperatures). The influence of the lateral advection and salinity on the shell ^{18}O in this part of the Fram Strait requires further investigations.

9. The isotope signal of *N. pachyderma* (s.) from the water column reflected the surface sediments in the Fram Strait, where the ^{18}O and ^{13}C values in the surface sediments were higher by 0.2 ‰ and 0.3 ‰, respectively.

6. References

- Aksu, A.E. and Vilks, G. (1987): Stable isotopes in planktonic and benthic foraminifera from the Arctic Ocean surface sediments. *Can. J. Earth Sci.*, 25: 701-709.
- Aldermann, S.E. (1996): Planktonic foraminifera in the Sea of Okhotsk: population and stable isotopic analysis from a sediment trap. M. S. thesis, Massachusetts Institute of Technology/Woods Hole Oceanographic Institute Joint Program, Woods Hole, MA.
- Almogi-Labin, A. (1984): Population dynamics of planktic foraminifera and pteropoda – Gulf of Aqaba, Red Sea. *Paleontol.*, 87: 481-511.
- Anderson, O.R., Spindler, M., Bé, A.W.H. and Hemleben, C. (1979): Trophic activity of planktonic foraminifera. *J. mar. biol. Assoc. U.K.*, 59: 791-799.
- Anderson, T.F. and Arthur, M.A. (1983): Stable isotopes of oxygen and carbon and their application to sedimentologic and paleoenvironmental problems. In: Stable isotopes in sedimentary geology: SEPM Short Course, 10: 1-151, Tulsa.
- Arikawa, R. (1983): Distribution and taxonomy of *Globigerina pachyderma* (Ehrenberg) off the Sanriku Coast, Northeast Honshu, Japan. Tohoku University Scientific Reports, Serie 2 (Geology), 53 (2): 103-157.
- Bauch, D., Carstens, J. and Wefer, G. (1997): Oxygen isotope composition of living *Neogloboquadrina pachyderma* (sin.) in the Arctic Ocean. *Earth Planet. Sci. Lett.*, 146: 47-58.
- Bauch, D., Carstens, J., Wefer, G. and Thiede, J. (1999): The imprint of anthropogenic CO₂ in the Arctic Ocean: evidence from planktic ¹³C data from watercolumn and sediment surfaces. *Deep-Sea Res. II*, 47 (9-11): 1791-1808.
- Bauerfeind, E., v. Bodungen B., Arndt, K. and Koeve, W. (1994): Particle flux, and composition of sedimenting matter, in the Greenland Sea. *J. Mar. Syst.*, 5: 411-423.
- Bé, A.W.H. (1977): An ecological, zoogeographic, and taxonomic review of recent planktonic foraminifera, In: Oceanic Micropaleontology. Ramsay, A.T.S. (ed.). Academic Press, London. p. 2-100.
- Bé, A.W.H. and Anderson, O.R. (1976): Gametogenesis in planktonic foraminifera. *Science*, 192: 890-892.
- Bé, A.W.H., Bishop J.K.B., Sverdløve, M.S. and Gardner, W.D. (1985): Standing stock vertical distribution and flux of planktonic foraminifera in the Panama Basin. *Mar. Micropaleontol.*, 9: 307-333.
- Bé, A.W.H. and Tolderlund, D.S. (1971): Distribution and ecology of living planktonic foraminifera in surface waters of the Atlantic and Indian Oceans. In: The Micropaleontology of the Oceans, Funnel, B.F. (ed). Cambridge University Press, New York. p.105-149.
- Bemis, B.E., Spero, H.J., Bijma, J. and Lea, D.W. (1998): Reevaluation of the oxygen isotopic composition of planktonic foraminifera: Experimental results and revised paleotemperature equations. *Paleoceanogr.*, 13 (2): 150-160.
- Berberich, D. (1996): Die planktische Foraminifere *Neogloboquadrina pachyderma* (Ehrenberg) im Weddellmeer, Antarktis. *Ber. zur Polarforschung*, 195: 1-193.
- Berger, W.H. (1969): Ecologic patterns of living planktonic Foraminifera. *Deep-Sea Res.*, 16: 1-24.
- Berger, W.H. (1970): Planktonic foraminifera: differential production and expatriation off Baja California. *Limnol. Oceanogr.*, 15: 183-204.
- Berger, W.H. (1981): Oxygen and carbon isotopes in foraminifera: An introduction. *Paleogeogr., Paleoclimatol., Paleoecol.*, 33: 3-7.
- Berger, W.H., Killingley, J.S. and Vincent, E. (1978): Stable isotopes in the deep-sea carbonates: box core ERDC-92, West Equatorial Pacific. *Oceanol. Acta*, 1: 203-216.
- Berger, W.H. and Piper, D.J.W. (1972): Planktonic foraminifera: differential settling, dissolution and redeposition. *Limnol. Oceanogr.*, 17: 275-287.

- Bijma, J., Erez, J. and Hemleben, C. (1990a): Lunar and semi-lunar reproductive cycles in some spinose planktonic foraminifers. *J. Foram. Res.*, 20 (2): 117-127.
- Bijma, J., Walter, W., Faber, Jr. and Hemleben, C. (1990b): Temperature and salinity limits for growth and survival of some planktonic foraminifers in laboratory cultures. *J. Foram. Res.*, 20 (2): 95-116.
- Bijma, J., Hemleben, C., Oberhänsli, H. and Spindler, M. (1992): The effects of increased water fertility on tropical spinose planktonic foraminifers in laboratory cultures. *J. Foram. Res.*, 22 (3): 242-256.
- Bodungen v., B., Antia, A., Bauerfeind, E., Haupt, O., Koeve, W., Machado, E., Peeken, I., Peinert, R., Reitmeier, S., Thomsen, C., Voss, M., Wunsch, M., Zeller, U. and Zeitschel, B. (1995): Pelagic processes and vertical flux of particles: an overview of a long-term comparative study in the Norwegian-Greenland Sea. *Geol. Rundschau*, 84: 11-27.
- Boltovskoy, E. (1971): Patchiness in the distribution of planktonic foraminifera. In: Proc. II Planktonic Conf., Roma, Rome, Farinacci, A. (ed.), p. 107-155.
- Bouvier-Soumagnac, Y. and Duplessy, J.-C. (1985): Carbon and oxygen isotopic composition of planktonic foraminifera from laboratory culture, plankton tows and recent sediment: implications for the reconstruction of paleoclimatic conditions and of the global carbon cycle. *J. Foram. Res.*, 15 (4): 302-320.
- Broecker, W.S. (1989): Oxygen isotope constraints on surface ocean temperatures. *Quat. Res.*, 26: 121-134.
- Broecker, W.S. and van Donk, J. (1970): Insolation changes, ice volumes, and the ^{18}O record in deep-sea cores. *Rev. Geophys. Space Phys.*, 8: 169-198.
- Broecker, W.S. and Peng, T.-H. (1982): Tracers in the Sea. Lamont-Doherty Geological Observatory, Columbia University, Palisades, New York, p. 690.
- Brown, J., Colling, A., Park, D., Phillips, J., Rothery, D. and Wright, J. (1991): Ocean Circulation. The Open University, Pergamon Press, Oxford, New York, Beijing, Frankfurt, Seoul, Sydney, Tokyo, p. 238.
- Brummer, G.-J.A., Hemleben, C. and Spindler, M. (1985): Planktonic foraminiferal ontogeny and new perspectives for micropaleontology. *Nature*, 319: 50-52.
- Brummer, G.-J.A., Hemleben, C. and Spindler, M. (1987): Ontogeny of extant globigerinid planktonic foraminifera: a concept exemplified by *Globigerinoides sacculifer* (Brady) and *G. ruber* (d'Orbigny). *Mar. Micropaleontol.*, 12: 357-381.
- Carstens, J. (1988): Verteilung planktischer Foraminiferen in Oberflächengewässern der Framstraße, Nordatlantik. Diplomarbeit, Universität Bremen.
- Carstens, J., Hebbeln, D. and Wefer, G. (1997): Distribution of planktonic foraminifera at the ice margin in the Arctic (Fram Strait). *Mar. Micropaleontol.*, 29: 257-269.
- Carstens, J. and Wefer, G. (1992): Recent distribution of planktonic foraminifera in the Nansen Basin, Arctic Ocean. *Deep-Sea Res.*, 39 (2): 507-524.
- Chappel, J. and Shackleton, N. (1986): Oxygen isotopes and sea level. *Nature*, 324: 137-140.
- Cifelli, R. (1973): Observations on *Globigerina pachyderma* (Ehrenberg) and *Globigerina incompta* Cifelli from the North Atlantic. *J. Foram. Res.*, 3 (4): 157-166.
- Curry, W.B. and Matthews, R.K. (1981): Equilibrium ^{18}O fractionation in small size fraction planktic foraminifera: evidence from recent Indian Ocean sediments. *Mar. Micropaleontol.*, 6: 327-337.
- Dansgaard, W. (1961): The isotopic composition of natural waters with special reference to the Greenland ice cap. *Meddr. Greenland*, 165: 1-120.
- Dansgaard, W. (1964): Stable isotopes in precipitation. *Tellus*, 16: 436-467.
- Dickson, B. (1997): From the Labrador Sea to global change. *Nature*, 386, 649-650.
- Dietrich, G., Kalle, K., Krauss, W., Siedler, G. (1975): Allgemeine Meereskunde – Eine Einführung in die Ozeanographie. Berlin, Stuttgart, Gebr. Bornträger, 593 S.

- Donner, B. and Wefer, G. (1994): Flux and stable isotope composition of *Neogloboquadrina pachyderma* and other planktonic foraminifera in the Southern Ocean (Atlantic sector). *Deep-Sea Res.*, 41 (11/12): 1733-1743.
- Duplessy, J.C., Bé, A.W.H. and Blanc, P.L. (1981a): Oxygen and carbon isotopic composition and biogeographic distribution of planktonic foraminifera in the Indian Ocean. *Paleogeogr., Paleoclimatol., Paleoecol.*, 33: 9-46.
- Duplessy, J.C., Blanc, P.L., Bé, A.W.H. (1981b): Oxygen-18 enrichment of planktonic foraminifera due to gametogenic calcification below the euphotic zone. *Science* 213: 1247-1250.
- Duplessy, J.-C., Labeyrie, L., Juillet-Leclerc, A., Maitre, F., Duprat, J. and Sarinthein, M. (1991): Surface salinity reconstruction of the North Atlantic Ocean during the last glacial maximum. *Oceanol. Acta*, 14: 311-324.
- Emiliani, C. (1954): Depth habitats of some species of pelagic foraminifera as indicated by oxygen isotope ratios. *Am. J. Sci.*, 252: 149-158.
- Emiliani, C. (1971): Depth habitats of growth stages of pelagic foraminifera. *Science*, 173: 1122-1124.
- Epstein, S., Buchsbaum, R., Lowenstam, H.A. and Urey, H.C. (1951): Carbonate-water isotopic temperature scale. *Geol. Soc. Am. Bull.*, 62: 417-426.
- Erez, J., Almogi-Labin, A. and Avraham, S. (1991): On the life history of planktonic foraminifera: lunar reproduction cycle in *Globigerinoides sacculifer* (Brady). *Paleoceanogr.*, 6 (3): 295-306.
- Erez, J. and Luz, B. (1982): Temperature control of oxygen-isotope fractionation of cultured planktonic foraminifera. *Nature*, 297: 220-223.
- Erez, J. and Luz, B. (1983): Experimental paleotemperature equation for planktonic foraminifera. *Geochim. Cosmochim. Acta*, 47: 1025-1031.
- Erlenkeuser, H., Spielhagen, R.F. and Taldenkova, E. (1999): Stable isotopes in modern water and bivalve samples from the southern Kara Sea. In: The Kara Sea expedition of RV "Akademik Boris Petrov" 1997: First results of a Joint Russian-German pilot study, Matthiessen, J. et al., (eds.). *Ber. zur Polarforschung*, 300: 80-90.
- Fairbanks, R.G., Wiebe, P.H. and Bé, A.W.H. (1979): Vertical distribution and isotopic composition of living planktonic foraminifera in the western North Atlantic. *Science*, 207: 61-63.
- Fairbanks, R.G. and Wiebe, P.H. (1980): Foraminifera and chlorophyll maximum: Vertical distribution, seasonal succession and paleoceanographic significance. *Science*, 209: 1524-1526.
- Fairbanks, R.G., Sverdrlove, M., Free, R., Wiebe, P.H. and Bé, A.W.H. (1982): Vertical distribution and isotopic fractionation of living planktonic foraminifera from the Panama Basin. *Nature*, 298: 841-844.
- Fontugne, M. and Duplessy, J.C. (1981): Organic carbon isotopic fractionation by marine plankton in the temperate range -1 to 31 °C. *Oceanol. Acta*, 4: 85-90.
- Hastenrath, S. and Merle, J. (1987): Annual cycle of subsurface thermal structure in the tropical Atlantic Ocean. *J. Phys. Oceanogr.*, 17(9): 1518-1538.
- Hecht, A.D. (1976): The oxygen isotope record of foraminifera in deep-sea sediment. In: Foraminifera, Hedley, R.H. and Adams, C.G. (eds.), London, 2: 1-43.
- Hemleben, C. and Auras, A. (1984): Variations in the calcite dissolution pattern on the Barbados ridge complex at Sites 541 and 543, Deep Sea Drilling Project Leg 78A. In: Initial Reports of the Deep Sea Drilling Project, Leg 78, Biju-Duval, B. and Moore, J.C., et al. (eds). Washington, p. 471-497.
- Hemleben, C. and Bijma, J. (1994): Foraminiferal population dynamics and stable carbon isotopes. In: Carbon Cycling in the Glacial Ocean: Constraints on the Ocean's role in Global Change, Zahn, R. et al., (eds.). Springer Verlag, 580 S.
- Hemleben, C. and Spindler, M. (1983): Recent advances in research on living planktonic foraminifera. In: Meulen-kamp J.E. (ed.) Reconstruction on marine paleoenvironments. *Utr. Micropaleontol. Bull.*, 30: 141-170.

- Hemleben, C., Spindler, M. and Anderson, O.R. (1989): Modern planktonic foraminifera. Springer Verlag, New York: 363 S.
- Hemleben, C., Spindler, M., Breitingner, I. and Deuser, W.G. (1985): Field and laboratory studies on the ontogeny and ecology of some globorotaliid species from the Sargasso sea off Bermuda. *J. Foram. Res.*, 15: 254-272.
- Herczeg, A.L. and Fairbanks, R.G. (1987): Anomalous carbon isotope fractionation between atmospheric CO₂ and dissolved inorganic carbon induced by intense photosynthesis. *Geochim. Cosmochim. Acta*, 51: 895-899.
- Hesse, M., Meier, H. and Zeeh, B. (1991): Spektroskopische Methoden in der organischen Chemie. Stuttgart, New York. Thieme Verlag, 336 S.
- Ivanova, E.M., Conan, S.M.-H., Peeters, F.J.C. and Troelstra, S.R. (1999): Living *Neogloboquadrina pachyderma* (sin.) and its distribution in the sediments from Oman and Somalia upwelling areas. *Mar. Micropaleontol.*, 36: 91-107.
- Jasper, J.P. and Gagosian, R.B. (1989): Glacial-interglacial climatically forced ¹³C variations in sedimentary organic matter. *Nature*, 342: 60-62.
- Jensen S. (1998): Planktische Foraminiferen im Europäischen Nordmeer: Verbreitung und Vertikalfluß sowie ihre Entwicklung während der letzten 15 000 Jahre. *Ber. aus dem Sonderforschungsbereich 313*, 75: 105 S.
- Kennett, J.P. and Srinivasan, M.S. (1983): Neogene Planktonic Foraminifera. A Phylogenetic Atlas. Hutchinson Ross Publishing Company, p. 265.
- Kennett, J. and Venz, K. (1995): Late Quaternary climatically related planktonic foraminiferal assemblage changes: Hole 893A Santa Barbara Basin, California. *Proc. ODP Sci. Res.*, 146: 281-293.
- Kohfeld, K.E. (1998): Geochemistry and ecology of polar planktonic Foraminifera, and applications to paleoceanographic reconstructions. Columbia University, p.1-252.
- Kohfeld, K.E. and Fairbanks, R.G. (1996): *Neogloboquadrina pachyderma* (sinistral coiling) as paleoceanographic tracers in polar oceans: Evidence from Northeast Polynya plankton tows, sediment traps, and surface sediments. *Paleoceanogr.*, 11 (6): 679-699.
- Kohfeld, K.E., Anderson, R.F. and Lynch-Stieglitz, J. (2000): Carbon isotopic disequilibrium in polar planktonic foraminifera and its impact on modern and Last Glacial Maximum reconstructions. *Paleoceanogr.*, 15 (1): 53-64.
- Kohly, A. (1998): Diatom flux and species composition in the Greenland Sea and Norwegian Sea in 1991-1992. *Mar. Geol.*, 145: 293-312.
- Koltermann, K.P. (1987): Die Tiefenzirkulation der Grönland-See als Folge des thermohalinen Systems des Europäischen Nordmeeres. Dissertation, Universität Hamburg.
- Kroon, D. (1988): The planktic ¹³C record, upwelling and climate. In: Planktonic Foraminifera as tracers of Ocean-Climate History. Brummer, D.A. and Kroon, D. (eds.). Amsterdam, p. 335-346.
- Lazier, J.R.N. (1973): The renewal of Labrador Sea water. *Deep-Sea Res.*, 20: 341-353.
- Lazier, J.R.N. and Wright, D.G. (1992): Annual velocity variations in the Labrador Current. *J. Phys. Oceanogr.*, 23: 659-678.
- Lee, J.J. and Anderson, O.R. (1991): Biology of Foraminifera. Academic Press, London. p. 1-368.
- Lohmann, G.P. (1995): A model for variation in the chemistry of planktonic foraminifera due to secondary calcification and selective dissolution. *Paleoceanogr.*, 10 (3): 445-457.
- Lynch-Stieglitz, J., Fairbanks, R.G. and Charles, C.D. (1994): Glacial-interglacial history of Antarctic intermediate Water: Relative strengths of Antarctic versus Indian Ocean sources. *Paleoceanogr.*, 9 (1): 7-29.
- Macdonald, R. (1996): Awakenings in the Arctic. *Nature*, 380: 286-287.
- McConnaughey, T. (1989): ¹³C and ¹⁸O isotopic disequilibrium in biological carbonates: I. *In vitro* simulation of kinetic isotope effects. *Geochim. Cosmochim. Acta*, 53: 163-171.

- Mulitza, S., Wolff, T., Pätzold, J., Hale, W. and Wefer, G. (1998): Temperature sensitivity of planktonic foraminifera and its influence on the oxygen isotope record. *Mar. Micropaleontol.*, 33: 223-240.
- Murray, J.W. (1991): Ecology and distribution of planktonic foraminifera. In: *Biology of Foraminifera*. Lee, J.J. and Anderson, O.R. (eds). Academic Press, p. 255-284.
- Olson, R. K. (1973): What is a kummerform planktonic foraminifer? *J. Paleontol.*, 47: 327-329.
- O'Neil, J.R., Clayton, R.N. and Mayeda, T.K. (1969): Oxygen isotope fractionation in divalent metal carbonates. *J. Chem. Phys.*, 15 (12): 5547-5558.
- Ortiz, J.D. and Mix, A.C. (1992): The spatial distribution and seasonal succession of planktonic foraminifera in the California Current off Oregon, September 1987-September 1988. *Geolog. Soc. Spec. Public.*, 64: 197-213.
- Ortiz, J.D., Mix, A.C. and Collier R.W. (1995): Environmental control of living symbiotic and asymbiotic foraminifera of the California Current. *Paleoceanogr.*, 10 (6): 987-1009.
- Ortiz, J.D., Mix, A.C., Rugh, W., Watkins, J.M. and Collier R.W. (1996): Deep-dwelling planktonic foraminifera of the northeastern Pacific Ocean reveal environmental control of oxygen and carbon isotopic disequilibria. *Geochim. Cosmochim. Acta*, 60 (22): 4509-4523.
- Quadfasel, D., Gascard, J.C. and Koltermann, K.P. (1987): Large-scale oceanography in Fram Strait during the 1984 Marginal Ice Zone Experiment. *J. Geophys. Res.*, 92: 6719-6728.
- Rau, G.H., Takahashi, T. and Des Marais, D.J. (1989): Latitudinal variations in plankton ^{13}C : implications for CO_2 and productivity in past oceans. *Nature*, 341: 516-518.
- Rau, G.H., Froehlich, P.N., Takahashi, T. and Des Marais, D.J. (1991): Does sedimentary organic ^{13}C record variations in Quaternary ocean (CO_2 (aq))? *Paleoceanogr.*, 6: 335-347.
- Ravelo, A.C. and Fairbanks, R.G. (1995): Carbon isotope fractionation in multiple species of planktonic foraminifera from core-tops in the tropical Atlantic. *J. Foram. Res.*, 25 (1): 53-74.
- Read, J.F. and Gould, W.J. (1992): Cooling and freshening of the subpolar North Atlantic Ocean since the 1960s. *Nature*, 360, 55-57.
- Reynolds, L.A. and Thunell, R.C. (1986): Seasonal production and morphologic variation of *Neogloboquadrina pachyderma* (Ehrenberg) in the Northeast Pacific. *Micropaleontol.*, 32 (1): 1-18.
- Reynolds Sautter, L.R. (1998): Morphologic and stable isotopic variability within the planktic foraminiferal genus *Neogloboquadrina*. *J. Foram. Res.*, 28 (3): 220-232.
- Romanek, C.S., Grossman, E.L. and Morse, J.W. (1992): Carbon isotopic fractionation in synthetic aragonite and calcite: Effects of temperature and precipitation rate. *Geochim. Cosmochim. Acta*, 56: 419-430.
- Sautter, L.R. and Thunell, R.C. (1989): Seasonal succession of planktonic foraminifera: Results from a four-year time-series sediment trap experiment in the Northeast Pacific. *J. Foram. Res.*, 19 (4): 253-267.
- Schweitzer, P.N. and Lohmann, G.P. (1991): Ontogeny and habitat of modern menardiform planktonic foraminifera. *J. Foram. Res.*, 21 (4): 332-346.
- Shackleton, N. J. (1974): Attainment of isotopic equilibrium between ocean water and the benthonic foraminifera genus *Uvigerina*: Isotopic changes in the ocean during the last glacial. *Collog. Internation. du C.N.R.S.*, 219: 203-209.
- Simstich, J. (1999): Die ozeanische Deckschicht des Europäischen Nordmeeres im Abbild stabiler Isotope von Kalkgehäusen unterschiedlicher Planktonforaminiferenarten. *Ber. des Institut für Geowissenschaften, Universität Kiel*. 2: 96 S.
- Spero, H.J. (1992): Do planktic foraminifera accurately record shifts in the carbon isotopic composition of sea water CO_2 ? *Mar. Micropaleontol.*, 19: 275-285.
- Spero, H.J., Bijma, J., Lea, D.W. and Bemis B.E. (1997): Effect of seawater carbonate concentration on foraminiferal carbon and oxygen isotopes. *Nature*, 390: 497-500.

- Spero, H.J. and Lea, D.W. (1993): Intraspecific stable isotope variability in the planktic foraminifera *Globigerinoides sacculifer*: Results from laboratory experiments. *Mar. Micropaleontol.*, 22: 221-234.
- Spero, H.J. and Lea, D.W. (1996): Experimental determination of stable isotope variability in *Globigerina bulloides*: implications for paleoceanographic reconstructions. *Mar. Micropaleontol.*, 28: 231-246.
- Spero, H.J. and Williams, D.F. (1988): Extracting environmental information from planktonic foraminiferal ^{13}C data. *Nature*, 335: 717-719.
- Spero, H.J. and Williams, D.F. (1989): Opening the carbon isotope "vital effect" black box. 1. Seasonal temperatures in the euphotic zone. *Paleoceanogr.*, 4 (6): 593-601.
- Spielhagen, R.F. and Erlenkeuser, H. (1994): Stable oxygen and carbon isotopes in planktonic foraminifers from Arctic Ocean surface sediments: Reflection of the low salinity surface water layer. *Mar. Geol.*, 199: 227-250.
- Spindler, M. (1996): On the salinity tolerance of the planktonic foraminifer *Neogloboquadrina pachyderma* from Antarctic sea ice. Proc. NIPR Symp. *Polar Biol.*, 9: 85-91.
- Spindler, M. and Dieckmann, G.S. (1986): Distribution and abundance of the planktonic foraminifer *Neogloboquadrina pachyderma* in sea ice of the Weddell Sea (Antarctica). *Polar Biol.*, 5: 185-191.
- Spindler, M., Hemleben, C., Bayer, U., Bé, A.W.H. and Anderson, O.R. (1979): Lunar periodicity of reproduction in the planktonic foraminifer *Hastigerina pelagica*. *Mar. Ecol. Prog. Ser. 1*, 1: 61-64.
- Spindler, M., Hemleben, C., Salomons, J.B. and Smit, L.P. (1984): Feeding behavior of some planktonic foraminifers in laboratory cultures. *J. Foram. Res.*, 14: 237-249.
- Srinivasan, M.S. and Kennett, J.P. (1974): Secondary calcification of the planktonic foraminifer *Neogloboquadrina pachyderma* as a climatic index. *Science*, 186: 630-631.
- Stehmann, C.F. (1972): Planktonic foraminifera in Baffin Bay, Davis Strait and the Labrador Sea. *Maritime Sediments*, 8: 13-19.
- Swift, J.H. (1986): The Arctic waters. In: The Nordic Seas, Hurdle, B.G. (ed.). Springer Verlag, 129-153.
- Sy, A., Rhein, M., Lazier, J.R.N., Kolterman, K. P., Meincke, J., Putzka, A. and Bersch, M. (1997): Surprisingly rapid spreading of newly formed intermediate waters across the North Atlantic Ocean. *Nature*, 386: 675-679.
- Takahashi, H. and Bé, A.W.H. (1984): Planktonic foraminifera: factors controlling sinking speeds. *Deep-Sea Res.*, 31: 1477-1500.
- Urey, H.C. (1947): The thermodynamic properties of isotopic substances. *J. Chem. Soc.*, 562-581.
- Urey, H.C., Lowenstam, H.A., Epstein, S. and McKinney, C.R. (1951): Measurements of paleotemperatures and temperatures of the Upper Cretaceous of England, Denmark and the southeastern United States. *Bull. Geo. Soc. of Am.*, 62: 399-416.
- Vergnaud-Grazzini, C. (1976): Non-equilibrium isotopic compositions of shells of planktonic foraminifera in the Mediterranean sea. *Palaeogeogr., Palaeoclimatol., Palaeoecol.*, 20: 263-276.
- Vilks, G. (1975): Comparison of *Globorotalia pachyderma* (Ehrenberg) in the water column and sediments of the Canadian Arctic. *J. Foram. Res.*, 5: 313-325.
- Vilks, G. (1973): A study of *Globorotalia pachyderma* (Ehrenberg) in the Canadian Arctic, Halifax, Nova Scotia. p. 216.
- Vincent, E. and Berger, W.H. (1981): Planktonic foraminifera and their use in paleoceanography. In: The Oceanic Lithosphere: The Sea, Emiliani, C. (ed.). New York, p. 1025-1119.
- Vogelsang, E. (1991): Paläo-Ozeanographie des Europäischen Nordmeeres anhand stabiler Kohlenstoff- und Sauerstoffisotope. *Ber. des Sonderforschungsbereich 313*, Universität Kiel, 23: 1-136.
- Volkman, R. (2000a): Planktic foraminifers in the outer Laptev Sea and the Fram Strait - Modern distribution and ecology. *J. Foram. Res.*, 30: 157-176.

References

- Volkman, R. (2000b): Planktic foraminifers ecology and stable isotope geochemistry in the Arctic Ocean: implications from water column and sediment surface studies for quantitative reconstructions of oceanic parameters. *Ber. zur Polarforschung*, 361: 1-96.
- Wefer, G. (1985): Die Verteilung stabiler Isotope in Kalkschalen mariner Organismen. *Geologisches Jahrbuch*, A 82: 3-111.
- Williams, N.H. (1992): Stable isotope differences among morphotypes of *Neogloboquadrina pachyderma* (Ehrenberg): implications for high-latitude palaeoceanographic studies. *Terra Nova*, 4: 693-700.
- Wu, G. and Hillaire-Marcel, C. (1994): Oxygen isotope composition of sinistral *Neogloboquadrina pachyderma* tests in surface sediments: North Atlantic Ocean. *Geochim. Cosmochim. Acta*, 58 (4): 1303-1312.
- Zahn, R. and Mix, A. C. (1991): Benthic foraminiferal ^{18}O in the ocean's temperature-salinity field: constraints on ice age thermohaline circulation. *Paleoceanogr.*, 6 (1): 1-20.

7. Appendix

Complete data sets (counting lists, stable isotope data, CTD data (Ark XV/2), *chl a* and SiO_4 data (Ark XV/1+2)) are available at <http://www.pangaea.de>.

List of Tables:

Table 1: Absolute Abundances of Planktonic Foraminifera ($\text{Ind}\cdot\text{m}^{-3}$) in the Labrador Sea (M 39/4).

Table 2: Frequency Distribution of *N. pachyderma* (s.) and *T. quinqueloba* in the Labrador Sea (M 39/4).

Table 3: Stable Isotope Data of *N. pachyderma* (s.) from the Labrador Sea (M 39/4).

Table 4: Absolute Abundances of Planktonic Foraminifera ($\text{Ind}\cdot\text{m}^{-3}$) in the Greenland Sea (Ark XV/1).

Table 5: Frequency Distribution of *N. pachyderma* (s.) and *T. quinqueloba* in the Greenland Sea (Ark XV/1).

Table 6: Absolute Abundances of Planktonic Foraminifera ($\text{Ind}\cdot\text{m}^{-3}$) in the Fram Strait (Ark XV/2).

Table 7: Frequency Distribution of *N. pachyderma* (s.) and *T. quinqueloba* in the Fram Strait (Ark XV/2).

Table 8: Stable Isotope Data of *N. pachyderma* (s.) and *T. quinqueloba* from the Fram Strait (Ark XV/2).

Appendix

Table 1: Absolute Abundances of Planktonic Foraminifera (Ind*m⁻³) in the Labrador Sea (M 39/4).

Station: 352								
Depth (m)	<i>N. pach.</i> (s.)	<i>N. pach.</i> (d.)	<i>T. quin.</i>	<i>G. bull.</i>	<i>G. glu.</i>	<i>G. uvul.</i>	<i>O. ried.</i>	other
63-125 µm								
0-50	6.24	0.16	2.48	0	7.44	1.12	0	0
50-100	3.52	0	9.36	0.16	2.4	0.08	0	0
100-200	0.56	0.08	3.44	0.08	0.04	0.16	0	0
200-300	0.12	0	0	0	0	0.04	0	0
300-500	1.44	0.08	11.68	0.08	0.3	0.14	0.02	0
125-250 µm								
0-50	5.6	0.16	1.12	0.08	0	0	0	0
50-100	2.72	0.16	5.2	0.16	0	0.16	0.08	0.08
100-200	0.8	0.08	2	0	0	0.12	0.04	0
200-300	0.08	0	0.08	0	0	0	0	0
300-500	0.9	0.18	3.24	0	0.02	0.04	0	0
250-500 µm								
0-50	0.72	0	0.16	0	0	0	0	0.08
50-100	0.8	0.08	0.08	0.48	0	0	0.08	0
100-200	0.08	0.04	0.08	0	0	0	0	0
200-300	0	0	0	0	0	0	0	0
300-500	0.12	0	0.08	0.04	0	0	0	0
total								
0-50	12.56	0.32	3.76	0.08	7.44	1.12	0	0.8
50-100	7.04	0.24	14.64	0.8	2.4	0.24	0.16	1.12
100-200	1.44	0.2	5.52	0.08	0.04	0.28	0.04	0.2
200-300	0.2	0	0.08	0	0	0.04	0	0.08
300-500	2.46	0.26	15	0.12	0.32	0.18	0.02	0.58
Station: 357								
Depth (m)	<i>N. pach.</i> (s.)	<i>N. pach.</i> (d.)	<i>T. quin.</i>	<i>G. bull.</i>	<i>G. glu.</i>	<i>G. uvul.</i>	<i>O. ried.</i>	other
63-125 µm								
0-50	4.88	0.24	8.64	3.76	8.08	0.32	0	0
50-100	0.96	0.32	4	1.68	8.72	1.68	0	0
100-200	1.16	0.76	2.48	0.28	6.2	0.92	0.08	0.04
200-300	2.24	1.12	3.12	0.16	5.96	1.12	0.04	0
300-500	1.16	0.18	11.6	0.22	5.82	0.94	0.06	0
125-250 µm								
0-50	4.8	2.48	16	6.56	0.56	0.16	0	0
50-100	0.88	0.48	3.28	0.96	0	0.56	0	0
100-200	1.16	1.44	3.2	0.28	1.68	0.52	0.56	0.08
200-300	1.12	1.04	1.84	0.2	0.64	0.28	0.36	0
300-500	0.68	0.22	2.06	0.12	0.24	0.18	0.2	0
250-500 µm								
0-50	0.4	0.32	0.16	1.52	0	0	0	0
50-100	0.08	0.16	0	0.08	0	0	0	0
100-200	0.24	0.16	0.16	0.68	0.16	0	0.04	0.04
200-300	0	0	0.04	0.2	0	0	0	0
300-500	0.02	0	0.04	0.02	0	0	0	0
total								
0-50	10.08	3.04	24.8	11.84	8.64	0.48	0	0.8
50-100	1.92	0.96	7.28	2.72	8.72	2.24	0	0.88
100-200	2.56	2.36	5.84	1.24	8.04	1.44	0.68	5.64
200-300	3.36	2.16	5	0.56	6.6	1.4	0.4	5.6
300-500	1.86	0.4	13.7	0.36	6.06	1.12	0.26	0.88
Station: 361								
Depth (m)	<i>N. pach.</i> (s.)	<i>N. pach.</i> (d.)	<i>T. quin.</i>	<i>G. bull.</i>	<i>G. glu.</i>	<i>G. uvul.</i>	<i>O. ried.</i>	other
63-125 µm								
0-50	10.16	2	10.88	3.2	22.32	1.68	0	0
50-100	3.2	0.56	4	2.16	8	1.36	0	0
100-200	0.92	0.12	0.84	0.16	0.4	0.08	0	0
200-300	0.68	0.4	0.72	0.08	0.16	0.08	0	0
300-500	6.22	0.92	9.24	0.38	0.22	0.18	0	0
125-250 µm								
0-50	12.4	3.36	8.24	5.92	3.28	0.72	0	0
50-100	10.48	1.84	5.6	2.88	0.32	0.24	0	0
100-200	13.04	0.64	2.76	0.24	0.04	0.08	0	0
200-300	0.68	0.24	0.64	0.2	0	0	0	0
300-500	6.78	0.3	2.86	0.84	0.02	0.12	0	0
250-500 µm								
0-50	1.2	0	0	0.88	0	0	0	0
50-100	2	0.08	0.16	0.56	0	0	0	0
100-200	8.32	0.16	0	0.08	0	0	0	0
200-300	0.28	0	0	0.04	0	0	0	0
300-500	0.5	0	0.04	0.12	0	0	0	0
total								
0-50	23.76	5.36	19.12	10	25.6	2.4	0	3.2
50-100	15.68	2.48	9.76	5.6	8.32	1.6	0	0.32
100-200	22.28	0.92	3.6	0.48	0.44	0.16	0	0.04
200-300	1.64	0.64	1.36	0.32	0.16	0.08	0	0.28
300-500	13.5	1.22	12.14	1.34	0.24	0.3	0	4.16

Appendix

Table 1: Continued.

Station:	366							
Depth (m)	<i>N. pach.</i> (s.)	<i>N. pach.</i> (d.)	<i>T. quin.</i>	<i>G. bull.</i>	<i>G. glu.</i>	<i>G. uvul.</i>	<i>O. ried.</i>	other
63-125 µm								
0-50	18.64	0.24	12.72	1.36	5.92	0.8	0	0
50-100	5.44	0.16	7.2	0.72	2.16	0.24	0	0
100-200	2.88	0.04	9.96	0.12	0.48	0.08	0	0
200-300	7.12	0.6	20.56	0.4	1.28	0.84	0	0
300-500	0	0	0.04	0	0	0	0	0
125-250 µm								
0-50	6.24	0.4	6.32	0	0	0	0	0
50-100	4.4	0.16	4	0.08	0	0	0	0
100-200	1.32	0.08	2.32	0.04	0	0	0	0
200-300	3	1.12	3.12	0.24	0	0	0	0
300-500	0.02	0	0.02	0	0	0	0	0
250-500 µm								
0-50	0.32	0	0	0	0	0	0	0
50-100	0.08	0	0	0	0	0	0	0
100-200	0.12	0	0	0.08	0	0	0	0
200-300	0.04	0	0	0.04	0	0	0	0
300-500	0	0	0	0	0	0	0	0
total								
0-50	25.2	0.64	19.04	1.36	5.92	0.8	0	0.4
50-100	9.92	0.32	11.2	0.8	2.16	0.24	0	1.52
100-200	4.32	0.12	12.28	0.24	0.48	0.08	0	0.28
200-300	10.16	1.72	23.68	0.68	1.28	0.84	0	3.32
300-500	0.02	0	0.06	0	0	0	0	0.08
Station: 376								
Depth (m)	<i>N. pach.</i> (s.)	<i>N. pach.</i> (d.)	<i>T. quin.</i>	<i>G. bull.</i>	<i>G. glu.</i>	<i>G. uvul.</i>	<i>O. ried.</i>	other
63-125 µm								
0-50	2	0.08	4.48	0.32	7.04	0.64	0	0
50-100	0.8	0	7.68	0.08	7.28	0.8	0	0
100-200	0.32	0.08	26.08	0.12	4.52	0.76	0	0
200-300	0.44	0.04	5.56	0.04	0.76	0.24	0	0
300-500	0.24	0	16.34	0.04	2.02	0.46	0	0
125-250 µm								
0-50	2.8	0.16	7.12	0.72	0.16	0.56	0	0
50-100	0.48	0.08	4.96	0.32	0	0.32	0	0
100-200	0.72	0	6	0.04	0.08	0.2	0	0
200-300	0.04	0	2.32	0.04	0	0.16	0	0
300-500	0.34	0	7.08	0.04	0.02	0.48	0	0
250-500 µm								
0-50	0.24	0	0.64	0.32	0	0	0	0
50-100	0.32	0	0	0.24	0	0	0	0
100-200	0.32	0	0.08	0.04	0	0	0	0
200-300	0.2	0	0.12	0	0	0	0	0
300-500	0	0	0.18	0	0	0	0	0
total								
0-50	5.04	0.24	12.24	1.36	7.2	1.2	0	1.52
50-100	1.6	0.08	12.64	0.64	7.28	1.12	0	2.08
100-200	1.36	0.08	32.16	0.2	4.6	0.96	0	0.72
200-300	0.68	0.04	8	0.08	0.76	0.4	0	0.36
300-500	0.58	0	23.6	0.08	2.04	0.94	0	0.46
Station: 381								
Depth (m)	<i>N. pach.</i> (s.)	<i>N. pach.</i> (d.)	<i>T. quin.</i>	<i>G. bull.</i>	<i>G. glu.</i>	<i>G. uvul.</i>	<i>O. ried.</i>	other
63-125 µm								
0-50	0.96	0.56	4.88	0.24	84.8	14.8	0.08	0
50-100	0.64	0.32	5.92	0.56	13.52	2.16	0	0
100-200	0.44	0.12	21.96	0.12	13.64	8.24	0.2	0.12
200-300	0.12	0.04	9.56	0.08	3.72	1.08	0	0
300-500	no data							
125-250 µm								
0-50	1.6	1.68	2.8	0.24	0.48	8.24	0.32	0
50-100	0.48	0.08	3.12	0.32	0.4	2.32	0	0
100-200	0.24	0.28	4	0.04	0.8	2.72	0.12	0.08
200-300	0.12	0.04	1.4	0	0.12	0.8	0	0
300-500	no data							
250-500 µm								
0-50	0.16	0.4	0.16	0.48	0	0	0.08	0
50-100	0.16	0.56	0.24	0.24	0.08	0	0	0
100-200	0.32	0.44	0.04	0.6	0.04	0	0	0
200-300	0	0.2	0.2	0.44	0	0	0	0
300-500	no data							
total								
0-50	2.72	2.64	7.84	0.96	85.28	23.04	0.48	3.76
50-100	1.28	0.96	9.28	1.12	14	4.48	0	2.56
100-200	1	0.84	26	0.76	14.48	10.96	0.32	2.16
200-300	0.24	0.28	11.16	0.52	3.84	1.88	0	0.12
300-500	no data							

Appendix

Table 1: Continued.

Station: 402								
Depth (m)	<i>N. pach.</i> (s.)	<i>N. pach.</i> (d.)	<i>T. quin.</i>	<i>G. bull.</i>	<i>G. glu.</i>	<i>G. uvul.</i>	<i>O. ried.</i>	other
63-125 µm								
0-50	33.12	0.4	28.8	0.56	149.84	6.32	0	0
50-100	no data							
100-200	1.12	0	18.2	0.04	6.04	1.6	0	0
200-300	1.96	0.24	38.44	0	4.24	0.48	0	0
300-500	0.54	0.02	24.72	0.02	3.54	0.36	0	0
125-250 µm								
0-50	68.48	2.64	14.32	2.48	18.64	7.2	0	0
50-100	no data							
100-200	3.52	0.12	8.48	0.04	2.6	1.08	0	0
200-300	4.28	0.12	12.64	0.12	0.88	1.04	0	0
300-500	1.3	0.14	4.98	0	0.24	0.26	0	0
250-500 µm								
0-50	19.2	0.56	1.44	1.28	0	0	0	0
50-100	no data							
100-200	1.2	0.08	0.68	0.6	0	0	0	0
200-300	1.36	0.08	0.96	0.24	0	0	0	0
300-500	0.38	0	0.34	0.04	0	0	0	0
total								
0-50	120.8	3.6	44.56	4.32	168.48	13.52	0	1.2
50-100	no data							
100-200	5.84	0.2	27.36	0.68	8.64	2.68	0	0
200-300	7.6	0.44	52.04	0.36	5.12	1.52	0	0.12
300-500	2.22	0.16	30.04	0.06	3.78	0.62	0	0.2
Station: 404								
Depth (m)	<i>N. pach.</i> (s.)	<i>N. pach.</i> (d.)	<i>T. quin.</i>	<i>G. bull.</i>	<i>G. glu.</i>	<i>G. uvul.</i>	<i>O. ried.</i>	other
63-125 µm								
0-50	1.28	0.16	125.04	2.24	73.2	0.56	0	1.76
50-100	0.08	0.08	16.96	0.56	7.6	0.48	0.08	0.96
100-200	0.44	0.04	30.36	0.92	12.8	0.8	0	0.76
200-300	0.12	0	11.28	0.4	3.92	0.24	0	0
300-500	0.58	0.18	41.7	1.12	26.62	0.4	0	0.5
125-250 µm								
0-50	3.84	2.32	18.08	3.2	1.12	0.64	0	3.76
50-100	0.56	0.96	5.92	1.52	0.8	0.24	0.16	1.44
100-200	1.4	0.76	7.52	1.64	1	0.44	0	0.24
200-300	0.28	0.16	3.6	0.28	0.32	0.16	0	0.04
300-500	0.44	0.2	8.52	0.86	0.52	0.22	0	0.32
250-500 µm								
0-50	0.88	1.76	0.24	0.64	0	0	0	2.88
50-100	0.08	0.96	0	2.64	0.08	0	0.08	3.04
100-200	0.24	1.04	0.08	2.04	0.04	0	0	0.52
200-300	0.04	0.2	0	0.2	0	0	0	0.8
300-500	0.08	0.08	0.14	0.14	0.02	0	0	0.2
total								
0-50	6	4.24	143.36	6.08	74.32	1.2	0	11.28
50-100	0.72	2	22.88	4.72	8.48	0.72	0.32	9.2
100-200	2.08	1.84	37.96	4.6	13.84	1.24	0	4.32
200-300	0.44	0.36	14.88	0.88	4.24	0.4	0	1.8
300-500	1.1	0.46	50.36	2.12	27.16	0.62	0	1.64

Appendix

Table 2: Frequency Distribution of *N. pachyderma* (s.) and *T. quinqueloba* in the Labrador Sea (M 39/4).

Station 352																					
<i>N. pach. (s.)</i>		0-50 m				50-100 m				100-200 m				200-300 m				300-500 m			
size-class	total	dead	kum.	calc.	total	dead	kum.	calc.	total	dead	kum.	calc.	total	dead	kum.	calc.	total	dead	kum.	calc.	
70	31	13	0	0	28	9	0	2	3	0	0	0	0	0	0	0	28	20	0	0	
93	31	8	0	1	8	4	1	0	8	6	0	0	0	0	0	0	34	26	0	1	
116	16	4	0	0	8	2	0	0	3	1	0	0	3	3	0	0	10	4	1	3	
139	21	4	0	2	8	2	0	1	5	1	0	1	0	0	0	0	9	5	1	2	
162	20	3	0	1	10	2	0	2	4	0	0	2	0	0	0	0	15	8	0	1	
186	16	3	0	0	6	0	1	3	2	1	0	0	1	1	0	0	12	5	0	0	
209	7	1	1	1	2	0	0	1	3	0	0	1	1	0	0	0	6	2	1	1	
232	6	0	0	1	8	1	1	5	6	1	0	2	0	0	0	0	3	1	0	2	
255	4	0	0	1	2	1	1	1	2	0	0	2	0	0	0	0	3	0	0	2	
278	3	1	0	0	5	0	2	5	0	0	0	0	0	0	0	0	2	0	1	2	
302	2	0	0	0	1	0	0	1	0	0	0	0	0	0	0	0	0	0	0	0	
325	0	0	0	0	1	0	0	1	0	0	0	0	0	0	0	0	1	0	1	1	
348	0	0	0	0	1	0	0	1	0	0	0	0	0	0	0	0	0	0	0	0	
371	0	0	0	0	0	0	0	0	0	0	0	0	0	0	0	0	0	0	0	0	
394	0	0	0	0	0	0	0	0	0	0	0	0	0	0	0	0	0	0	0	0	
418	0	0	0	0	0	0	0	0	0	0	0	0	0	0	0	0	0	0	0	0	
<i>T. quin.</i>	total	dead	kum.	calc.	total	dead	kum.	calc.	total	dead	kum.	calc.	total	dead	kum.	calc.	total	dead	kum.	calc.	
70	7	3	0	0	64	9	0	0	15	1	0	0	0	0	0	0	232	38	0	0	
93	16	7	0	0	32	11	0	0	45	5	0	0	0	0	0	0	282	68	0	0	
116	8	4	0	0	21	10	0	2	26	4	0	0	0	0	0	0	70	49	0	0	
139	4	2	0	0	17	7	0	1	13	2	0	0	0	0	0	0	32	30	0	0	
162	4	3	0	0	28	14	0	1	21	2	0	0	1	1	0	0	69	59	0	0	
186	2	1	0	0	13	5	0	1	6	0	0	2	1	0	0	0	41	29	0	0	
209	1	0	0	0	3	0	0	1	4	0	0	1	0	0	0	0	11	10	0	0	
232	3	1	0	1	4	1	0	0	6	1	0	2	0	0	0	0	9	8	0	0	
255	1	1	0	0	0	0	0	0	2	0	0	1	0	0	0	0	3	1	0	1	
278	1	0	0	1	1	0	0	0	0	0	0	0	0	0	0	0	0	0	0	0	
302	0	0	0	0	0	0	0	0	0	0	0	0	0	0	0	0	1	1	0	0	
325	0	0	0	0	0	0	0	0	0	0	0	0	0	0	0	0	0	0	0	0	
348	0	0	0	0	0	0	0	0	0	0	0	0	0	0	0	0	0	0	0	0	

Station 357																					
<i>N. pach. (s.)</i>		0-50 m				50-100 m				100-200 m				200-300 m				300-500 m			
size-class	total	dead	kum.	calc.	total	dead	kum.	calc.	total	dead	kum.	calc.	total	dead	kum.	calc.	total	dead	kum.	calc.	
70	12	2	0	0	3	1	0	0	9	3	0	1	30	6	0	0	15	9	0	0	
93	36	7	0	0	6	1	0	0	13	5	0	0	22	9	0	0	28	12	0	0	
116	13	1	0	0	3	2	0	0	7	3	1	2	4	3	1	0	15	9	0	1	
139	12	1	1	1	3	1	0	0	6	0	0	1	7	3	0	0	6	2	0	1	
162	18	1	0	0	2	0	0	0	14	6	0	1	13	11	2	0	14	6	1	2	
186	11	2	0	0	3	1	0	1	4	1	0	1	4	2	0	0	11	2	2	6	
209	12	1	0	1	2	1	0	1	4	1	1	1	4	2	2	0	3	1	0	0	
232	7	0	0	0	1	0	0	0	1	0	1	1	0	0	0	0	0	0	0	0	
255	4	0	0	1	1	0	0	1	2	0	1	2	0	0	0	0	0	0	0	0	
278	1	0	0	0	0	0	0	0	2	0	0	2	0	0	0	0	0	0	0	0	
302	0	0	0	0	0	0	0	0	2	0	1	2	0	0	0	0	0	0	0	0	
325	0	0	0	0	0	0	0	0	0	0	0	0	0	0	0	0	1	0	1	1	
348	0	0	0	0	0	0	0	0	0	0	0	0	0	0	0	0	0	0	0	0	
371	0	0	0	0	0	0	0	0	0	0	0	0	0	0	0	0	0	0	0	0	
394	0	0	0	0	0	0	0	0	0	0	0	0	0	0	0	0	0	0	0	0	
418	0	0	0	0	0	0	0	0	0	0	0	0	0	0	0	0	0	0	0	0	
<i>T. quin.</i>	total	dead	kum.	calc.	total	dead	kum.	calc.	total	dead	kum.	calc.	total	dead	kum.	calc.	total	dead	kum.	calc.	
70	16	13	0	0	11	8	0	0	17	5	0	0	22	15	0	0	149	23	0	0	
93	36	28	0	0	28	14	0	0	25	10	0	0	45	23	0	0	349	143	0	0	
116	55	39	0	0	11	9	0	0	20	9	0	0	11	11	0	0	82	65	0	0	
139	54	38	0	0	6	6	0	0	16	6	0	0	8	7	0	0	22	19	0	0	
162	59	44	0	0	18	12	0	1	20	15	0	0	15	13	0	0	29	27	0	0	
186	42	30	0	1	11	5	0	0	20	15	0	1	9	7	0	0	30	30	0	0	
209	34	24	0	1	4	3	1	12	10	3	0	2	8	8	0	0	12	12	0	0	
232	12	7	0	0	2	0	0	0	9	5	0	1	6	5	0	0	10	10	0	0	
255	1	1	0	0	0	0	0	0	3	3	0	0	1	1	0	0	1	1	0	0	
278	1	0	0	0	0	0	0	0	0	0	0	0	0	0	0	0	1	0	0	1	
302	0	0	0	0	0	0	0	0	0	0	0	0	0	0	0	0	0	0	0	0	
325	0	0	0	0	0	0	0	0	0	0	0	0	0	0	0	0	0	0	0	0	
348	0	0	0	0	0	0	0	0	0	0	0	0	0	0	0	0	0	0	0	0	

Station 361																					
<i>N. pach. (s.)</i>		0-50 m				50-100 m				100-200 m				200-300 m				300-500 m			
size-class	total	dead	kum.	calc.	total	dead	kum.	calc.	total	dead	kum.	calc.	total	dead	kum.	calc.	total	dead	kum.	calc.	
70	12	1	0	0	2	1	0	0	3	2	0	0	1	0	0	0	72	27	0	0	
93	48	7	0	0	7	2	0	0	12	6	0	1	14	2	0	0	157	103	0	0	
116	65	13	0	0	31	12	0	0	10	8	0	0	2	2	0	0	84	64	0	4	
139	43	3	0	0	31	10	0	3	42	27	0	4	11	3	0	1	100	76	0	8	
162	37	6	2	1	28	6	0	10	64	32	1	27	4	0	0	0	110	74	0	8	
186	31	5	2	4	25	3	1	8	48	23	1	21	0	0	0	0	50	33	0	7	
209	33	3	0	3	26	7	1	15	73	20	0	49	1	0	0	0	48	26	0	10	
232	14	0	1	5	23	6	3	17	97	17	2	81	1	0	0	0	28	9	0	5	
255	8	0	1	4	13	3	1	12	68	7	1	59	0	0	0	0	13	6	0	7	
278	3	0	0	1	4	1	0	7	43	7	3	37	3	0	1	3	6	1	0	5	
302	2	0	1	2	3	0	0	3	33	2	3	29	2	0	0	2	0	0	0	0	
325	0	0	0	0	0	0	0	0	30	0	4	29	0	0	0	0	3	0	0	3	
348	1	1	1	1	0	0	0	0	18	0	3	18	2	0	0	2	3	0	0	3	
371	0	0	0	0	0	0	0	0	9	0	0	9	0	0	0	0	1	0	0	1	
394	0	0	0	0	0	0	0	0	7	0	3	7	0	0	0	0	0	0	0	0	
418	0	0	0	0	0	0	0	0	1	0	1	1	0	0	0	0	0	0	0	0	
<i>T. quin.</i>	total	dead	kum.	calc.	total	dead	kum.	calc.	total	dead	kum.	calc.	total	dead	kum.	calc.	total	dead	kum.	calc.	
70	11	3	0	0	2	1	0	0	0	0	0	0	0	0	0	0	14	4	0	0	
93	60	22	0	0	23	18	0	0	7	4	0	0	12	3	0	0	256	41	0	0	
116	66	13	0	0	26	16	0	0	15	7	0	0	13	4	0	0	193	51	0	0	
139	45	7	0	0	21	14	0	0	15	10	0	2	6	1	0	1	58	35	0	0	
162	33	10	1	3	22	10	0	5	32	9	0	12	6	4	0	1	61	44	0	5	
186	11	1	0	0	15	3	0	11	19	7	0										

Appendix

Table 2: Continued.

Station 366		0-50 m				50-100 m				100-200 m				200-300 m				300-500 m			
<i>N. pach.</i> (<i>s.</i>)	size-class	total	dead	kum.	calc.	total	dead	kum.	calc.	total	dead	kum.	calc.	total	dead	kum.	calc.	total	dead	kum.	calc.
70		57	37	0	0	34	19	0	1	14	9	0	0	55	35	0	0	0	0	0	0
93		113	69	0	1	22	7	0	3	47	26	0	0	86	60	0	2	0	0	0	0
116		62	39	0	0	12	2	0	0	11	3	0	1	37	28	0	3	0	0	0	0
139		34	16	0	0	17	3	0	7	11	6	0	2	26	14	1	3	0	0	0	0
162		24	10	0	0	15	5	0	6	9	3	0	4	21	15	0	7	1	0	0	0
186		12	4	0	1	10	1	0	4	5	1	0	2	18	9	1	7	0	0	0	0
209		4	1	0	2	11	2	0	8	6	0	1	4	4	2	0	2	0	0	0	0
232		5	1	0	1	2	0	0	2	2	0	1	1	6	2	0	2	0	0	0	0
255		2	0	0	0	1	0	0	1	0	0	0	0	1	0	0	1	0	0	0	0
278		1	0	0	0	0	0	0	0	3	0	2	3	0	0	0	0	0	0	0	0
302		1	0	0	0	0	0	0	0	0	0	0	0	0	0	0	0	0	0	0	0
325		0	0	0	0	0	0	0	0	0	0	0	0	0	0	0	0	0	0	0	0
348		0	0	0	0	0	0	0	0	0	0	0	0	0	0	0	0	0	0	0	0
371		0	0	0	0	0	0	0	0	0	0	0	0	0	0	0	0	0	0	0	0
394		0	0	0	0	0	0	0	0	0	0	0	0	0	0	0	0	0	0	0	0
418		0	0	0	0	0	0	0	0	0	0	0	0	0	0	0	0	0	0	0	0
<i>T. quin.</i>		total	dead	kum.	calc.	total	dead	kum.	calc.	total	dead	kum.	calc.	total	dead	kum.	calc.	total	dead	kum.	calc.
70		26	24	0	0	56	38	0	0	70	38	0	0	125	60	0	0	0	0	0	0
93		80	54	0	0	22	12	0	0	147	102	0	0	331	224	0	3	2	1	0	0
116		54	44	0	0	12	10	0	0	32	23	0	0	71	50	0	2	0	0	0	0
139		29	25	0	0	9	6	0	0	17	13	0	1	33	25	0	1	1	0	0	0
162		30	21	0	0	23	19	0	0	30	19	0	2	31	31	0	2	0	0	0	0
186		10	5	0	0	12	9	0	0	8	6	0	1	13	12	0	3	0	0	0	0
209		7	5	0	1	4	2	0	0	3	1	0	1	3	2	0	0	0	0	0	0
232		3	3	0	0	2	2	0	0	0	0	0	0	2	1	0	0	0	0	0	0
255		0	0	0	0	0	0	0	0	0	0	0	0	0	0	0	0	0	0	0	0
278		0	0	0	0	0	0	0	0	0	0	0	0	0	0	0	0	0	0	0	0
302		0	0	0	0	0	0	0	0	0	0	0	0	0	0	0	0	0	0	0	0
325		0	0	0	0	0	0	0	0	0	0	0	0	0	0	0	0	0	0	0	0
348		0	0	0	0	0	0	0	0	0	0	0	0	0	0	0	0	0	0	0	0

Station 376		0-50 m				50-100 m				100-200 m				200-300 m				300-500 m			
<i>N. pach.</i> (<i>s.</i>)	size-class	total	dead	kum.	calc.	total	dead	kum.	calc.	total	dead	kum.	calc.	total	dead	kum.	calc.	total	dead	kum.	calc.
70		9	1	0	0	5	2	0	0	0	0	0	0	6	3	0	0	2	2	0	0
93		9	3	0	0	4	2	0	0	5	1	0	0	4	3	0	0	10	6	0	1
116		7	0	0	0	1	0	0	0	4	2	0	0	1	0	0	0	0	0	0	0
139		2	0	0	0	1	0	0	1	3	1	0	2	1	0	0	0	1	1	0	0
162		10	3	0	1	1	0	0	0	2	0	0	1	0	0	0	0	6	4	0	0
186		9	0	0	1	3	0	0	2	6	1	0	4	0	0	0	0	5	3	0	0
209		10	2	0	2	0	0	0	0	4	0	0	4	0	0	0	0	3	3	0	2
232		4	0	0	0	1	0	0	1	2	0	1	2	0	0	0	0	2	1	0	0
255		2	0	0	0	2	0	0	2	3	0	0	3	2	0	1	2	0	0	0	0
278		1	0	0	1	0	0	0	0	2	0	0	2	1	0	0	0	0	0	0	0
302		0	0	0	0	1	0	0	1	1	0	0	1	1	0	0	1	0	0	0	0
325		0	0	0	0	1	0	0	1	2	0	0	2	1	0	0	1	0	0	0	0
348		0	0	0	0	0	0	0	0	0	0	0	0	0	0	0	0	0	0	0	0
371		0	0	0	0	0	0	0	0	0	0	0	0	0	0	0	0	0	0	0	0
394		0	0	0	0	0	0	0	0	0	0	0	0	0	0	0	0	0	0	0	0
418		0	0	0	0	0	0	0	0	0	0	0	0	0	0	0	0	0	0	0	0
<i>T. quin.</i>		total	dead	kum.	calc.	total	dead	kum.	calc.	total	dead	kum.	calc.	total	dead	kum.	calc.	total	dead	kum.	calc.
70		16	5	0	0	33	12	0	0	268	15	0	0	29	10	0	0	237	76	0	0
93		31	11	0	0	43	17	0	0	282	41	0	1	80	26	0	0	419	201	0	5
116		9	4	0	0	20	13	0	0	103	34	0	0	30	26	0	0	160	136	0	14
139		17	3	0	0	14	8	0	0	46	15	0	3	19	17	0	1	110	110	0	32
162		28	6	0	0	21	14	0	0	46	24	0	3	20	18	0	3	92	89	0	31
186		17	4	0	0	13	8	0	0	28	12	1	8	9	8	0	4	94	88	0	38
209		11	2	0	0	10	5	0	0	16	10	0	7	6	5	0	4	41	37	0	22
232		16	4	0	0	4	4	0	0	13	7	0	0	4	3	0	0	18	17	0	11
255		5	0	0	0	0	0	0	0	2	0	0	1	2	1	1	2	7	6	0	6
278		3	0	0	0	0	0	0	0	0	0	0	0	1	1	0	0	2	2	1	1
302		0	0	0	0	0	0	0	0	0	0	0	0	0	0	0	0	0	0	0	0
325		0	0	0	0	0	0	0	0	0	0	0	0	0	0	0	0	0	0	0	0
348		0	0	0	0	0	0	0	0	0	0	0	0	0	0	0	0	0	0	0	0

Station 381		0-50 m				50-100 m				100-200 m				200-300 m				300-500 m			
<i>N. pach.</i> (<i>s.</i>)	size-class	total	dead	kum.	calc.	total	dead	kum.	calc.	total	dead	kum.	calc.	total	dead	kum.	calc.	total	dead	kum.	calc.
70		9	5	0	0	3	0	0	0	2	1	0	0	1	1	0	0	no data			
93		2	0	0	0	4	0	0	1	8	4	1	1	2	1	0	1				
116		1	1	0	0	1	1	0	0	1	0	0	0	0	0	0	0				
139		6	0	0	0	1	0	0	0	1	0	0	1	0	0	0	0				
162		4	0	0	0	3	2	0	0	4	2	0	1	2	0	0	2				
186		6	0	0	0	1	0	0	0	0	0	0	0	1	0	0	1				
209		2	0	0	0	1	0	0	0	1	0	0	0	0	0	0	0				
232		2	0	0	2	1	0	0	1	1	0	0	1	0	0	0	0				
255		1	0	0	1	0	0	0	1	1	0	0	1	0	0	0	0				
278		1	0	0	0	1	0	0	1	1	0	1	1	0	0	0	0				
302		0	0	0	0	0	0	0	0	0	0	0	0	0	0	0	0				
325		0	0	0	0	0	0	0	0	4	0	1	4	0	0	0	0				
348		0	0	0	0	0	0	0	0	0	0	0	0	0	0	0	0				
371		0	0	0	0	0	0	0	0	2	0	0	0	0	0	0	0				
394		0	0	0	0	0	0	0	0	0	0	0	0	0	0	0	0				
418		0	0	0	0	0	0	0	0	0	0	0	0	0	0	0	0				
<i>T. quin.</i>		total	dead	kum.	calc.	total	dead	kum.	calc.	total	dead	kum.	calc.	total	dead	kum.	calc.	total	dead	kum.	calc.
70		22	5	0	0	16	6	0	0	229	44	0	0	39	6	0	0	no data			
93		22	9	0	0	33	18	0	0	271	39	0	0	166	23	0	0				
116		17	2	0	0	25	5	0	0	50	23	0	0	34	11	0	0				

Appendix

Table 2: Continued.

Station N. pach. (s.)		402				50-100 m				100-200 m				200-300 m				300-500 m			
size-class	total	dead	kum.	calc.	total	dead	kum.	calc.	total	dead	kum.	calc.	total	dead	kum.	calc.	total	dead	kum.	calc.	
70	159	27	3	0	no data				13	6	3	0	18	14	2	1	9	6	1	1	
93	143	19	4	0	no data				5	2	0	0	23	19	4	3	7	5	2	0	
116	112	8	6	1	no data				11	5	4	1	8	4	1	3	11	10	5	3	
139	162	12	8	0	no data				22	9	5	2	18	13	1	12	12	9	0	5	
162	197	9	9	1	no data				20	8	1	3	24	13	1	16	11	5	1	10	
186	189	7	2	3	no data				16	9	4	7	29	23	0	9	14	9	3	12	
209	151	2	1	2	no data				11	5	1	2	23	16	0	11	14	10	2	12	
232	158	9	2	12	no data				18	5	0	3	13	9	1	6	14	6	1	11	
255	111	0	5	15	no data				12	5	2	7	18	10	1	14	11	8	0	8	
278	95	0	6	9	no data				11	3	2	6	10	5	0	8	3	0	0	3	
302	23	0	1	5	no data				3	0	0	1	5	2	1	4	1	1	0	1	
325	10	1	3	2	no data				1	0	0	0	1	0	0	1	1	1	0	1	
348	0	0	0	0	no data				3	0	0	3	0	0	0	0	2	2	1	2	
371	0	0	0	0	no data				0	0	0	0	0	0	0	0	0	0	0	0	
394	0	0	0	0	no data				0	0	0	0	0	0	0	0	1	1	1	1	
418	0	0	0	0	no data				0	0	0	0	0	0	0	0	0	0	0	0	
<i>T.quin.</i>	total	dead	kum.	calc.	total	dead	kum.	calc.	total	dead	kum.	calc.	total	dead	kum.	calc.	total	dead	kum.	calc.	
70	223	79	0	0	no data				208	159	0	0	385	170	0	0	534	393	0	0	
93	99	40	0	0	no data				167	134	0	0	447	198	0	0	575	452	0	0	
116	39	12	0	0	no data				78	64	0	0	128	91	0	0	126	99	0	0	
139	43	13	0	0	no data				77	67	0	0	139	131	3	0	106	104	0	0	
162	48	14	0	0	no data				67	63	0	0	79	78	7	0	74	71	0	0	
186	23	9	0	0	no data				31	28	0	0	30	27	0	0	36	36	0	0	
209	36	5	0	0	no data				19	18	0	0	41	41	1	0	20	19	0	0	
232	30	9	0	0	no data				19	19	0	0	27	25	1	0	13	12	0	0	
255	8	2	0	0	no data				9	8	0	0	14	14	2	0	14	13	0	0	
278	9	0	0	0	no data				8	6	0	0	8	7	0	0	2	2	0	0	
302	0	0	0	0	no data				0	0	0	0	0	0	0	0	0	0	0	0	
325	0	0	0	0	no data				0	0	0	0	1	1	0	0	2	2	0	0	
348	0	0	0	0	no data				0	0	0	0	0	0	0	0	0	0	0	0	

Station N. pach. (s.)		404				50-100 m				100-200 m				200-300 m				300-500 m			
size-class	total	dead	kum.	calc.	total	dead	kum.	calc.	total	dead	kum.	calc.	total	dead	kum.	calc.	total	dead	kum.	calc.	
70	3	0	0	1	0	0	0	0	0	0	0	0	0	0	0	0	9	6	0	2	
93	6	1	0	0	0	0	0	0	6	2	0	2	2	2	0	1	14	10	0	6	
116	6	2	0	1	1	0	0	0	5	2	0	2	1	1	0	0	6	5	0	3	
139	4	1	0	0	5	0	0	0	5	2	1	3	2	2	0	0	13	11	0	12	
162	17	6	1	2	0	0	0	0	12	1	1	9	1	0	0	0	4	3	0	2	
186	7	3	0	0	2	0	0	0	9	3	1	5	1	0	0	0	2	0	0	1	
209	10	2	0	0	0	0	0	0	3	3	0	1	2	0	0	1	2	0	0	1	
232	10	2	0	3	0	0	0	0	6	0	1	3	1	0	0	1	1	1	0	1	
255	5	2	0	1	0	0	0	0	3	1	1	1	0	0	0	0	1	0	0	0	
278	4	0	0	2	1	0	0	0	1	0	1	1	0	0	0	0	1	1	0	1	
302	1	0	0	0	0	0	0	0	1	0	0	0	0	0	0	0	2	0	0	1	
325	0	0	0	0	0	0	0	0	1	0	0	1	0	0	0	0	0	0	0	0	
348	1	0	0	1	0	0	0	0	0	0	0	0	1	0	1	1	0	0	0	0	
371	0	0	0	0	0	0	0	0	0	0	0	0	0	0	0	0	0	0	0	0	
394	0	0	0	0	0	0	0	0	0	0	0	0	0	0	0	0	0	0	0	0	
418	0	0	0	0	0	0	0	0	0	0	0	0	0	0	0	0	0	0	0	0	
<i>T.quin.</i>	total	dead	kum.	calc.	total	dead	kum.	calc.	total	dead	kum.	calc.	total	dead	kum.	calc.	total	dead	kum.	calc.	
70	968	739	0	0	94	75	0	0	246	179	0	0	72	44	0	0	871	707	0	0	
93	502	399	0	0	96	85	0	0	393	305	0	0	158	127	0	0	1053	992	0	0	
116	95	58	0	0	23	19	0	0	119	101	0	0	53	44	0	0	163	155	0	0	
139	82	61	0	0	21	17	0	0	64	51	0	0	36	31	0	0	167	167	0	0	
162	67	43	0	0	29	21	0	0	84	61	0	0	25	23	0	0	146	142	0	0	
186	51	33	0	0	14	9	0	0	28	17	0	0	20	20	0	0	68	65	0	0	
209	15	7	0	0	5	0	0	0	8	4	0	0	8	8	0	0	35	35	0	0	
232	9	2	0	0	4	2	0	0	4	4	0	0	0	0	0	0	7	7	0	0	
255	1	1	0	0	0	0	0	0	2	2	0	0	0	0	0	0	5	5	0	0	
278	1	1	0	0	0	0	0	0	0	0	0	0	0	0	0	0	2	2	0	0	
302	1	1	0	0	0	0	0	0	0	0	0	0	0	0	0	0	0	0	0	0	
325	0	0	0	0	0	0	0	0	0	0	0	0	0	0	0	0	0	0	0	0	
348	0	0	0	0	0	0	0	0	0	0	0	0	0	0	0	0	0	0	0	0	

Appendix

Table 3: Stable Isotope Data of *N. pachyderma* (s.) from the Labrador Sea (M 39/4).

station	depth (m)	max. Diameter (μm)	n	^{13}C	$\pm\text{s}13$	^{18}O	$\pm\text{s}18$	Calc. Group
361	0-50	137	40	-0.88	0.01	1.14	0.02	nonencrusted
361	0-50	171	32	-0.70	0.01	1.28	0.02	nonencrusted
361	0-50	194	19	-0.53	0.02	1.18	0.04	nonencrusted
361	0-50	205	21	-0.25	0.01	1.24	0.01	nonencrusted
361	0-50	228	17	-0.12	0.02	1.38	0.03	nonencrusted
361	50-100	137	52	-0.83	0.01	1.49	0.03	nonencrusted
361	50-100	171	20	-0.40	0.02	1.49	0.04	nonencrusted
361	50-100	194	15	-0.24	0.02	1.74	0.04	nonencrusted
361	50-100	205	12	-0.41	0.02	1.45	0.06	nonencrusted
361	50-100	228	14	-0.12	0.01	1.77	0.02	nonencrusted
361	50-100	182	17	-0.02	0.02	2.12	0.03	heavily+encrusted
361	50-100	228	6	0.29	0.02	2.26	0.02	heavily+encrusted
361	50-100	262	13	0.07	0.01	1.78	0.04	nonencrusted
361	50-100	262	3	0.30	0.02	2.04	0.03	heavily encrusted
361	100-200	137	40	-0.84	0.01	1.50	0.02	nonencrusted
361	100-200	171	29	-0.52	0.01	1.72	0.02	nonencrusted
361	100-200	194	14	-0.36	0.03	1.75	0.03	nonencrusted
361	100-200	205	13	-0.30	0.01	1.61	0.03	nonencrusted
361	100-200	205	12	-0.28	0.01	1.72	0.03	nonencrusted
361	100-200	228	10	-0.24	0.02	1.41	0.03	nonencrusted
361	100-200	160	12	-0.37	0.01	2.11	0.04	encrusted
361	100-200	194	11	-0.02	0.01	2.17	0.03	encrusted
361	100-200	217	8	0.02	0.01	2.17	0.03	encrusted
361	100-200	228	9	0.05	0.02	2.16	0.05	encrusted
361	100-200	239	5	0.12	0.02	2.11	0.05	encrusted
361	100-200	239	5	0.15	0.02	2.23	0.04	encrusted
361	100-200	160	12	-0.33	0.01	2.24	0.01	heavily encrusted
361	100-200	182	6	-0.03	0.05	2.45	0.06	heavily encrusted
361	100-200	194	10	-0.08	0.02	2.19	0.03	heavily encrusted
361	100-200	205	7	0.16	0.01	2.43	0.03	heavily encrusted
361	100-200	205	7	0.20	0.01	2.27	0.02	heavily encrusted
361	100-200	217	4	0.17	0.01	2.21	0.03	heavily encrusted
361	100-200	217	4	0.10	0.01	2.37	0.02	heavily encrusted
361	100-200	217	4	0.23	0.02	2.29	0.02	heavily encrusted
361	100-200	217	4	0.11	0.02	2.32	0.04	heavily encrusted
361	100-200	217	5	0.40	0.10	2.54	0.13	heavily encrusted
361	100-200	228	5	-0.01	0.10	2.27	0.09	heavily encrusted
361	100-200	228	5	0.16	0.02	2.20	0.02	heavily encrusted
361	100-200	228	5	0.22	0.01	2.31	0.03	heavily encrusted
361	100-200	228	4	0.30	0.03	2.49	0.04	heavily encrusted
361	100-200	228	4	0.37	0.01	2.27	0.03	heavily encrusted
361	100-200	239	4	0.29	0.02	2.39	0.03	heavily encrusted
361	100-200	239	4	0.19	0.01	2.30	0.03	heavily encrusted
361	100-200	239	3	0.26	0.02	2.25	0.04	heavily encrusted
361	100-200	239	3	0.04	0.01	2.29	0.03	heavily encrusted
361	100-200	251	10	0.11	0.01	1.93	0.01	nonencrusted
361	100-200	262	6	-0.15	0.01	1.80	0.04	nonencrusted
361	100-200	296	7	0.09	0.01	1.74	0.02	nonencrusted
361	100-200	251	7	0.21	0.02	2.26	0.04	encrusted
361	100-200	262	3	0.28	0.01	2.31	0.02	encrusted
361	100-200	262	3	0.27	0.02	2.11	0.03	encrusted
361	100-200	285	2	0.30	0.01	2.33	0.03	encrusted
361	100-200	285	3	0.36	0.01	2.26	0.03	encrusted
361	100-200	296	3	0.25	0.01	2.32	0.02	encrusted
361	100-200	296	3	0.40	0.01	2.29	0.01	encrusted
361	100-200	296	3	0.28	0.03	2.34	0.04	encrusted
361	100-200	296	3	0.29	0.02	2.35	0.02	encrusted
361	100-200	296	5	0.31	0.02	2.09	0.03	encrusted
361	100-200	308	2	0.16	0.02	2.34	0.04	encrusted
361	100-200	308	2	0.45	0.03	2.18	0.05	encrusted
361	100-200	308	2	0.34	0.01	2.31	0.03	encrusted
361	100-200	308	2	0.29	0.07	2.22	0.10	encrusted
361	100-200	308	2	0.35	0.01	2.16	0.03	encrusted
361	100-200	319	2	0.41	0.01	2.32	0.04	encrusted
361	100-200	319	3	0.21	0.01	2.22	0.02	encrusted
361	100-200	331	3	0.56	0.07	2.38	0.12	encrusted
361	100-200	342	2	0.45	0.02	2.32	0.03	encrusted
361	100-200	342	3	0.43	0.01	2.17	0.02	encrusted
361	100-200	353	2	0.29	0.01	2.10	0.03	encrusted
361	100-200	353	2	0.34	0.02	2.08	0.02	encrusted
361	100-200	353	2	0.43	0.03	2.57	0.03	encrusted
361	100-200	353	3	0.35	0.02	2.19	0.02	encrusted
361	100-200	365	2	0.24	0.02	2.71	0.04	encrusted
361	100-200	365	2	0.50	0.01	2.38	0.03	encrusted
361	100-200	365	2	0.18	0.02	2.13	0.04	encrusted
361	100-200	365	2	0.39	0.01	2.16	0.03	encrusted
361	100-200	365	2	0.55	0.01	2.25	0.01	encrusted
361	100-200	388	2	0.51	0.01	2.45	0.03	encrusted
361	100-200	388	2	0.49	0.01	2.26	0.02	encrusted
361	100-200	388	3	0.45	0.01	2.23	0.02	encrusted
361	100-200	399	1	0.42	0.02	2.12	0.03	encrusted
361	100-200	251	3	0.14	0.01	2.30	0.02	heavily encrusted
361	100-200	251	4	0.17	0.01	2.27	0.02	heavily encrusted
361	100-200	251	4	0.28	0.01	2.28	0.02	heavily encrusted
361	100-200	262	3	0.35	0.02	2.40	0.03	heavily encrusted
361	100-200	262	4	0.40	0.01	2.33	0.02	heavily encrusted
361	100-200	262	4	0.19	0.02	2.31	0.04	heavily encrusted
361	100-200	274	3	0.25	0.01	2.30	0.03	heavily encrusted
361	100-200	274	4	0.27	0.01	2.20	0.02	heavily encrusted
361	100-200	285	2	0.31	0.01	2.17	0.03	heavily encrusted
361	100-200	285	2	0.07	0.02	2.18	0.03	heavily encrusted

Appendix

Table 3: Continued.

station	depth (m)	max. Diameter (μm)	n	^{13}C	$\pm\text{s}13$	^{18}O	$\pm\text{s}18$	Calc. Group
361	100-200	285	2	0.35	0.01	2.17	0.04	heavily encrusted
361	100-200	296	2	0.16	0.03	2.14	0.03	heavily encrusted
361	100-200	296	3	0.06	0.02	1.84	0.01	heavily encrusted
361	100-200	308	3	0.34	0.01	2.29	0.03	heavily encrusted
361	200-300	331	2	0.22	0.02	2.23	0.04	encrusted
361	200-300	262	3	-0.07	0.02	1.95	0.04	encrusted
361	200-300	274	2	-0.05	0.01	1.97	0.03	heavily encrusted
361	300-500	125	59	-1.46	0.01	1.97	0.04	nonencrusted
361	300-500	148	56	-1.36	0.01	1.91	0.03	nonencrusted
361	300-500	171	33	-1.00	0.02	1.90	0.06	nonencrusted
361	300-500	182	22	-0.89	0.02	1.94	0.02	nonencrusted
361	300-500	182	17	-0.86	0.02	1.84	0.03	nonencrusted
361	300-500	205	24	-1.32	0.02	1.88	0.05	nonencrusted
361	300-500	228	11	-0.43	0.01	1.77	0.04	nonencrusted
361	300-500	194	16	-0.43	0.01	2.28	0.02	encrusted
361	300-500	160	8	-0.45	0.01	2.26	0.03	heavily encrusted
361	300-500	217	5	-0.37	0.01	2.39	0.03	heavily encrusted
361	300-500	228	4	0.15	0.01	2.49	0.03	heavily encrusted
361	300-500	251	7	-1.11	0.01	2.00	0.03	nonencrusted
361	300-500	262	5	-0.19	0.02	2.12	0.03	encrusted
361	300-500	319	3	0.55	0.02	2.79	0.07	encrusted
361	300-500	251	4	0.12	0.02	2.48	0.03	heavily encrusted
361	300-500	342	5	0.41	0.02	2.48	0.04	heavily encrusted
402	0-50	125	58	-1.05	0.02	0.32	0.02	nonencrusted
402	0-50	137	39	-0.96	0.02	0.40	0.02	nonencrusted
402	0-50	148	34	-0.82	0.02	0.57	0.02	nonencrusted
402	0-50	148	34	-0.87	0.03	0.35	0.04	nonencrusted
402	0-50	160	33	-0.66	0.02	0.30	0.03	nonencrusted
402	0-50	160	34	-0.76	0.01	0.48	0.02	nonencrusted
402	0-50	171	30	-0.49	0.01	0.44	0.05	nonencrusted
402	0-50	171	30	-0.52	0.01	0.70	0.02	nonencrusted
402	0-50	171	29	-0.47	0.01	0.36	0.02	nonencrusted
402	0-50	182	23	-0.35	0.02	0.61	0.03	nonencrusted
402	0-50	182	23	-0.40	0.02	0.75	0.04	nonencrusted
402	0-50	182	22	-0.31	0.01	0.79	0.03	nonencrusted
402	0-50	182	26	-0.44	0.02	0.58	0.03	nonencrusted
402	0-50	194	22	-0.23	0.02	0.68	0.02	nonencrusted
402	0-50	194	22	-0.16	0.03	0.95	0.03	nonencrusted
402	0-50	194	22	-0.27	0.01	0.49	0.02	nonencrusted
402	0-50	194	18	-0.25	0.01	0.26	0.04	nonencrusted
402	0-50	205	17	-0.11	0.06	0.63	0.09	nonencrusted
402	0-50	205	17	-0.17	0.01	0.77	0.03	nonencrusted
402	0-50	205	17	-0.15	0.01	0.67	0.03	nonencrusted
402	0-50	205	19	-0.19	0.01	0.95	0.01	nonencrusted
402	0-50	217	12	-0.08	0.01	0.59	0.04	nonencrusted
402	0-50	217	12	-0.15	0.01	0.59	0.02	nonencrusted
402	0-50	217	12	0.02	0.03	0.56	0.03	nonencrusted
402	0-50	217	12	0.06	0.03	0.68	0.02	nonencrusted
402	0-50	217	11	-0.04	0.02	0.54	0.03	nonencrusted
402	0-50	228	12	0.08	0.05	0.69	0.08	nonencrusted
402	0-50	228	12	-0.01	0.03	0.71	0.04	nonencrusted
402	0-50	228	12	-0.03	0.01	0.74	0.02	nonencrusted
402	0-50	228	12	-0.02	0.01	0.90	0.03	nonencrusted
402	0-50	228	12	-0.04	0.06	0.72	0.08	nonencrusted
402	0-50	239	13	0.12	0.01	0.80	0.02	nonencrusted
402	0-50	239	13	0.15	0.01	1.01	0.03	nonencrusted
402	0-50	239	13	0.11	0.03	1.15	0.03	nonencrusted
402	0-50	239	13	0.06	0.01	0.75	0.02	nonencrusted
402	0-50	239	13	0.14	0.01	0.94	0.03	nonencrusted
402	0-50	189	2	0.08	0.01	1.21	0.02	heavily+encrusted
402	0-50	239	5	0.27	0.01	1.02	0.04	encrusted
402	0-50	251	9	0.12	0.01	0.91	0.03	nonencrusted
402	0-50	251	9	0.20	0.03	0.79	0.02	nonencrusted
402	0-50	251	9	0.21	0.02	0.76	0.04	nonencrusted
402	0-50	251	9	0.23	0.01	0.90	0.03	nonencrusted
402	0-50	251	10	0.11	0.01	0.85	0.03	nonencrusted
402	0-50	262	8	0.24	0.02	0.78	0.03	nonencrusted
402	0-50	262	8	0.30	0.01	0.79	0.03	nonencrusted
402	0-50	262	9	0.35	0.01	0.86	0.02	nonencrusted
402	0-50	262	9	0.19	0.02	1.19	0.03	nonencrusted
402	0-50	262	9	0.26	0.02	0.86	0.02	nonencrusted
402	0-50	274	8	0.34	0.02	0.95	0.03	nonencrusted
402	0-50	274	8	0.27	0.02	0.99	0.03	nonencrusted
402	0-50	274	9	0.24	0.03	0.66	0.02	nonencrusted
402	0-50	274	9	0.26	0.01	1.12	0.02	nonencrusted
402	0-50	274	8	0.25	0.02	0.67	0.04	nonencrusted
402	0-50	285	6	0.25	0.01	0.65	0.02	nonencrusted
402	0-50	285	6	0.36	0.02	1.19	0.04	nonencrusted
402	0-50	285	6	0.44	0.03	1.05	0.03	nonencrusted
402	0-50	296	7	0.51	0.03	1.21	0.02	nonencrusted
402	0-50	296	7	0.33	0.02	1.07	0.04	nonencrusted
402	0-50	308	5	0.35	0.01	1.38	0.03	nonencrusted
402	0-50	314	5	0.49	0.02	0.96	0.05	nonencrusted
402	0-50	262	2	0.37	0.01	1.55	0.03	encrusted
402	0-50	291	4	0.46	0.01	0.97	0.02	encrusted

Appendix

Table 4: Absolute Abundances of Planktonic Foraminifera (Ind*m⁻³) in the Greenland Sea (Ark XV/1).

Station: 55/18								
Depth (m)	<i>N. pach.</i> (s.)	<i>N. pach.</i> (d.)	<i>T. quin.</i>	<i>G. bull.</i>	<i>G. glu.</i>	<i>G. uvul.</i>	<i>O. ried.</i>	other
63-125 µm								
0-50	3.92	0.08	10.08	0	0	0	0	0
50-100	5.92	0.24	13.04	0	0.16	0	0	0
100-200	12.28	0.32	33.6	0	0.12	0.04	0	0
200-300	6.28	0	23.96	0	0	0.04	0	0
300-500	6.86	0.14	23.68	0.02	0	0.06	0	0
125-250 µm								
0-50	5.28	0.24	2.16	0	0	0	0	0
50-100	11.92	0.4	5.52	0.16	0	0	0	0
100-200	22.24	0.68	14.52	0.16	0	0	0	0.04
200-300	10.32	0.44	2.32	0	0	0	0	0
300-500	6.22	0.18	2.18	0.06	0	0	0.04	0.02
250-500 µm								
0-50	0.56	0	0	0	0	0	0	0
50-100	1.2	0	0	0	0	0	0	0
100-200	1.36	0	0.04	0.08	0	0	0	0
200-300	0.52	0.04	0	0	0	0	0	0
300-500	0.2	0	0.02	0	0	0	0	0
total								
0-50	9.76	0.32	12.24	0	0	0	0	0
50-100	19.04	0.64	18.56	0.16	0.16	0	0	0
100-200	35.88	1	48.16	0.24	0.12	0.04	0	0.04
200-300	17.12	0.48	26.28	0	0	0.04	0	0
300-500	13.28	0.32	25.88	0.08	0	0.06	0.04	0.02
Station: 55/19								
Depth (m)	<i>N. pach.</i> (s.)	<i>N. pach.</i> (d.)	<i>T. quin.</i>	<i>G. bull.</i>	<i>G. glu.</i>	<i>G. uvul.</i>	<i>O. ried.</i>	other
63-125 µm								
0-50	1.52	0	3.28	0	0.08	0	0	0
50-100	7.44	0.16	17.2	0	0.08	0	0	0
100-200	25.68	0.32	94.28	0	0.12	0	0	0
200-300	5.28	0	14.8	0	0	0.04	0	0
300-500	1.88	0.04	5.1	0	0	0	0	0
125-250 µm								
0-50	2.32	0.08	1.12	0	0	0	0	0
50-100	19.04	0.4	11.76	0.16	0	0	0	0.08
100-200	53.96	1.64	34.8	0.48	0	0	0	0
200-300	9.72	0.36	4.64	0.08	0	0	0	0
300-500	4.86	0.1	2.08	0.02	0	0	0	0.02
250-500 µm								
0-50	0.08	0	0	0	0	0	0	0
50-100	1.36	0.08	0	0	0	0	0	0
100-200	3.64	0.24	0.04	0.16	0	0	0	0
200-300	0.36	0.04	0	0	0	0	0	0
300-500	0.26	0.02	0	0	0	0	0	0
total								
0-50	3.92	0.08	4.4	0	0.08	0	0	0
50-100	27.84	0.64	28.96	0.16	0.08	0	0	0.08
100-200	83.28	2.2	129.12	0.64	0.12	0	0	0
200-300	15.36	0.4	19.44	0.08	0	0.04	0	0
300-500	7	0.16	7.18	0.02	0	0	0	0.02
Station: 55/25								
Depth (m)	<i>N. pach.</i> (s.)	<i>N. pach.</i> (d.)	<i>T. quin.</i>	<i>G. bull.</i>	<i>G. glu.</i>	<i>G. uvul.</i>	<i>O. ried.</i>	other
63-125 µm								
0-50	26.56	0	44.16	0	0	0	0	0
50-100	7.76	0	12.48	0	0.08	0.08	0.08	0
100-200	8.88	0.08	20.36	0	0.08	0	0	0
200-300	4.64	0.04	13.72	0	0.08	0.04	0	0
300-500	3.9	0.02	25.3	0	0.08	0.06	0.02	0
125-250 µm								
0-50	76.16	0.32	40.96	0.64	0	0	0	0
50-100	35.76	0.48	9.12	0.16	0	0	0	0
100-200	22.88	0.28	8.28	0.2	0	0	0	0
200-300	7.4	0.12	3	0.08	0	0	0	0
300-500	8.62	0.26	4.16	0.14	0	0.02	0	0
250-500 µm								
0-50	2.24	0	1.28	0	0	0	0	0
50-100	2.24	0	0.08	0.08	0	0	0	0
100-200	1.76	0.08	0.04	0.16	0	0	0	0
200-300	0.28	0	0	0.04	0	0	0	0
300-500	0.44	0	0	0.04	0	0	0	0
total								
0-50	104.96	0.32	86.4	0.64	0	0	0	0
50-100	45.76	0.48	21.68	0.24	0.08	0.08	0.08	0
100-200	33.52	0.44	28.68	0.36	0.08	0	0	0
200-300	12.32	0.16	16.72	0.12	0.08	0.04	0	0
300-500	12.96	0.28	29.46	0.18	0.08	0.08	0.02	0

Appendix

Table 4: Continued.

Station: 55/30									
Depth (m)	<i>N. pach.</i> (s.)	<i>N. pach.</i> (d.)	<i>T. quin.</i>	<i>G. bull.</i>	<i>G. glu.</i>	<i>G. uvul.</i>	<i>O. ried.</i>	other	
63-125 µm									
0-50	5.36	0	11.6	0	0	0.08	0	0	
50-100	45.12	0.64	103.04	0.64	0	0	0	0	
100-200	18.24	0.64	100	0.16	0.32	0	0	0	
200-300	7.84	0.16	41.12	0	0	0	0	0	
300-500	3.72	0.08	29.54	0.1	0	0.02	0	0	
125-250 µm									
0-50	17.68	0.32	8.48	0.08	0	0	0	0	
50-100	124.48	1.92	49.6	1.28	0	0	0	0	
100-200	33.12	0.96	36.16	0	0	0	0	0	
200-300	12.48	0.48	20.16	0.32	0	0	0	0	
300-500	6.4	0.12	15.22	0.16	0.06	0	0	0	0.02
250-500 µm									
0-50	0.48	0.08	0.08	0	0	0	0	0	
50-100	4.48	0	0	0.32	0	0	0	0	
100-200	2.08	0.16	0	0	0	0	0	0	
200-300	0.48	0	0	0	0	0	0	0	
300-500	0.08	0	0	0	0	0	0	0	
total									
0-50	23.52	0.4	20.16	0.08	0	0.08	0	0	
50-100	174.08	2.56	152.64	2.24	0	0	0	0	
100-200	53.44	1.76	136.16	0.16	0.32	0	0	0	
200-300	20.8	0.64	61.28	0.32	0	0	0	0	
300-500	10.2	0.2	44.76	0.26	0.06	0.02	0	0	0.02
Station: 55/37									
Depth (m)	<i>N. pach.</i> (s.)	<i>N. pach.</i> (d.)	<i>T. quin.</i>	<i>G. bull.</i>	<i>G. glu.</i>	<i>G. uvul.</i>	<i>O. ried.</i>	other	
63-125 µm									
0-50	227.84	3.84	469.76	0	0	0	0	0	1.28
50-100	110.08	2.56	258.56	0	0	0	0	0	0
100-200	23.68	0.64	187.52	0	0	0	0	0	0
200-300	10.24	0	131.84	0	0	0	0	0	0
300-500	13.28	0.24	92.48	0	0	0	0	0	0
125-250 µm									
0-50	291.84	2.56	121.6	1.28	0	0	0	0	0
50-100	117.76	2.56	58.88	0	0	0	0	0	0
100-200	51.84	0.64	95.36	0	0	0	0	0	0
200-300	15.04	0.32	62.4	0.32	0	0	0	0	0
300-500	15.12	0.4	40.96	0.16	0.08	0	0	0	0
250-500 µm									
0-50	2.56	1.28	0	0	0	0	0	0	0
50-100	2.56	0	0	0	0	0	0	0	0
100-200	2.56	0	0	0	0	0	0	0	0
200-300	0.64	0	0	0	0	0	0	0	0
300-500	0.4	0.08	0	0	0	0	0	0	0
total									
0-50	522.24	7.68	591.36	1.28	0	0	0	0	1.28
50-100	230.4	5.12	317.44	0	0	0	0	0	0
100-200	78.08	1.28	282.88	0	0	0	0	0	0
200-300	25.92	0.32	194.24	0.32	0	0	0	0	0
300-500	28.8	0.72	133.44	0.16	0.08	0	0	0	0
Station: 55/43									
Depth (m)	<i>N. pach.</i> (s.)	<i>N. pach.</i> (d.)	<i>T. quin.</i>	<i>G. bull.</i>	<i>G. glu.</i>	<i>G. uvul.</i>	<i>O. ried.</i>	other	
63-125 µm									
0-50	212.48	3.84	576	0	0	0	0	0	0
50-100	203.52	2.56	1003.52	1.28	0	0	0	0	0
100-200	14.08	0	231.04	0	0	0	0	0	0
200-300	8.96	0	81.6	0	0	0	0	0	0
300-500	8	0	141.76	0	0	0	0	0	0
125-250 µm									
0-50	510.72	7.68	176.64	2.56	0	0	0	0	0
50-100	294.4	6.4	275.2	3.84	0	0	0	0	0
100-200	51.2	1.28	316.16	0.64	0	0	0	0	0
200-300	18.88	0.96	121.6	0	0.32	0.32	0	0	0
300-500	10.24	0.32	42.56	0	0	0	0	0	0
250-500 µm									
0-50	30.72	0	1.28	1.28	0	0	0	0	0
50-100	10.24	0	1.28	0	0	0	0	0	0
100-200	6.4	0.64	0	0	0	0	0	0	0
200-300	1.6	0	0	0	0	0	0	0	0.32
300-500	0.32	0	0.32	0	0	0	0	0	0
total									
0-50	753.92	11.52	753.92	3.84	0	0	0	0	0
50-100	508.16	8.96	1280	5.12	0	0	0	0	0
100-200	71.68	1.92	547.2	0.64	0	0	0	0	0
200-300	29.44	0.96	203.2	0	0.32	0	0	0	0.32
300-500	18.56	0.32	184.64	0	0	0	0	0	0

Appendix

Table 4: Continued.

Station: 55/51								
Depth (m)	<i>N. pach.</i> (s.)	<i>N. pach.</i> (d.)	<i>T. quin.</i>	<i>G. bull.</i>	<i>G. glu.</i>	<i>G. uvul.</i>	<i>O. ried.</i>	other
63-125 µm								
0-50	97.28	1.28	509.44	0	71.68	10.24	0	0
50-100	113.92	1.28	949.76	0	14.08	5.12	1.28	0
100-200	36.48	0	231.04	0	14.08	0.64	0	0
200-300	32	0	121.92	0	15.68	3.04	0	0
300-500	7.76	0.16	29.28	0	4.24	2.96	0	0
125-250 µm								
0-50	98.56	2.56	236.8	2.56	0	6.4	0	0
50-100	161.28	6.4	259.84	0	0	6.4	0	0
100-200	61.44	4.48	66.56	0	0	0	0	0
200-300	28.32	0.64	15.84	0.16	0	1.44	0	0
300-500	10.32	0.32	16.8	0	0	0.16	0	0
250-500 µm								
0-50	10.24	0	12.8	0	0	0	0	0
50-100	23.04	0	12.8	0	0	0	0	0
100-200	0.64	0	1.28	0	0	0	0	0
200-300	1.12	0.16	0.48	0	0	0	0	0
300-500	0.48	0	1.2	0	0	0	0	0
total								
0-50	206.08	3.84	759.04	2.56	71.68	16.64	0	0
50-100	298.24	7.68	1222.4	0	14.08	11.52	1.28	0
100-200	98.56	4.48	298.88	0	14.08	0.64	0	0
200-300	61.44	0.8	138.24	0.16	15.68	4.48	0	0
300-500	18.56	0.48	47.28	0	4.24	3.12	0	0
Station: 55/63								
Depth (m)	<i>N. pach.</i> (s.)	<i>N. pach.</i> (d.)	<i>T. quin.</i>	<i>G. bull.</i>	<i>G. glu.</i>	<i>G. uvul.</i>	<i>O. ried.</i>	other
63-125 µm								
0-50	12.16	0	99.84	0.32	60.48	4.48	0.32	0
50-100	8.96	0	256	0	24.32	5.12	0	0
100-200	8.96	0	339.84	0	12.16	3.84	0	0
200-300	3.52	0	34.56	0	1.44	1.6	0.16	0
300-500	3.52	0.08	28.96	0	4.08	1.52	0	0
125-250 µm								
0-50	29.76	0.64	130.88	0.96	1.92	4.16	0.64	0
50-100	17.92	1.28	188.16	1.28	0	3.84	0	0
100-200	7.68	0.64	96	0	0	2.56	0.64	0
200-300	4	0.16	34.56	0	0.32	0.48	0	0
300-500	2.88	0.24	18.32	0	0	0.4	0	0
250-500 µm								
0-50	4.8	0	6.72	0	0	0	0	0
50-100	19.2	1.28	3.84	0	0	0	0	0
100-200	1.28	0	1.92	0	0	0	0	0
200-300	0.64	0	0.96	0	0	0	0	0
300-500	1.12	0	1.04	0	0	0	0	0
total								
0-50	46.72	0.64	237.44	1.28	62.4	8.64	0.96	0
50-100	46.08	2.56	448	1.28	24.32	8.96	0	0
100-200	17.92	0.64	437.76	0	12.16	6.4	0.64	0
200-300	8.16	0.16	70.08	0	1.76	2.08	0.16	0
300-500	7.52	0.32	48.32	0	4.08	1.92	0	0
Station: 55/66								
Depth (m)	<i>N. pach.</i> (s.)	<i>N. pach.</i> (d.)	<i>T. quin.</i>	<i>G. bull.</i>	<i>G. glu.</i>	<i>G. uvul.</i>	<i>O. ried.</i>	other
63-125 µm								
0-50	11.2	0	216.32	0	50.88	3.84	0	0
50-100	8.96	0	443.84	0	16.96	9.92	0.32	0
100-200	9.92	0	94.72	0	8.48	2.72	0	0.16
200-300	1.52	0	4.64	0	0.72	0.44	0.04	0
300-500	1.76	0	15.84	0	2.08	0.64	0	0
125-250 µm								
0-50	11.52	0.32	122.56	0.64	0.96	2.24	0.64	0
50-100	33.92	0.32	159.04	0	0.32	6.72	0.64	0
100-200	17.44	0.48	55.04	0.16	0.32	2.24	0.16	0
200-300	4.24	0.12	7.32	0.04	0	0.08	0	0
300-500	5.12	0.08	8.8	0.08	0.08	0.4	0.08	0
250-500 µm								
0-50	3.84	0	4.48	0	0	0	0	0
50-100	16	0	4.48	0	0	0	0	0
100-200	4.48	0	1.12	0.16	0	0	0	0
200-300	0.52	0	0.48	0	0	0	0	0
300-500	0.64	0	1.28	0	0	0	0	0
total								
0-50	26.56	0.32	343.36	0.64	51.84	6.08	0.64	0
50-100	58.88	0.32	607.36	0	17.28	16.64	0.96	0
100-200	31.84	0.48	150.88	0.32	8.8	4.96	0.16	0.16
200-300	6.28	0.12	12.44	0.04	0.72	0.52	0.04	0
300-500	7.52	0.08	25.92	0.08	2.16	1.04	0.08	0

Appendix

Table 5: Continued.

Station 51 N. pach. (s.)		0-50 m				50-100 m				100-200 m				200-300 m				300-500 m			
size-class	total	dead	kum.	calc.	total	dead	kum.	calc.	total	dead	kum.	calc.	total	dead	kum.	calc.	total	dead	kum.	calc.	
70	18	8	0	0	10	4	0	0	3	1	0	0	7	3	0	0	4	2	0	0	
93	25	13	0	0	33	9	1	0	27	4	0	0	69	26	2	2	21	12	0	1	
116	33	14	0	0	46	6	0	0	27	5	2	1	124	44	4	15	72	38	4	17	
139	20	5	3	0	33	4	0	0	34	4	9	13	69	19	12	18	47	20	9	21	
162	25	7	1	1	35	3	3	4	34	3	8	10	51	25	8	26	35	12	3	9	
186	11	2	0	0	25	3	3	1	18	2	8	10	24	7	3	8	29	6	3	8	
209	5	0	0	0	24	2	4	7	4	1	2	3	25	9	2	9	12	2	1	3	
232	16	3	3	3	9	1	1	1	6	2	0	3	8	2	1	1	6	1	1	1	
255	4	0	0	0	13	1	4	6	0	0	0	0	5	1	2	4	5	1	2	3	
278	3	0	1	1	1	0	0	1	1	1	0	1	2	0	0	1	1	1	1	1	
302	0	0	0	0	3	0	1	2	0	0	0	0	0	0	0	0	0	0	0	0	
325	1	0	0	1	1	0	0	1	0	0	0	0	0	0	0	0	0	0	0	0	
348	0	0	0	0	0	0	0	0	0	0	0	0	0	0	0	0	0	0	0	0	
371	0	0	0	0	0	0	0	0	0	0	0	0	0	0	0	0	0	0	0	0	
394	0	0	0	0	0	0	0	0	0	0	0	0	0	0	0	0	0	0	0	0	
418	0	0	0	0	0	0	0	0	0	0	0	0	0	0	0	0	0	0	0	0	
<i>T.qum.</i>	total	dead	kum.	calc.	total	dead	kum.	calc.	total	dead	kum.	calc.	total	dead	kum.	calc.	total	dead	kum.	calc.	
70	230	91	0	0	328	56	0	0	133	17	0	0	255	63	0	0	100	19	0	1	
93	104	40	0	0	243	37	0	0	154	41	0	1	327	104	1	15	164	78	1	21	
116	64	22	1	1	171	18	0	0	74	24	1	5	180	78	2	31	102	58	1	43	
139	52	12	0	0	74	8	0	2	39	22	0	12	41	27	1	17	42	30	4	21	
162	61	17	0	1	54	7	2	10	31	14	1	14	32	20	2	19	47	37	6	35	
186	36	12	1	2	46	6	3	20	14	9	2	14	12	6	1	9	50	46	8	46	
209	20	7	1	1	18	1	5	16	11	7	2	10	8	5	0	5	50	41	4	42	
232	16	5	1	3	11	2	1	7	9	7	0	9	6	6	1	5	21	21	6	20	
255	8	1	1	3	9	1	1	8	2	1	0	1	3	3	0	3	10	8	1	8	
278	2	0	0	1	1	0	0	1	0	0	0	0	0	0	0	0	4	3	0	3	
302	0	0	0	0	0	0	0	0	0	0	0	0	0	0	0	0	1	1	0	1	
325	0	0	0	0	0	0	0	0	0	0	0	0	0	0	0	0	0	0	0	0	
348	0	0	0	0	0	0	0	0	0	0	0	0	0	0	0	0	0	0	0	0	
371	0	0	0	0	0	0	0	0	0	0	0	0	0	0	0	0	0	0	0	0	
394	0	0	0	0	0	0	0	0	0	0	0	0	0	0	0	0	0	0	0	0	
418	0	0	0	0	0	0	0	0	0	0	0	0	0	0	0	0	0	0	0	0	
<i>T.qum.</i>	total	dead	kum.	calc.	total	dead	kum.	calc.	total	dead	kum.	calc.	total	dead	kum.	calc.	total	dead	kum.	calc.	
70	9	1	0	0	2	0	0	0	0	0	0	0	5	3	0	2	7	5	0	2	
93	8	3	1	0	3	1	0	0	4	1	1	0	6	4	0	2	12	10	3	5	
116	21	5	1	2	2	0	0	0	10	5	1	1	11	10	4	5	25	23	2	8	
139	22	8	0	2	3	0	0	0	5	1	0	2	9	6	1	2	15	13	4	4	
162	17	1	2	0	6	0	1	1	3	2	0	0	3	3	0	0	10	8	0	0	
186	17	1	2	1	4	1	0	0	3	3	0	0	6	2	1	1	6	4	1	1	
209	21	2	1	0	1	0	0	0	0	0	0	0	1	1	0	0	2	1	1	0	
232	16	2	2	2	0	0	0	0	1	0	0	0	5	1	0	0	3	0	1	1	
255	8	0	1	1	4	0	1	4	0	0	0	0	1	0	0	0	8	3	2	2	
278	3	0	1	1	5	0	4	3	2	0	2	2	2	0	0	0	3	1	1	1	
302	2	0	0	0	4	0	1	4	0	0	0	0	1	0	0	0	1	0	0	0	
325	1	0	0	0	1	0	0	1	0	0	0	0	0	0	0	0	1	0	0	1	
348	1	0	0	1	1	0	1	1	0	0	0	0	0	0	0	0	1	1	0	1	
371	0	0	0	0	0	0	0	0	0	0	0	0	0	0	0	0	0	0	0	0	
394	0	0	0	0	0	0	0	0	0	0	0	0	0	0	0	0	0	0	0	0	
418	0	0	0	0	0	0	0	0	0	0	0	0	0	0	0	0	0	0	0	0	
<i>T.qum.</i>	total	dead	kum.	calc.	total	dead	kum.	calc.	total	dead	kum.	calc.	total	dead	kum.	calc.	total	dead	kum.	calc.	
70	127	41	0	1	83	3	0	0	271	20	0	1	50	14	0	4	157	66	2	23	
93	86	27	0	1	65	8	0	0	153	15	0	4	71	39	1	24	120	77	2	26	
116	99	35	0	7	52	8	0	0	107	22	4	18	95	47	2	55	85	67	1	46	
139	112	35	3	10	53	3	0	0	59	16	4	37	86	63	5	66	78	68	5	51	
162	127	24	2	5	51	6	0	2	66	12	5	35	72	60	10	65	99	82	12	76	
186	76	14	1	1	22	2	0	1	21	4	7	14	30	18	8	23	31	20	4	19	
209	52	12	0	3	13	3	1	1	2	1	1	0	9	4	0	5	10	6	0	6	
232	42	8	1	4	8	0	0	2	2	0	1	0	19	13	2	9	11	6	3	5	
255	14	1	0	1	1	0	0	1	2	0	0	2	4	4	0	3	9	4	0	6	
278	7	1	1	2	2	0	0	0	1	1	0	1	2	2	1	1	3	3	2	2	
302	0	0	0	0	0	0	0	0	0	0	0	0	0	0	0	0	1	0	1	0	
325	0	0	0	0	0	0	0	0	0	0	0	0	0	0	0	0	0	0	0	0	
348	0	0	0	0	0	0	0	0	0	0	0	0	0	0	0	0	0	0	0	0	
371	0	0	0	0	0	0	0	0	0	0	0	0	0	0	0	0	0	0	0	0	
394	0	0	0	0	0	0	0	0	0	0	0	0	0	0	0	0	0	0	0	0	
418	0	0	0	0	0	0	0	0	0	0	0	0	0	0	0	0	0	0	0	0	
<i>T.qum.</i>	total	dead	kum.	calc.	total	dead	kum.	calc.	total	dead	kum.	calc.	total	dead	kum.	calc.	total	dead	kum.	calc.	
70	316	84	0	1	621	32	0	1	185	25	0	4	45	15	0	14	42	16	0	4	
93	191	60	0	0	426	32	0	2	229	43	0	4	30	17	1	13	89	44	2	23	
116	169	50	0	1	340	41	1	1	178	39	0	15	41	23	0	27	67	36	2	15	
139	140	44	0	0	187	23	2	3	130	36	7	27	37	28	3	27	39	30	3	8	
162	118	31	1	3	171	29	6	13	108	34	11	47	67	54	7	47	30	22	4	11	
186	51	8	1	0	71	11	4	14	60	13	14	46	47	31	10	32	21	15	2	9	
209	45	3	1	2	41	2	10	28	33	6	8	20	19	16	2	13	8	6	2	2	
232	29	4	4	3	27	1	7	25	13	2	2	7	13	6	2	8	12	10	4	9	
255	12	4	3	4	9	0	1	8	5	0	1	4	9	6	1	7	7	5	0	6	
278	2	0	0	0	4	0	0	3	2	0	0	2	2	0	0	1	8	8	1	8	
302	0	0	0	0	1	0	0	0	0	0	0	0	0	0	0	0	1	0	0	0	
325	0	0	0	0	0	0	0	0	0	0	0	0	0	0	0	0	0	0	0	0	
348	0	0	0	0	0	0	0	0	0	0	0	0	0	0	0	0	0	0	0	0	
371	0	0	0	0	0	0	0	0	0	0	0	0	0	0	0	0	0	0	0	0	
394	0	0	0	0	0	0	0	0	0	0	0	0	0	0	0	0	0	0	0	0	
418	0	0	0	0	0	0	0	0	0	0	0	0	0	0	0	0	0	0	0	0	
<i>T.qum.</i>	total	dead	kum.	calc.	total	dead	kum.	calc.	total	dead	kum.	calc.	total	dead	kum.	calc.	total	dead	kum.	calc.	
70	13	5	0	0	8	3	0	0	2	1	1	1	5	4	0	0	1	1	0	0	
93	7	4	0	0	4	2	0	0	16	7	2	3	10	9	2	2	6	4	1	3	
116	15	5	1	0	16	4	0</														

Appendix

Table 6: Absolute Abundances of Planktonic Foraminifera (Ind*m⁻³) in the Fram Strait (Ark XV/2).

Station: 55/77								
Depth (m)	<i>N. pach.</i> (s.)	<i>N. pach.</i> (d.)	<i>T. quin.</i>	<i>G. bull.</i>	<i>G. glu.</i>	<i>G. uvul.</i>	<i>O. ried.</i>	other
63-125 µm								
0-50	0.08	0	84.48	0	1.76	0.24	0	0
50-100	0.16	0	93.68	0.08	0.32	0.16	0.08	0
100-200	0.28	0	59.56	0	0.8	0.28	0.12	0
200-300	0	0	7.96	0	0.24	0.08	0	0
300-500	0.02	0	11.48	0	0.4	0.16	0	0
125-250 µm								
0-50	4.8	0.08	37.76	0.16	0	0	0	0.08
50-100	12.32	0	60.08	0	0	0	0.32	0
100-200	9.36	0.08	29.76	0	0	0	0.32	0
200-300	2.72	0.04	11.4	0.08	0	0	0.04	0
300-500	1.62	0	9.9	0	0	0	0	0
250-500 µm								
0-50	0.08	0	0	0	0	0	0	0
50-100	1.12	0	0.32	0	0	0	0	0
100-200	0.96	0.04	0.16	0	0	0	0	0
200-300	0.16	0	0.16	0	0	0	0	0
300-500	0.12	0	0.06	0	0	0	0	0
total								
0-50	4.96	0.08	122.24	0.16	1.76	0.24	0	0.08
50-100	13.6	0	154.08	0.08	0.32	0.16	0.4	0
100-200	10.6	0.12	89.48	0	0.8	0.28	0.44	0
200-300	2.88	0.04	19.52	0.08	0.24	0.08	0.04	0
300-500	1.76	0	21.44	0	0.4	0.16	0	0
Station: 55/78								
Depth (m)	<i>N. pach.</i> (s.)	<i>N. pach.</i> (d.)	<i>T. quin.</i>	<i>G. bull.</i>	<i>G. glu.</i>	<i>G. uvul.</i>	<i>O. ried.</i>	other
63-125 µm								
0-50	0.88	0	37.92	0.16	1.84	0.24	0	0
50-100	3.84	0	248.88	0.08	1.28	0.48	0.48	0.24
100-200	1.52	0	39.92	0	0.44	0	0	0
200-300	0.96	0.04	3.68	0	0.16	0.04	0	0.04
300-500	0.34	0	7.36	0.02	0.32	0.04	0	0.06
125-250 µm								
0-50	5.2	0.16	35.6	0.08	0.08	0	0	0
50-100	15.68	0.24	231.92	0.16	0	0	0.96	0.16
100-200	24.52	0.28	37.44	0.04	0.04	0	0	0.16
200-300	2.6	0	2.96	0	0	0	0	0
300-500	2.9	0.02	7.98	0	0.02	0	0.04	0.02
250-500 µm								
0-50	0.4	0	0.08	0	0	0	0	0
50-100	0.72	0	0.88	0	0	0	0	0.08
100-200	0.84	0	0.48	0	0	0	0	0.04
200-300	0.08	0	0.04	0	0	0	0	0
300-500	0.12	0	0.1	0	0	0	0	0
total								
0-50	6.48	0.16	73.6	0.24	0.08	0.16	0	0
50-100	20.24	0.24	481.68	0.24	1.28	0.48	1.44	0.48
100-200	26.88	0.28	77.84	0.04	0.48	0	0	0.2
200-300	3.64	0.04	6.68	0	0.16	0.04	0	0.04
300-500	3.36	0.02	15.44	0.02	0.34	0.04	0.04	0.08
Station: 55/79								
Depth (m)	<i>N. pach.</i> (s.)	<i>N. pach.</i> (d.)	<i>T. quin.</i>	<i>G. bull.</i>	<i>G. glu.</i>	<i>G. uvul.</i>	<i>O. ried.</i>	other
63-125 µm								
0-50	0.88	0	65.04	0.08	0.64	0.4	0	0
50-100	2.8	0	97.12	0	2.16	0.4	0	0
100-200	0	0	82.48	0	0.4	0.08	0	0
200-300	0.28	0	22.2	0	0.24	0.08	0	0
300-500	0	0	8.36	0	0.08	0.06	0	0
125-250 µm								
0-50	13.12	0.16	33.36	0.32	0	0	0	0.08
50-100	21.44	0.16	123.12	0.16	0	0.08	0	0
100-200	7	0.16	71.04	0.04	0	0	0	0
200-300	4.92	0	10.04	0.04	0	0	0	0
300-500	2.86	0	7.72	0	0	0	0.02	0
250-500 µm								
0-50	3.68	0.08	1.12	0.08	0	0.08	0	0
50-100	1.84	0	0.56	0	0	0	0	0
100-200	1.32	0	0.12	0	0	0	0	0
200-300	0.56	0.04	0	0	0	0	0	0
300-500	0.12	0	0	0	0	0	0	0
total								
0-50	17.68	0.24	99.52	0.48	0.64	0.48	0	0.08
50-100	26.08	0.16	220.8	0.16	2.16	0.48	0	0
100-200	8.32	0.16	153.64	0.04	0.4	0.08	0	0
200-300	5.76	0.04	32.24	0.04	0.24	0.08	0	0
300-500	2.98	0	16.08	0	0.08	0.06	0.02	0

Appendix

Table 6: Continued.

Station:	55/80							
Depth (m)	<i>N. pach.</i> (s.)	<i>N. pach.</i> (d.)	<i>T. quin.</i>	<i>G. bull.</i>	<i>G. glu.</i>	<i>G. uvul.</i>	<i>O. ried.</i>	other
63-125 µm								
0-50	0.48	0	79.36	0.08	0.96	0.24	0	0
50-100	2.64	0	48.16	0.08	0.32	0.08	0	0
100-200	0.12	0	69.4	0.04	0.04	0.04	0.04	0
200-300	1.12	0	11.44	0	0.04	0.04	0.08	0.08
300-500	0.72	0	6.76	0	0.06	0.06	0.04	0.04
125-250 µm								
0-50	10.24	0.24	22.08	0.16	0.08	0.08	0	0
50-100	10.16	0.24	28	0.16	0	0	0	0
100-200	8.12	0.24	48.68	0.28	0	0	0.12	0
200-300	2.44	0.04	4.36	0	0	0	0	0
300-500	2.26	0.04	2.76	0	0	0	0	0
250-500 µm								
0-50	1.12	0.08	0	0.08	0	0	0	0
50-100	0.72	0	0.16	0.08	0	0	0	0
100-200	1.24	0	0.16	0	0	0	0	0
200-300	0.36	0	0.04	0	0	0	0	0
300-500	0.22	0	0	0	0	0	0	0
total								
0-50	11.84	0.32	101.44	0.32	1.04	0.32	0	0
50-100	13.52	0.24	76.32	0.32	0.32	0.08	0	0
100-200	9.48	0.24	118.24	0.32	0.04	0.04	0.16	0
200-300	3.92	0.04	15.84	0	0.04	0.04	0.08	0.08
300-500	3.2	0.04	9.52	0	0.06	0.06	0.04	0.04
Station: 55/81								
Depth (m)	<i>N. pach.</i> (s.)	<i>N. pach.</i> (d.)	<i>T. quin.</i>	<i>G. bull.</i>	<i>G. glu.</i>	<i>G. uvul.</i>	<i>O. ried.</i>	other
63-125 µm								
0-50	4.64	0	39.2	0	0.72	0.16	0.16	0
50-100	10.24	0.08	604.24	0	1.12	0	0.32	0
100-200	6.32	0.04	193.24	0.08	0.92	0.08	1.12	0.32
200-300	1.56	0	22.68	0	0.08	0.08	0	0
300-500	0.34	0	10.22	0	0.18	0.04	0	0
125-250 µm								
0-50	4.96	0	10.4	0	0	0	0	0
50-100	21.6	0.48	451.2	0.4	0.16	0	2.64	0
100-200	11.88	0.32	204.96	0.12	0	0	0.84	0.16
200-300	3.96	0.08	20.72	0	0	0	0.04	0
300-500	3.74	0.1	20.3	0	0	0.02	0.02	0.04
250-500 µm								
0-50	0.4	0	0	0	0	0	0	0
50-100	2.08	0.08	0.96	0	0	0	0	0
100-200	0.92	0	0.32	0	0	0	0	0
200-300	0.12	0	0	0	0	0	0	0
300-500	0.14	0	0.02	0	0	0	0	0
total								
0-50	10	0	49.6	0	0.72	0.16	0.16	0
50-100	33.92	0.64	1056.4	0.4	1.28	0	2.96	0
100-200	19.12	0.36	398.52	0.2	0.92	0.08	1.96	0.48
200-300	5.64	0.08	43.4	0	0.08	0.08	0.04	0
300-500	4.22	0.1	30.54	0	0.18	0.06	0.02	0.04
Station: 55/82								
Depth (m)	<i>N. pach.</i> (s.)	<i>N. pach.</i> (d.)	<i>T. quin.</i>	<i>G. bull.</i>	<i>G. glu.</i>	<i>G. uvul.</i>	<i>O. ried.</i>	other
63-125 µm								
0-50	2.32	0.08	5.76	0.08	0	0.16	0	0
50-100	3.76	0	25.52	0.08	0.16	0	0	0.16
100-200	1.4	0	32.2	0.04	0.12	0.04	0	0.08
200-300	1.44	0	7.68	0	0.2	0.04	0	0.04
300-500	0.1	0.02	2.76	0	0	0	0	0.02
125-250 µm								
0-50	3.92	0.08	2.08	0	0.08	0	0	0
50-100	20.48	0.56	29.2	0.4	0	0	0	0.08
100-200	8.12	0.28	34.88	0.24	0	0	0.08	0.12
200-300	2.56	0.2	7.28	0.08	0	0	0.08	0
300-500	1.22	0.02	5.56	0	0	0	0	0
250-500 µm								
0-50	0.4	0	0.08	0.08	0	0	0	0
50-100	2.16	0	0.08	0.16	0	0	0	0
100-200	1.44	0.04	0.04	0.12	0	0	0	0
200-300	0.12	0	0.04	0.04	0	0	0	0
300-500	0	0	0	0	0	0	0	0
total								
0-50	6.64	0.16	7.92	0.16	0.08	0.16	0	0
50-100	26.4	0.56	54.8	0.64	0.16	0	0	0.24
100-200	10.96	0.32	67.12	0.4	0.12	0.04	0.08	0.2
200-300	4.12	0.2	15	0.12	0.2	0.04	0.08	0.04
300-500	1.32	0.04	8.32	0	0	0	0	0.02

Appendix

Table 6: Continued.

Station: 55/83									
Depth (m)	<i>N. pach.</i> (s.)	<i>N. pach.</i> (d.)	<i>T. quin.</i>	<i>G. bull.</i>	<i>G. glu.</i>	<i>G. uvul.</i>	<i>O. ried.</i>	other	
63-125 µm									
0-50	2.56	0.08	7.52	0.08	0	0	0	0.16	
50-100	4.16	0.16	10	0	0.08	0	0	0.08	
100-200	2.4	0	4.96	0	0	0	0	0	
200-300	1.4	0	3.12	0	0	0	0	0	
300-500	0.62	0	6.82	0.02	0.06	0.04	0	0	
125-250 µm									
0-50	12.08	1.12	8.16	0.48	0	0	0	0	
50-100	18.72	0.32	8.08	0.24	0.08	0	0	0	
100-200	10.2	0.32	4.28	0.36	0	0.04	0	0.04	
200-300	2.56	0.04	1.76	0	0	0	0	0	
300-500	1.14	0.08	4.46	0.04	0.04	0	0	0	
250-500 µm									
0-50	5.92	0.16	0.48	0	0	0	0	0	
50-100	9.76	0.24	0.48	0	0	0	0	0	
100-200	5.04	0	0.08	0.08	0	0	0	0.04	
200-300	0.16	0	0	0	0	0	0	0	
300-500	0.18	0	0.04	0	0	0	0	0	
total									
0-50	20.56	1.36	16.16	0.56	0	0	0	0.16	
50-100	32.64	0.72	18.56	0.24	0.16	0	0	0.08	
100-200	17.64	0.32	9.32	0.44	0	0.04	0	0.08	
200-300	4.12	0.04	4.88	0	0	0	0	0	
300-500	1.94	0.08	11.32	0.06	0.1	0.04	0	0	

Station: 55/84									
Depth (m)	<i>N. pach.</i> (s.)	<i>N. pach.</i> (d.)	<i>T. quin.</i>	<i>G. bull.</i>	<i>G. glu.</i>	<i>G. uvul.</i>	<i>O. ried.</i>	other	
63-125 µm									
0-50	6	0.48	9.2	0	0	0	0	0.56	
50-100	3.28	0	1.44	0	0	0	0	0.08	
100-200	0.28	0	0.96	0	0	0	0	0	
200-300	0.48	0	0.6	0	0	0	0	0	
300-500	0.14	0	0.26	0	0	0	0	0	
125-250 µm									
0-50	8.64	0.56	3.28	0	0	0	0	0	
50-100	6.96	0.08	0.8	0	0.08	0	0	0	
100-200	5.6	0.12	1.32	0	0	0	0	0	
200-300	1.64	0	0.64	0	0	0	0	0	
300-500	0.62	0.02	0.34	0	0	0	0	0	
250-500 µm									
0-50	1.92	0.16	0.08	0	0	0	0	0	
50-100	3.76	0.16	0	0	0	0	0	0	
100-200	3.52	0.04	0.08	0	0	0	0	0	
200-300	0.4	0	0.04	0	0	0	0	0	
300-500	0.12	0	0	0	0	0	0	0	
total									
0-50	16.56	1.2	12.56	0	0	0	0	0.56	
50-100	14	0.24	2.24	0	0.08	0	0	0.08	
100-200	9.4	0.16	2.36	0	0	0	0	0	
200-300	2.52	0	1.28	0	0	0	0	0	
300-500	0.88	0.02	0.6	0	0	0	0	0	

Table 7: Frequency Distribution of *N. pachyderma* (s.) and *T. quinqueloba* in the Fram Strait (Ark XV/2).

Station77																				
<i>N. pach.</i> (s.) size-class	0-50 m				50-100 m				100-200 m				200-300 m				300-500 m			
	total	dead	kum.	calc.	total	dead	kum.	calc.	total	dead	kum.	calc.	total	dead	kum.	calc.	total	dead	kum.	calc.
70	7	6	0	0	15	3	0	0	33	20	0	2	9	2	0	0	2	1	0	0
93	13	2	1	2	27	8	0	0	69	28	9	11	14	6	5	5	19	19	5	8
116	11	2	1	2	31	6	2	2	63	13	13	27	17	4	6	9	22	18	6	16
139	17	7	3	4	18	1	3	4	65	23	22	35	14	3	3	5	35	34	17	21
162	13	3	4	5	33	9	2	4	80	17	20	30	17	8	5	5	47	41	8	18
186	12	0	2	3	21	2	5	7	50	15	16	19	10	2	3	3	24	15	2	5
209	4	2	0	2	18	1	6	6	15	2	2	4	5	1	1	1	8	5	1	1
232	2	0	1	1	5	1	1	2	14	1	5	7	5	2	3	3	4	3	0	1
255	1	1	0	1	4	0	0	2	2	0	1	2	2	0	0	1	3	2	2	2
278	0	0	0	0	0	0	0	0	1	0	0	1	0	0	0	0	0	0	0	0
302	0	0	0	0	1	0	0	1	0	0	0	0	1	0	0	0	0	0	0	0
325	0	0	0	0	2	0	1	2	1	0	1	1	0	0	0	0	0	0	0	0
348	0	0	0	0	0	0	0	0	1	1	1	1	0	0	0	0	0	0	0	0
371	0	0	0	0	0	0	0	0	0	0	0	0	0	0	0	0	0	0	0	0
394	0	0	0	0	0	0	0	0	0	0	0	0	0	0	0	0	0	0	0	0
418	0	0	0	0	0	0	0	0	0	0	0	0	0	0	0	0	0	0	0	0
<i>T. quin.</i>	total	dead	kum.	calc.	total	dead	kum.	calc.	total	dead	kum.	calc.	total	dead	kum.	calc.	total	dead	kum.	calc.
70	335	94	0	2	418	60	0	1	395	176	3	18	97	41	2	24	157	101	2	38
93	189	48	0	3	379	62	1	6	380	141	7	98	99	53	3	42	229	174	5	107
116	108	25	3	5	240	27	1	15	240	50	7	125	66	45	6	28	159	134	11	97
139	130	22	3	5	141	31	0	13	111	35	9	53	47	36	1	25	117	104	7	88
162	118	22	3	7	132	14	4	14	100	31	11	0	48	26	2	23	123	109	15	90
186	52	12	3	7	66	7	8	16	57	11	7	35	18	11	1	8	66	56	12	59
209	10	2	0	2	37	1	5	18	23	2	7	16	4	2	0	2	23	23	4	18
232	9	0	1	3	11	1	1	5	10	1	1	7	4	3	0	2	7	7	1	4
255	0	0	0	0	2	0	0	2	2	0	0	1	1	0	1	1	1	1	0	1
278	0	0	0	0	0	0	0	0	3	0	0	3	0	0	0	0	1	0	0	0
302	0	0	0	0	0	0	0	0	0	0	0	0	0	0	0	0	0	0	0	0
325	0	0	0	0	0	0	0	0	0	0	0	0	0	0	0	0	0	0	0	0
348	0	0	0	0	0	0	0	0	0	0	0	0	0	0	0	0	0	0	0	0

Appendix

Table 7: Continued.

Station 82																				
<i>N. pach.</i> (s.)																				
size-class	0-50 m				50-100 m				100-200 m				200-300 m				300-500 m			
	total	dead	kum.	calc.	total	dead	kum.	calc.	total	dead	kum.	calc.	total	dead	kum.	calc.	total	dead	kum.	calc.
70	2	0	0	0	11	7	0	0	12	6	0	0	11	9	0	0	4	2	0	0
93	2	0	0	0	11	3	0	0	11	3	0	1	17	7	4	5	3	1	0	0
116	4	0	0	0	12	1	1	1	23	14	1	3	15	6	2	5	10	8	4	6
139	10	0	0	0	15	3	0	0	27	7	3	8	8	4	1	1	9	6	1	2
162	3	0	0	0	41	3	0	1	43	17	6	7	8	2	0	1	11	2	2	2
186	6	0	0	0	28	3	0	0	29	10	2	4	3	1	1	2	8	4	2	2
209	10	4	0	0	18	7	2	1	28	1	6	8	3	1	1	1	9	5	2	3
232	6	0	0	1	18	4	1	0	15	1	4	10	2	0	1	0	2	0	0	0
255	2	0	0	0	5	0	1	1	9	1	3	6	2	1	1	1	1	1	0	1
278	2	0	0	0	9	2	2	1	11	1	5	6	3	1	0	2	0	0	0	0
302	1	0	0	0	1	0	0	0	0	0	0	0	0	0	0	0	0	0	0	0
325	0	0	0	0	2	0	0	2	3	0	1	3	1	1	0	0	0	0	0	0
348	0	0	0	0	0	0	0	0	1	0	1	0	0	0	0	0	0	0	0	0
371	0	0	0	0	0	0	0	0	0	0	0	0	0	0	0	0	0	0	0	0
394	0	0	0	0	0	0	0	0	0	0	0	0	0	0	0	0	0	0	0	0
418	0	0	0	0	0	0	0	0	0	0	0	0	0	0	0	0	0	0	0	0
<i>T.quin.</i>	total	dead	kum.	calc.	total	dead	kum.	calc.	total	dead	kum.	calc.	total	dead	kum.	calc.	total	dead	kum.	calc.
70	27	6	0	0	141	17	0	0	304	70	1	13	75	45	1	20	33	23	4	21
93	36	6	0	1	136	14	1	2	304	52	2	16	82	61	6	29	35	27	2	26
116	4	0	0	0	112	7	1	0	259	37	4	24	50	41	1	11	76	65	9	33
139	4	2	0	1	106	5	0	0	219	30	7	53	42	32	2	15	59	53	7	40
162	11	4	1	1	107	10	2	2	189	23	11	52	45	32	1	21	61	52	9	42
186	1	0	0	0	51	10	2	3	99	15	17	34	24	17	3	9	50	46	8	43
209	0	0	0	0	13	5	2	1	52	11	11	29	14	8	2	4	39	34	7	23
232	2	0	0	0	6	2	0	0	8	2	1	6	10	6	0	6	7	7	1	1
255	0	0	0	0	1	0	0	1	0	0	0	0	0	0	0	0	1	1	0	1
278	0	0	0	0	1	0	0	0	0	0	0	0	0	0	0	0	0	0	0	0
302	0	0	0	0	0	0	0	0	0	0	0	0	0	0	0	0	0	0	0	0
325	0	0	0	0	0	0	0	0	0	0	0	0	0	0	0	0	0	0	0	0
348	0	0	0	0	0	0	0	0	0	0	0	0	0	0	0	0	0	0	0	0

Station 83																				
<i>N. pach.</i> (s.)																				
size-class	0-50 m				50-100 m				100-200 m				200-300 m				300-500 m			
	total	dead	kum.	calc.	total	dead	kum.	calc.	total	dead	kum.	calc.	total	dead	kum.	calc.	total	dead	kum.	calc.
70	9	1	0	0	17	6	0	0	14	2	0	0	10	3	1	1	24	19	0	0
93	7	1	0	0	14	0	0	0	20	3	0	0	14	1	0	0	23	17	1	2
116	8	1	0	0	25	8	0	0	35	8	0	0	16	6	1	0	11	9	0	0
139	18	3	0	0	23	0	0	0	46	5	1	0	13	3	1	0	14	10	2	3
162	23	2	0	0	58	4	0	2	69	3	2	3	10	2	1	1	14	5	1	1
186	25	1	1	1	30	1	0	0	39	1	3	2	8	2	0	0	4	2	0	0
209	25	0	0	0	27	2	2	0	33	0	4	4	4	0	1	1	8	5	0	2
232	37	1	1	0	56	0	8	5	29	0	8	8	3	0	1	1	1	0	1	1
255	22	1	5	2	36	0	5	4	29	0	17	18	2	1	2	2	0	0	0	0
278	21	3	4	1	25	1	2	3	28	0	11	21	0	0	0	0	3	2	0	3
302	3	0	0	0	13	0	4	6	12	0	8	12	0	0	0	0	2	2	1	1
325	0	0	5	0	8	0	3	5	11	0	8	9	0	0	0	0	4	4	2	3
348	2	0	0	0	0	0	0	0	4	0	2	4	0	0	0	0	0	0	0	0
371	0	0	0	0	0	0	0	0	0	0	0	0	0	0	0	0	0	0	0	0
394	0	0	0	0	0	0	0	0	0	0	0	0	0	0	0	0	0	0	0	0
418	0	0	0	0	0	0	0	0	0	0	0	0	0	0	0	0	0	0	0	0
<i>T.quin.</i>	total	dead	kum.	calc.	total	dead	kum.	calc.	total	dead	kum.	calc.	total	dead	kum.	calc.	total	dead	kum.	calc.
70	34	9	0	0	71	19	0	0	67	11	0	0	50	19	0	0	169	109	4	55
93	42	8	0	0	39	13	0	0	38	4	0	1	13	8	0	1	90	63	3	35
116	35	5	1	0	30	6	0	1	39	10	0	2	15	9	1	5	74	62	6	32
139	25	3	1	0	27	6	0	0	35	3	0	1	7	3	1	2	51	44	2	17
162	29	4	1	0	20	3	0	0	22	4	1	2	15	8	1	6	51	46	5	28
186	9	2	1	1	13	4	0	0	15	3	0	6	3	0	0	0	27	20	5	17
209	4	0	0	0	8	1	0	0	6	1	1	4	0	0	0	0	9	6	1	4
232	9	1	1	0	9	0	0	0	3	0	0	1	0	0	0	0	2	1	0	1
255	1	0	0	0	6	1	0	0	1	0	0	0	0	0	0	0	0	0	0	0
278	6	0	0	0	6	0	0	0	0	0	0	0	0	0	0	0	0	0	0	0
302	0	0	0	0	3	0	1	1	1	0	0	0	0	0	0	0	0	0	0	0
325	0	0	0	0	1	0	0	0	0	0	0	0	0	0	0	0	0	0	0	0
348	0	0	0	0	0	0	0	0	0	0	0	0	0	0	0	0	0	0	0	0

Station 84																				
<i>N. pach.</i> (s.)																				
size-class	0-50 m				50-100 m				100-200 m				200-300 m				300-500 m			
	total	dead	kum.	calc.	total	dead	kum.	calc.	total	dead	kum.	calc.	total	dead	kum.	calc.	total	dead	kum.	calc.
70	24	15	0	0	9	3	0	0	4	1	0	0	1	1	0	0	0	0	0	0
93	16	5	2	0	6	2	0	0	4	1	0	0	1	1	0	0	3	2	0	0
116	14	1	0	0	7	0	0	0	6	2	0	0	4	2	0	0	6	2	0	0
139	14	2	0	0	7	0	0	0	6	1	1	1	1	1	0	0	7	3	0	0
162	17	2	1	0	12	0	1	0	24	0	2	3	10	6	0	0	4	2	0	0
186	9	0	0	0	14	1	0	0	30	2	4	4	12	6	3	3	2	0	0	0
209	9	0	0	0	7	0	0	0	21	0	3	5	7	2	2	2	2	0	0	0
232	9	4	0	0	22	0	1	1	24	0	9	9	6	3	1	2	3	0	0	1
255	8	0	5	2	14	0	2	2	33	1	17	22	3	1	1	1	1	0	0	0
278	6	0	1	1	7	0	4	5	15	0	5	11	2	1	1	1	1	0	0	0
302	2	0	1	0	7	0	6	3	12	0	4	9	0	0	0	0	0	0	0	0
325	1	0	1	0	2	0	1	1	4	0	1	3	0	0	0	0	0	0	0	0
348	0	0	0	0	0	0	0	0	1	0	1	0	0	0	0	0	0	0	0	0
371	0	0	0	0	0	0	0	0	0	0	0	0	0	0	0	0	0	0	0	0
394	0	0	0	0	0	0	0	0	0	0	0	0	0	0	0	0	0	0	0	0
418	0	0	0	0	0	0	0	0	0	0	0	0	0	0	0	0	0	0	0	0
<i>T.quin.</i>	total	dead	kum.	calc.	total	dead	kum.	calc.	total	dead	kum.	calc.	total	dead	kum.	calc.	total	dead	kum.	calc.
70	75	12	0	0	23	4	0	0	16	5	0	0	7	5	0	0	7	4	0	3
93	35	6	0	0	11	1	0	0	15	4	0	0	8	7	0	0	5	4	1	0
116	29	6	0	0	6	2	0	0	9	4	0	0	4	3	0	0	5	4	0	2
139	11	2	0	0	1	0	0	1	10	3	1	1	2	2	0	0	3	3	0	1
162	17	1	0	0	4	1	0	0	12	5	0	1	5	3	0	3	6	6	0	2
186	7	0	0	0	5	0	0	0	6	0	0	3	4	2	0	2	2	1	0	0
209	2	0	0	1	3	0	0	1	2	1	0									

Appendix

Table 8: Stable Isotope Data of *N. pachyderma* (s.) and *T. quinqueloba* from the Fram Strait (Ark XV/2).

station	depth (m)	species	max. Diameter (μm)	n	^{13}C	$\pm\text{s13}$	^{18}O	$\pm\text{s18}$	Living/Dead	Calc. Group
84	0-50	<i>N.pach.</i> (s.)	290	9	0.56	0.01	2.46	0.02	living	nonencrusted
84	0-50	<i>N.pach.</i> (s.)	255	6	0.46	0.01	2.19	0.03	living	nonencrusted
84	50-100	<i>N.pach.</i> (s.)	314	9	0.64	0.01	2.61	0.03	living	nonencrusted
84	50-100	<i>N.pach.</i> (s.)	267	11	0.54	0.02	2.51	0.02	living	nonencrusted
84	100-200	<i>N.pach.</i> (s.)	302	5	0.46	0.09	2.78	0.11	living	encrusted
84	100-200	<i>N.pach.</i> (s.)	255	6	0.40	0.02	3.00	0.03	living	encrusted
84	100-200	<i>N.pach.</i> (s.)	278	5	0.55	0.02	2.95	0.02	living	encrusted
84	100-200	<i>N.pach.</i> (s.)	255	6	0.53	0.01	3.01	0.04	living	nonencrusted
84	100-200	<i>N.pach.</i> (s.)	278	6	0.56	0.01	3.02	0.03	living	nonencrusted
84	100-200	<i>N.pach.</i> (s.)	314	7	0.60	0.01	2.96	0.02	living	nonencrusted
84	200-300	<i>N.pach.</i> (s.)	232	10	0.45	0.01	3.28	0.03	living+dead	encrusted
83	0-50	<i>N.pach.</i> (s.)	255	6	0.35	0.02	1.64	0.03	living	nonencrusted
83	0-50	<i>N.pach.</i> (s.)	278	9	0.44	0.02	1.86	0.01	living	nonencrusted
83	0-50	<i>N.pach.</i> (s.)	314	5	0.52	0.00	1.54	0.01	living	nonencrusted
83	50-100	<i>N.pach.</i> (s.)	255	9	0.50	0.02	2.47	0.02	living	nonencrusted
83	50-100	<i>N.pach.</i> (s.)	278	7	0.40	0.01	2.26	0.03	living	nonencrusted
83	50-100	<i>N.pach.</i> (s.)	302	7	0.61	0.01	2.69	0.02	living	nonencrusted
83	50-100	<i>N.pach.</i> (s.)	267	4	0.44	0.01	2.74	0.01	living	encrusted
83	50-100	<i>N.pach.</i> (s.)	302	7	0.54	0.01	2.68	0.03	living	encrusted
83	50-100	<i>N.pach.</i> (s.)	325	4	0.70	0.01	2.62	0.02	living	encrusted
83	100-200	<i>N.pach.</i> (s.)	267	6	0.46	0.01	2.76	0.04	living	nonencrusted
83	100-200	<i>N.pach.</i> (s.)	302	6	0.68	0.02	2.78	0.03	living	nonencrusted
83	100-200	<i>N.pach.</i> (s.)	325	4	0.49	0.01	2.78	0.03	living	nonencrusted
83	100-200	<i>N.pach.</i> (s.)	360	5	0.69	0.02	2.58	0.03	living	nonencrusted
83	100-200	<i>N.pach.</i> (s.)	278	4	0.60	0.01	2.95	0.01	living	encrusted
83	100-200	<i>N.pach.</i> (s.)	278	5	0.63	0.01	2.95	0.03	living	encrusted
83	100-200	<i>N.pach.</i> (s.)	302	4	0.53	0.01	3.00	0.02	living	encrusted
83	100-200	<i>N.pach.</i> (s.)	325	3	0.76	0.02	2.94	0.02	living	encrusted
83	200-300	<i>N.pach.</i> (s.)	220	5	0.43	0.01	3.20	0.03	living+dead	encrusted
83	300-500	<i>N.pach.</i> (s.)	221	3	0.55	0.02	3.28	0.03	living+dead	encrusted
83	300-500	<i>N.pach.</i> (s.)	278	3	0.60	0.01	2.83	0.04	living+dead	encrusted
83	300-500	<i>N.pach.</i> (s.)	302	3	0.65	0.02	2.90	0.03	dead	encrusted
83	300-500	<i>N.pach.</i> (s.)	325	3	0.64	0.01	2.70	0.02	dead	encrusted
82	0-50	<i>N.pach.</i> (s.)	198	14	-0.29	0.02	2.96	0.05	living+dead	nonencrusted
82	0-50	<i>N.pach.</i> (s.)	232	4	-0.01	0.02	2.92	0.05	living	nonencrusted
82	0-50	<i>N.pach.</i> (s.)	279	5	0.35	0.02	3.14	0.04	living	nonencrusted
82	50-100	<i>N.pach.</i> (s.)	255	5	0.10	0.03	2.91	0.03	living	nonencrusted
82	50-100	<i>N.pach.</i> (s.)	278	5	0.10	0.02	3.20	0.03	living+dead	nonencrusted
82	50-100	<i>N.pach.</i> (s.)	302	3	0.52	0.01	3.30	0.02	living	nonencrusted
82	100-200	<i>N.pach.</i> (s.)	255	4	0.27	0.02	3.27	0.02	living	encrusted
82	100-200	<i>N.pach.</i> (s.)	290	4	0.35	0.02	3.36	0.04	living	encrusted
82	100-200	<i>N.pach.</i> (s.)	325	2	0.66	0.01	3.14	0.03	living	encrusted
82	200-300	<i>N.pach.</i> (s.)	244	6	0.25	0.01	3.29	0.03	living+dead	encrusted
81	0-50	<i>N.pach.</i> (s.)	198	12	-0.05	0.02	2.88	0.03	living+dead	nonencrusted
81	0-50	<i>N.pach.</i> (s.)	221	6	0.03	0.03	2.94	0.06	living	nonencrusted
81	0-50	<i>N.pach.</i> (s.)	255	2	-1.00	0.08	1.81	0.09	living	nonencrusted
81	50-100	<i>N.pach.</i> (s.)	255	7	0.13	0.01	2.96	0.05	living	nonencrusted
81	50-100	<i>N.pach.</i> (s.)	278	3	0.32	0.04	3.29	0.08	living	nonencrusted
81	50-100	<i>N.pach.</i> (s.)	325	2	0.31	0.02	3.34	0.04	living	nonencrusted
81	50-100	<i>N.pach.</i> (s.)	232	9	-0.31	0.01	2.32	0.02	living	encrusted
81	100-200	<i>N.pach.</i> (s.)	221	7	-0.01	0.03	2.71	0.05	living	nonencrusted
81	100-200	<i>N.pach.</i> (s.)	255	7	1.25	0.08	2.40	0.05	living+dead	nonencrusted
81	100-200	<i>N.pach.</i> (s.)	232	3	-0.01	0.02	2.62	0.03	living+dead	encrusted
81	100-200	<i>N.pach.</i> (s.)	255	6	0.13	0.02	2.84	0.04	living+dead	encrusted
81	100-200	<i>N.pach.</i> (s.)	278	3	0.03	0.01	2.88	0.03	living+dead	encrusted
81	100-200	<i>N.pach.</i> (s.)	314	2	0.06	0.04	2.17	0.08	living	encrusted
81	200-300	<i>N.pach.</i> (s.)	279	7	0.38	0.01	3.36	0.01	living+dead	encrusted
81	300-500	<i>N.pach.</i> (s.)	209	16	-0.40	0.04	2.52	0.05	dead	encrusted
80	0-50	<i>N.pach.</i> (s.)	255	7	0.15	0.02	3.48	0.05	living+dead	nonencrusted
80	0-50	<i>N.pach.</i> (s.)	278	3	0.51	0.04	2.79	0.11	living	nonencrusted
80	0-50	<i>N.pach.</i> (s.)	302	3	0.35	0.02	3.18	0.04	living+dead	nonencrusted
80	100-200	<i>N.pach.</i> (s.)	255	4	0.26	0.01	3.28	0.02	living+dead	encrusted
80	100-200	<i>N.pach.</i> (s.)	278	6	0.15	0.02	3.22	0.06	living	encrusted
80	100-200	<i>N.pach.</i> (s.)	325	4	0.37	0.01	3.36	0.01	living	encrusted
80	200-300	<i>N.pach.</i> (s.)	244	5	0.23	0.01	3.42	0.02	living+dead	encrusted
80	300-500	<i>N.pach.</i> (s.)	221	6	-0.19	0.02	2.91	0.02	living+dead	encrusted
79	0-50	<i>N.pach.</i> (s.)	255	6	-0.13	0.02	3.35	0.02	living	nonencrusted
79	0-50	<i>N.pach.</i> (s.)	278	7	0.12	0.06	3.27	0.02	living	nonencrusted
79	0-50	<i>N.pach.</i> (s.)	302	2	-0.17	0.03	3.37	0.06	living	nonencrusted
79	50-100	<i>N.pach.</i> (s.)	255	3	-0.28	0.05	2.45	0.06	living	nonencrusted
79	50-100	<i>N.pach.</i> (s.)	278	4	0.27	0.01	2.87	0.03	living+dead	nonencrusted
79	50-100	<i>N.pach.</i> (s.)	314	2	0.28	0.02	3.09	0.04	living	nonencrusted
79	100-200	<i>N.pach.</i> (s.)	255	9	0.16	0.03	3.09	0.06	living	encrusted
79	100-200	<i>N.pach.</i> (s.)	278	2	0.19	0.02	3.28	0.03	living	encrusted
79	100-200	<i>N.pach.</i> (s.)	302	5	0.27	0.02	3.36	0.04	living	encrusted
79	100-200	<i>N.pach.</i> (s.)	348	2	0.62	0.03	3.63	0.07	living	encrusted
79	100-200	<i>N.pach.</i> (s.)	279	1	0.18	0.07	3.02	0.09	living	nonencrusted
79	200-300	<i>N.pach.</i> (s.)	198	5	0.17	0.01	2.63	0.04	living+dead	encrusted
79	200-300	<i>N.pach.</i> (s.)	255	4	0.30	0.01	3.06	0.01	living+dead	encrusted
79	300-500	<i>N.pach.</i> (s.)	198	4	0.06	0.02	2.96	0.03	dead	encrusted
79	300-500	<i>N.pach.</i> (s.)	232	3	0.19	0.02	2.61	0.05	living+dead	encrusted
79	300-500	<i>N.pach.</i> (s.)	255	2	0.24	0.02	2.98	0.03	dead	encrusted
79	300-500	<i>N.pach.</i> (s.)	325	1	0.33	0.03	3.12	0.05	dead	encrusted
78	50-100	<i>N.pach.</i> (s.)	232	10	-0.24	0.04	2.28	0.11	living	nonencrusted
78	50-100	<i>N.pach.</i> (s.)	278	3	0.34	0.02	3.04	0.04	living	nonencrusted
78	50-100	<i>N.pach.</i> (s.)	209	4	-0.12	0.01	2.68	0.01	living	encrusted
78	100-200	<i>N.pach.</i> (s.)	232	5	-0.02	0.02	2.75	0.05	living+dead	nonencrusted
78	100-200	<i>N.pach.</i> (s.)	267	5	0.39	0.02	2.77	0.02	living+dead	nonencrusted
78	100-200	<i>N.pach.</i> (s.)	255	3	0.17	0.06	2.82	0.07	living	encrusted
78	100-200	<i>N.pach.</i> (s.)	290	3	0.30	0.01	2.86	0.03	living	encrusted
78	300-500	<i>N.pach.</i> (s.)	255	5	0.49	0.01	2.95	0.03	dead	encrusted
77	50-100	<i>N.pach.</i> (s.)	290	5	0.21	0.01	2.39	0.03	living	encrusted

Appendix

Table 8: Continued.

station	depth (m)	species	max. Diameter (μm)	n	^{13}C	$\pm\text{s}13$	^{18}O	$\pm\text{s}18$	Living/Dead	Calc. Group
77	100-200	<i>N.pach.</i> (s.)	232	3	0.25	0.02	2.54	0.02	living	encrusted
77	100-200	<i>N.pach.</i> (s.)	267	2	0.25	0.03	2.44	0.03	living	encrusted
77	100-200	<i>N.pach.</i> (s.)	325	1	0.28	0.03	2.29	0.05	living	encrusted
77	200-300	<i>N.pach.</i> (s.)	174	6	-0.27	0.02	2.72	0.05	living+dead	encrusted
77	200-300	<i>N.pach.</i> (s.)	221	5	0.23	0.02	3.13	0.03	living+dead	encrusted
77	300-500	<i>N.pach.</i> (s.)	197	12	-0.03	0.01	2.96	0.02	living+dead	encrusted
84	0-50	<i>T. quin.</i>	232	12	0.34	0.01	1.57	0.02	living+dead	nonencrusted
84	50-100	<i>T. quin.</i>	244	12	0.01	0.01	2.26	0.02	living	nonencrusted
84	100-200	<i>T. quin.</i>	232	16	0.16	0.02	2.51	0.03	living+dead	nonencrusted
83	0-50	<i>T. quin.</i>	232	21	0.10	0.02	1.49	0.03	living+dead	nonencrusted
83	50-100	<i>T. quin.</i>	267	16	0.39	0.01	2.64	0.02	living+dead	nonencrusted
83	100-200	<i>T. quin.</i>	197	20	-0.99	0.01	2.68	0.02	living+dead	non+encrusted
83	200-300	<i>T. quin.</i>	163	13	-1.07	0.01	2.25	0.04	living+dead	non+encrusted
83	300-500	<i>T. quin.</i>	209	24	-1.35	0.01	2.53	0.04	living+dead	encrusted
82	50-100	<i>T. quin.</i>	186	17	-0.98	0.08	1.56	0.16	living	nonencrusted
82	50-100	<i>T. quin.</i>	209	9	-1.17	0.01	2.63	0.03	living	non+encrusted
82	100-200	<i>T. quin.</i>	198	20	-1.14	0.01	2.71	0.02	living+dead	encrusted
82	100-200	<i>T. quin.</i>	244	9	-1.09	0.05	2.58	0.07	living+dead	encrusted
82	200-300	<i>T. quin.</i>	209	21	-1.25	0.01	2.57	0.01	living+dead	encrusted
82	300-500	<i>T. quin.</i>	209	20	-1.27	0.01	2.62	0.02	dead	encrusted
82	300-500	<i>T. quin.</i>	186	18	-1.24	0.01	2.72	0.03	dead	encrusted
81	0-50	<i>T. quin.</i>	209	30	-1.06	0.01	2.54	0.01	living+dead	encrusted
81	50-100	<i>T. quin.</i>	186	30	-1.42	0.02	2.34	0.04	living	nonencrusted
81	50-100	<i>T. quin.</i>	209	30	-1.46	0.02	2.22	0.04	living	nonencrusted
81	50-100	<i>T. quin.</i>	232	11	-1.25	0.02	2.50	0.04	living	nonencrusted
81	50-100	<i>T. quin.</i>	209	26	-1.22	0.01	2.53	0.03	living	encrusted
81	50-100	<i>T. quin.</i>	232	15	-1.31	0.02	2.27	0.02	living	encrusted
81	100-200	<i>T. quin.</i>	209	24	-1.40	0.05	2.31	0.07	living	encrusted
81	100-200	<i>T. quin.</i>	232	12	-1.35	0.01	2.38	0.03	living	encrusted
81	200-300	<i>T. quin.</i>	209	24	-1.13	0.08	2.61	0.10	dead	encrusted
81	200-300	<i>T. quin.</i>	232	12	-1.26	0.01	2.51	0.03	dead	encrusted
81	200-300	<i>T. quin.</i>	186	11	-1.33	0.02	2.51	0.03	dead	encrusted
81	300-500	<i>T. quin.</i>	209	21	-1.42	0.02	2.36	0.02	dead	encrusted
81	300-500	<i>T. quin.</i>	232	20	-1.24	0.02	2.42	0.02	dead	encrusted
80	100-200	<i>T. quin.</i>	162	19	-1.22	0.02	2.94	0.03	living	encrusted
80	100-200	<i>T. quin.</i>	186	20	-1.17	0.02	2.78	0.03	living	encrusted
80	100-200	<i>T. quin.</i>	221	9	-1.09	0.02	2.95	0.04	living	encrusted
80	200-300	<i>T. quin.</i>	162	13	-1.21	0.01	2.85	0.02	dead	encrusted
80	200-300	<i>T. quin.</i>	198	13	-1.16	0.02	2.72	0.02	living+dead	encrusted
80	300-500	<i>T. quin.</i>	186	10	-1.17	0.01	2.79	0.02	dead	encrusted
80	300-500	<i>T. quin.</i>	151	14	-1.25	0.02	2.76	0.03	living+dead	encrusted
79	0-50	<i>T. quin.</i>	186	14	-1.51	0.01	2.32	0.02	living+dead	nonencrusted
79	0-50	<i>T. quin.</i>	209	21	-0.92	0.01	2.77	0.02	living+dead	non+encrusted
79	0-50	<i>T. quin.</i>	162	12	-1.41	0.03	2.53	0.03	living+dead	nonencrusted
79	50-100	<i>T. quin.</i>	209	15	-1.55	0.02	2.25	0.03	living	nonencrusted
79	50-100	<i>T. quin.</i>	244	21	-1.40	0.02	2.28	0.04	living	nonencrusted
79	50-100	<i>T. quin.</i>	186	12	-1.66	0.02	2.18	0.02	living+dead	nonencrusted
79	100-200	<i>T. quin.</i>	186	22	-1.42	0.01	2.48	0.03	living+dead	nonencrusted
79	100-200	<i>T. quin.</i>	221	23	-1.40	0.01	2.45	0.02	living+dead	encrusted
79	100-200	<i>T. quin.</i>	209	20	-1.18	0.03	2.83	0.04	living+dead	encrusted
79	100-200	<i>T. quin.</i>	186	18	-1.12	0.03	2.96	0.02	living+dead	encrusted
79	200-300	<i>T. quin.</i>	198	30	-1.05	0.02	2.97	0.03	living+dead	encrusted
79	200-300	<i>T. quin.</i>	162	13	-1.08	0.03	2.88	0.06	living+dead	encrusted
79	300-500	<i>T. quin.</i>	186	11	-1.18	0.02	2.91	0.03	dead	encrusted
79	300-500	<i>T. quin.</i>	221	24	-1.04	0.02	2.86	0.03	dead	encrusted
79	300-500	<i>T. quin.</i>	162	13	-1.24	0.02	2.80	0.05	dead	encrusted
78	0-50	<i>T. quin.</i>	186	11	-1.73	0.02	2.07	0.03	living+dead	nonencrusted
78	0-50	<i>T. quin.</i>	221	24	-1.64	0.02	2.13	0.04	living+dead	nonencrusted
78	50-100	<i>T. quin.</i>	209	23	-1.37	0.02	2.42	0.04	living	encrusted
78	50-100	<i>T. quin.</i>	232	20	-1.19	0.01	2.71	0.04	living	encrusted
78	100-200	<i>T. quin.</i>	209	25	-1.08	0.02	2.82	0.03	living	encrusted
78	100-200	<i>T. quin.</i>	232	24	-1.25	0.01	2.67	0.02	living	encrusted
78	300-500	<i>T. quin.</i>	209	22	-1.30	0.02	2.63	0.04	living+dead	encrusted
78	300-500	<i>T. quin.</i>	232	18	-1.16	0.01	2.64	0.03	living+dead	encrusted
77	0-50	<i>T. quin.</i>	209	22	-1.44	0.01	2.24	0.03	living+dead	nonencrusted
77	0-50	<i>T. quin.</i>	197	14	-1.01	0.03	2.81	0.04	living+dead	encrusted
77	50-100	<i>T. quin.</i>	209	10	-1.18	0.02	2.54	0.03	living+dead	encrusted
77	50-100	<i>T. quin.</i>	232	14	-1.28	0.01	2.47	0.03	living+dead	encrusted
77	50-100	<i>T. quin.</i>	174	10	-1.22	0.02	2.62	0.02	living+dead	encrusted
77	100-200	<i>T. quin.</i>	209	16	-1.46	0.02	2.49	0.04	living+dead	encrusted
77	100-200	<i>T. quin.</i>	174	14	-1.29	0.01	2.61	0.02	living+dead	encrusted
77	100-200	<i>T. quin.</i>	244	23	-1.08	0.02	2.43	0.05	living+dead	encrusted
77	200-300	<i>T. quin.</i>	163	6	-1.23	0.01	2.75	0.03	living+dead	encrusted
77	200-300	<i>T. quin.</i>	221	15	-0.94	0.02	2.41	0.05	living+dead	encrusted
77	300-500	<i>T. quin.</i>	232	6	-1.25	0.02	2.29	0.04	dead	encrusted
77	300-500	<i>T. quin.</i>	209	6	-1.21	0.02	2.52	0.05	dead	encrusted
77	300-500	<i>T. quin.</i>	186	13	-1.33	0.01	2.50	0.03	dead	encrusted

Acknowledgements

Für die Betreuung dieser Arbeit bedanke ich mich bei Prof. M. Spindler recht herzlich. Bei Herrn Prof. J. Thiede und Frau Dr. D. Bauch bedanke ich mich besonders für die Vergabe der Arbeit und ausdauernde Betreuung.

Bei Dr. U. Pflaumann und Dr. S. Jensen, die mich bei bei taxonomischen Fragen unterstützten, bedanke ich mich recht herzlich. Herrn Dr. H. Erlenkeuser und den Mitarbeitern des C¹⁴-Labors gilt ein besonderer Dank für die Messung stabiler Isotope. Herrn Dr. J. Simstich möchte ich für seine Diskussionsbereitschaft, konstruktive Kritik und die Korrektur dieser Arbeit danken.

Frau K. Fürhaupter für die geleistete Vorarbeit, die für das Gelingen dieser Dissertation von großer Bedeutung war, danke ich besonders. Der studentischen Hilfskraft J. Netzer bin ich für die Unterstützung im Projekt und auf See zu großem Dank verpflichtet. Weiterhin möchte ich mich bei der Crew des F.S *Polarstern* bedanken, die mir während der ARK XV Fahrtabschnitte 1 und 2 an Bord mit tatkräftiger Unterstützung zur Seite gestanden haben. Mein großer Dank gilt auch den Mitarbeitern des Instituts für Polarökologie und IfM, die zur Vorbereitung der ARK-Expedition massgeblich beigetragen haben: Herrn P. Rapp, P. Fritsche und Frau A. Scheltz.

Bedanken möchte ich mich auch bei Herrn Dr. J. Schönfeld und Dr. M. Hüls für ihre Unterstützung und motivierende Gespräche. Herrn T. Baumann und J. Ford danke ich für die Beratung in der englischen Sprache.

Mein größter Dank gilt meinen Freunden (Sascha, Stefan, André, Aziz) und meiner Familie, die in schwierigen Zeiten für mich da waren. Danke!!!